



**STUDY AND DEVELOPMENT OF THE DRAG REDUCTION SYSTEM FOR  
GO-KART**

**JULIANOUS KETIHUS**

**A report in partial fulfilment of the requirements for the degree of Bachelor of  
Mechatronics Engineering**

اونيورسيتي تیکنیکل ملیسیا ملاک  
UNIVERSITI TEKNIKAL MALAYSIA MELAKA

**Faculty of Electrical Engineering**

**UNIVERSITI TEKNIKAL MALAYSIA MELAKA**

**2014**


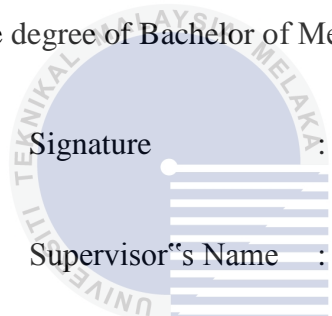
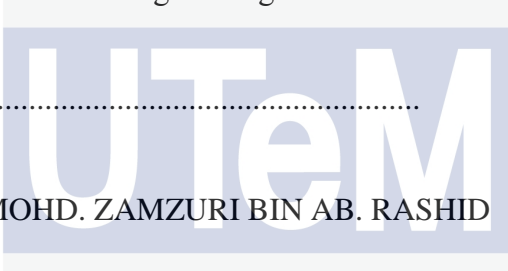
“I hereby declare that I have read through this report entitle “Study and Development of The Drag Reduction System for Go-kart” and found that it has comply the partial fulfilment for awarding the degree of Bachelor of Mechatronics Engineering”

Signature : .....

Supervisor's Name : MOHD. ZAMZURI BIN AB. RASHID

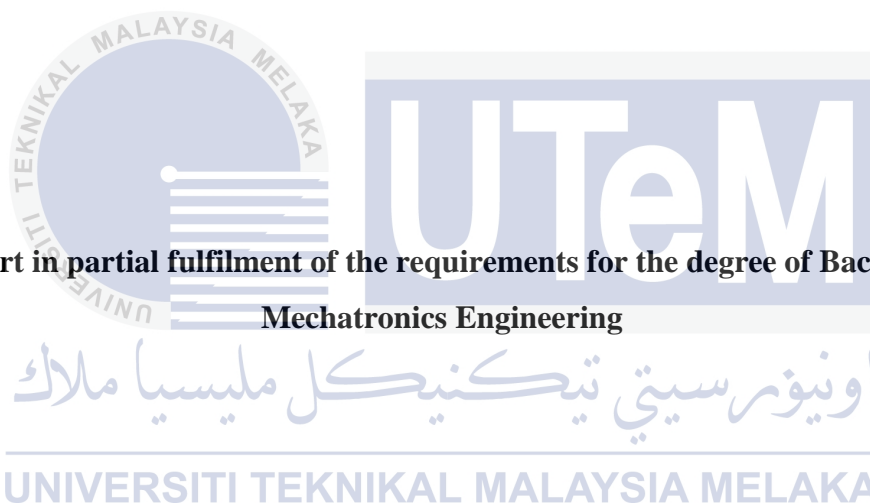
Date : .....

UNIVERSITI TEKNIKAL MALAYSIA MELAKA



**STUDY AND DEVELOPMENT OF THE DRAG REDUCTION SYSTEM FOR  
GO-KART**

**JULIANOUS KETIHUS**



**Faculty of Electrical Engineering  
UNIVERSITI TEKNIKAL MALAYSIA MELAKA**

**2014**

I declare that this report entitle “Study and development of Drag Reduction System for Go-kart” is the result of my own research except as cited in the references. The report has not been accepted for any degree and is not concurrently submitted in candidature of any other degree.

Signature	:	.....
Name	:	JULIANOUS KETIHUS
Date	:	.....



اونيورسيتي تيكنيكل مليسيا ملاك

---

UNIVERSITI TEKNIKAL MALAYSIA MELAKA



To my beloved mother and father



## ACKNOWLEDGEMENT

First of all, I would like to thanks to Almighty God, who has blessed and guided me for completion of this report as a partial fulfilment for awarding the degree of Bachelor of Mechatronics Engineering at Universiti Teknikal Malaysia Melaka. A special gratitude and sincerely thanks to my project supervisor, Encik Mohd Zamzuri bin Abdul Rashid, for encouragements, guidance critics and correction for this report from the beginning until the end of this report writing.

In this special moment, I would like to express my deepest thanks to my beloved parents, Ketihus bin John and Iren binti Angkarul for their love encouragement and supports both financially and mentally that made me to finishing this report as well as my study.

Last but not least, sincere thanks to all my friends and others who have provided assistance and contributing their ideas in completing this report. Without their support and efforts to help me, this project would not have been same as presented here.

اونيورسيتي تيكنيكل مليسيا ملاك  
UNIVERSITI TEKNIKAL MALAYSIA MELAKA

## ABSTRACT

Aerodynamic is an important element that needs to be considered in designation of a race car to achieve the top speed instead of depending only on the engine horsepower. In development of race car, engineer's goal is to provide enough downforce, and minimum aerodynamic drag. The innovative of aerodynamic design affects the speed of a race car, means the more aerodynamic of the car, the faster the speed of the vehicle and vice versa. However, there are two enemies or constrains that may affect speed in race car aerodynamics which is excess in drag force and lack of downforce. The drag is the resultant force in the direction of the upstream velocity; it opposes the forward motion of the vehicle. Excess in drag (wind resistance) reducing the effectiveness of the time and requires more horsepower for the engine to achieve top speed. Lack of downforce can reduce the traction and road grip. Therefore, this paper addresses the study and development of Drag Reduction System (DRS) for go-kart, a current technology in aerodynamics world. DRS are an adjustable rear wings used in Formula One cars to facilitate overtaking by reducing the drag and at the same time reducing downforce. In order to prove this hypothesis, DRS need to be developed in this project. Then its performance is tested in simulation and real world test (static test). In the same time, front and rear wing also required to be fabricated. Development of wings and DRS begins with conducting a literature study on previous research by several experts and follow by designing wings model. Process continues with fabrication and development. The final product are tested in real world environment and simulated by using Solidworks Flow Simulation. The purpose of this tests are to obtain the performance of the final product and comparing both results in term of aerodynamics element. The reduction of both aerodynamics forces must be at least reducing lower than the initial values.

## ABSTRAK

Aerodinamik memainkan peranan penting dalam setiap kereta lumba untuk mencapai kelajuan tinggi dan tidak hanya bergantung kepada kuasa enjin. Dalam pembangunan kereta lumba, matlamat jurutera adalah untuk menghasilkan kuasa teras yang mencukupi, dan meminimumkan seretan aerodinamik. Reka bentuk aerodinamik yang inovatif memberi kesan kepada kelajuan kereta lumba, dimana jika kereta yang lebih bersifat aerodinamik, kelajuan kenderaan lebih tinggi dan begitu juga sebaliknya. Walau bagaimanapun, terdapat dua musuh kelajuan dalam aerodinamik kereta lumba, iaitu yang berlebihan dalam daya seretan dan kekurangan daya teras. Kedua-dua daya adalah kekangan utama dalam setiap kereta lumba untuk mencapai kelajuan tertinggi. Seretan adalah daya paduan yang menentang gerakan ke depan kenderaan. Berlebihan dalam seretan (rintangan angin) mengurangkan keberkesanan masa dan memerlukan lebih kuasa kuda enjin untuk mencapai kelajuan tertinggi. Kekurangan daya teras boleh mengurangkan daya tarikan dan cengkaman kereta. Oleh itu, projek ini menumpukan kajian dan pembangunan Sistem Pengurangan Drag (DRS) untuk go-kart, iaitu teknologi terkini di dunia aerodinamik. DRS adalah sayap belakang yang boleh laras digunakan dalam kereta Formula Satu untuk memudahkan memotong dengan mengurangkan seretan dan pada masa yang sama mengurangkan daya teras. Dalam usaha untuk membuktikan hipotesis ini, DRS perlu dibangunkan dalam projek ini dan menguji prestasi dalam simulasi dan ujian dunia sebenar (ujian statik). Dalam masa yang sama, sayap depan dan belakang juga perlu direka. Pembangunan sayap dan DRS bermula dengan menjalankan kajian literatur mengenai penyelidikan oleh beberapa pakar dan diikuti dengan mereka bentuk model sayap depan dan belakang. Proses berterusan dengan fabrikasi dan pembangunan. Produk akhir diuji dalam persekitaran dunia sebenar dan simulasi dengan menggunakan Solidworks Aliran Simulasi. Tujuan ini menguji adalah untuk mendapatkan prestasi produk akhir dan membandingkan kedua-dua keputusan dalam elemen-elemen aerodinamik. Pengurangan kedua-dua angkatan aerodinamik mesti sekurang-kurangnya lebih rendah daripada nilai awal.

## TABLE OF CONTENTS

<b>ACKNOWLEDGEMENT .....</b>	<b>V</b>
<b>ABSTRACT .....</b>	<b>VI</b>
<b>ABSTRAK.....</b>	<b>VII</b>
<b>TABLE OF CONTENTS.....</b>	<b>VIII</b>
<b>LIST OF TABLES .....</b>	<b>X</b>
<b>LIST OF FIGURES .....</b>	<b>XI</b>
<b>LIST OF ABBREVIATIONS.....</b>	<b>XV</b>
<b>LIST OF APPENDICES.....</b>	<b>XVI</b>
<b>CHAPTER 1 .....</b>	<b>1</b>
<b>INTRODUCTION .....</b>	<b>1</b>
1.1 Motivation.....	1
1.2 Problem Statement.....	5
1.3 Objectives .....	5
1.4 Scopes .....	6
1.5 Report Organization.....	7
<b>CHAPTER 2 .....</b>	<b>8</b>
<b>LITERATURE REVIEW .....</b>	<b>8</b>
2.1 Introduction.....	8
2.2 Analysis of information .....	9
2.3 Synthesis of information .....	12
2.4 Evaluation of infomation .....	15
<b>CHAPTER 3 .....</b>	<b>16</b>
<b>METHODOLOGY .....</b>	<b>16</b>
3.1 Introduction.....	16
3.2 Project Gantt Chart .....	18
3.3 Project Methodology Flow Chart.....	19

3.4	Fabrication Methodology Flow Chart.....	24
3.5	System Block Diagram .....	26
3.6	Process Flow Chart .....	28
3.7	Components selection .....	29
3.8	Front and Rear Wings Design.....	29
3.9	Wings Fabrication.....	30
3.10	Validity of Data.....	33
3.11	Reliability of Data.....	39
3.12	Summary .....	39
<b>CHAPTER 4</b>	<b>.....</b>	<b>40</b>
RESULTS AND DISCUSSION.....		40
4.1	Introduction.....	40
4.2	Solidworks Simulation.....	41
4.2.1	Front wing Simulation.....	41
4.2.2	Rear Wing Simulation.....	47
4.2.3	Full Scale Go-kart Simulation.....	57
4.3	Static Test (Real World Test) .....	67
4.4	Analysis.....	73
4.5	Discussion.....	87
<b>CHAPTER 5</b>	<b>.....</b>	<b>89</b>
CONCLUSION AND RECOMMENDATIONS .....		89
5.1	Introduction.....	89
5.2	Conclusion .....	89
5.3	Recommendation .....	90
<b>REFERENCES</b> .....		<b>91</b>
<b>APPENDICES</b> .....		<b>93</b>

## LIST OF TABLES

TABLE	TITLE	PAGE
2.1	Front and Rear Wing Comparison	13
2.2	Drag Force and Downforce comparison	14
3.1	Project Gantt Chart	18
3.2	Input Data Table	33
3.3	Rear Wing Size Parameter	34
3.4	Front Wing Size Parameter	34
3.5	Full Scale Size Parameter	34
4.1	Front wing Goal Plot Table Result	42
4.2	Rear Wing (DRS OFF) Goal Plot Table Result	47
4.3	Rear Wing (DRS ON) Goal Plot Table Result	52
4.4	Full Scale (DRS OFF) Goal Plot Table Result	57
4.5	Full Scale (DRS ON) Goal Plot Table Result	60
4.6	Go-kart's Front Wing Pressure Simulation Result comparison	73
4.7	DRS OFF and DRS ON of Rear Wing comparison	75
4.8	DRS ON and DRS OFF of Full Scale Go-kart comparison	80
4.9	Flow trajectories of Rear Wing comparison (Isometric View)	85
4.10	Flow trajectories of Rear Wing comparison (Side View)	85
4.11	Flow trajectories of Rear Wing comparison (Isometric View)	86

## LIST OF FIGURES

<b>FIGURE</b>	<b>TITLE</b>	<b>PAGE</b>
1.1	Drag reduction system	3
1.2	DRS Deactivated	3
1.3	DRS Activated	3
1.4	Front Wing	4
2.1	Forces acting on a car	8
2.2	Three components of aerodynamic force	11
3.1 (a)	Project flow chart (part 1)	19
3.1 (b)	Project flow chart (part 2)	21
3.1 (c)	Project flow chart (part 3)	22
3.2	Experimental and setup flow chart	24
3.3	DRS Block Diagram	26
3.4	Open-Loop DRS Block Diagram	27
3.5	Process flow chart	28
3.6	Front Wing Final Design	29
3.7	Rear Wing Final Design	30
3.8	Front Wing Fabricated using PVC Foam	30
3.9	Linkage of Servo Motor	31
3.10	DRS Control Unit	32
3.11	Canopy Tent	36
3.12	Go-kart under Static Test	36
3.13	Front Wing Dimension in millimetre (mm)	37
3.14	Rear Wing Dimension in millimetre (mm)	37
4.1	Element in Aerodynamics	40
4.2	Front Wing	42
4.3	Isometric View for Pressure Flow Trajectories	42
4.4	Front View for Pressure Flow Trajectories	43



<b>FIGURE</b>	<b>TITLE</b>	<b>PAGE</b>
4.5	Side View for Pressure Flow Trajectories	43
4.6	Top View for Pressure Flow Trajectories	44
4.7	Isometric View for Surface Plot Pressure	44
4.8	Front View for Surface Plot Pressure	45
4.9	Side View for Surface Plot Pressure	45
4.10	Top View for Surface Plot Pressure	46
4.11	Rear Wing	47
4.12	Isometric View for Pressure Flow Trajectories (DRS OFF)	48
4.13	Front View for Pressure Flow Trajectories (DRS OFF)	48
4.14	Top View for Pressure Flow Trajectories (DRS OFF)	49
4.15	Top View for Pressure Flow Trajectories (DRS OFF)	49
4.16	Isometric View for Pressure Surface Plot (DRS OFF)	50
4.17	Front View for Pressure Surface Plot (DRS OFF)	50
4.18	Side View for Pressure Surface Plot (DRS OFF)	51
4.19	Top View for Pressure Surface Plot (DRS OFF)	51
4.20	Isometric View for Pressure Flow Trajectories (DRS ON)	52
4.21	Front View for Pressure Flow Trajectories (DRS ON)	53
4.22	Top View for Pressure Flow Trajectories (DRS ON)	53
4.23	Top View for Pressure Flow Trajectories (DRS ON)	54
4.24	Isometric View for Pressure Surface Plot (DRS ON)	54
4.25	Front View for Pressure Surface Plot (DRS ON)	55
4.26	Side View for Pressure Surface Plot (DRS ON)	55
4.27	Top View for Pressure Surface Plot (DRS ON)	56
4.28	Full Scale Go-kart Solidworks Drawing	57
4.29	Isometric View for Pressure Flow Trajectories (DRS OFF)	58
4.30	Front View for Pressure Flow Trajectories (DRS OFF)	58
4.31	Side View for Pressure Flow Trajectories (DRS OFF)	59
4.32	Isometric View for Pressure Surface Plot (DRS OFF)	60
4.33	Front View for Pressure Surface Plot (DRS OFF)	60
4.34	Side View for Pressure Surface Plot (DRS OFF)	61
4.35	Top View for Pressure Surface Plot (DRS OFF)	61
4.36	Isometric View for Pressure Flow Trajectories (DRS ON)	62

<b>FIGURE</b>	<b>TITLE</b>	<b>PAGE</b>
4.37	Front View for Pressure Flow Trajectories (DRS ON)	63
4.38	Side View for Pressure Flow Trajectories (DRS ON)	63
4.39	Top View for Pressure Flow Trajectories (DRS ON)	64
4.40	Isometric View for Pressure Surface Plot (DRS ON)	65
4.41	Front View for Pressure Surface Plot (DRS ON)	65
4.42	Side View for Pressure Surface Plot (DRS ON)	66
4.43	Top View for Pressure Surface Plot (DRS ON)	66
4.44	Go-kart	67
4.45	Go-kart's Front Wing	67
4.46	Go-kart's Front Wing Testing (a)	68
4.47	Go-kart's Front Wing Testing (b)	68
4.48	Go-kart's Front Wing Testing (c)	69
4.49	Go-kart's Front Wing Testing (d)	69
4.50	Go-kart's Rear Wing	70
4.51	Go-kart's Front Wing (DRS OFF) Testing (a)	70
4.52	Go-kart's Front Wing (DRS OFF) Testing (b)	71
4.53	Go-kart's Front Wing (DRS OFF) Testing (c)	71
4.54	Go-kart's Front Wing (DRS ON) Testing (a)	72
4.55	Go-kart's Front Wing (DRS ON) Testing (b)	72
4.56	Go-kart's Front Wing (DRS ON) Testing (c)	73
4.57	Graph of Drag Force of a Rear Wing during DRS ON and DRS OFF Comparison	76
4.58	Graph of Downforce of a Rear Wing during DRS ON and DRS OFF Comparison	77
4.59	Graph of Drag Coefficient of a Rear Wing during DRS ON and DRS OFF Comparison	78
4.60	Graph of Downforce Coefficient of a Rear Wing during DRS ON and DRS OFF Comparison	79
4.61	Graph of Drag Force of a Rear Wing during DRS ON and DRS OFF Comparison	81
4.62	Graph of Downforce of a Rear Wing during DRS ON and DRS OFF Comparison	82

<b>FIGURE</b>	<b>TITLE</b>	<b>PAGE</b>
4.63	Graph of Drag Coefficient of a Rear Wing during DRS ON and DRS OFF Comparison	63
4.64	Graph of Drag Force of a Rear Wing during DRS ON and DRS OFF Comparison	64
A1	Front wing solidworks drawing dimension	94
A2	Front wing solidworks drawing dimension	95
A3	Rear wing solidworks drawing dimension	96
A4	Rear wing solidworks drawing dimension	97
C1	Circuit Diagram	102
C2	Circuit Schematic	102



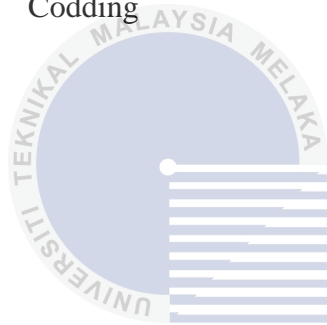
## LIST OF ABBREVIATIONS

- DRS - Drag Reduction System  
FYP - Final Year Project



**LIST OF APPENDICES**

<b>APPENDIX</b>	<b>TITLE</b>	<b>PAGE</b>
A	Solidworks Drawing	93
B	Turnitin Report	98
C	Circuit Design	100
D	Codding	102



اونيورسيتي تيكنيكل مليسيا ملاك

UNIVERSITI TEKNIKAL MALAYSIA MELAKA



# CHAPTER 1

## INTRODUCTION

### 1.1 Motivation

Aerodynamic plays important role in every race car to achieve the top speed instead of depend only on the engine horsepower. The innovative of aerodynamic design affects the speed of a race car, means the more aerodynamic of the car, the faster the speed of the vehicle and vice versa. The most important in aerodynamic research and development is to produce downforce, minimum aerodynamic drag and good directional stability [1]. The aim of every aerodynamic research is to channel the airflows perfectly through the car body, in order to generate as much downforce as possible; therefore the downforce will thrust the car down to onto the road and decreasing the clearance between the lower body parts to the road. This permits shorter braking distance and higher cornering speed [2].

The rear wing and front wing are crucial components for the performance of a race car that aims to reduce the lift and drag force on the car. The rear wing of a race car contribute approximately a third of the car's total downforce [2]. Basically rear wing consist of two sets of aerofoil connected to each other by the wing endplate. The angle between this aerofoil will affect the downforce and drag force of a car. Thus adjustable rear wing is the solution for this matter in order to adjust the angle between aerofoil automatically in certain condition. The front wing has a lot constrain too like the rear wing. Front wing produce in drag force which improving the car stability, especially in high speed cornering [2].

According to [3], DRS are adjustable rear wings used in Formula One cars for facilitate overtaking only. The DRS consists of two elements which is the main plane and the flap. The main plane remains fixed and the flap is adjustable which able to pivot between 10mm to 50mm from the main plane. DRS can be activated and deactivated depending on several conditions. When the DRS is activated, the flap wing at 50mm distance from main plane and when disabled, the flap wing returns to original position, 10mm from main plane as shown in Figure 1.1. However, DRS can be activated only for overtaking in a straight line condition. When the flap wing at 10mm position from main plane (DRS deactivate), the air stream ideally connected with wing contours and without any turbulence as shown in Figure 1.2. This provides the car with full of downforce efficiency and improving level of grip (stability). At the 50mm away from the main plane (DRS activate), both wings stop acting in harmony and airflow around the wing separated as shown in Figure 1.3. This condition decreasing the effectiveness of the wings (downforce decrease) and reduce drag force, but in the same time improving the straight line speeds of the car. Decrease in downforce can cause the handling to change from understeer to oversteer (car losing stability). This is the reason why DRS only can be activated during overtaking in straight line but not in cornering condition. During high speed cornering, car required more downforce to increase car's stability (grip).

اويونرسيتي تيكنيكل مليسيا ملاك

UNIVERSITI TEKNIKAL MALAYSIA MELAKA



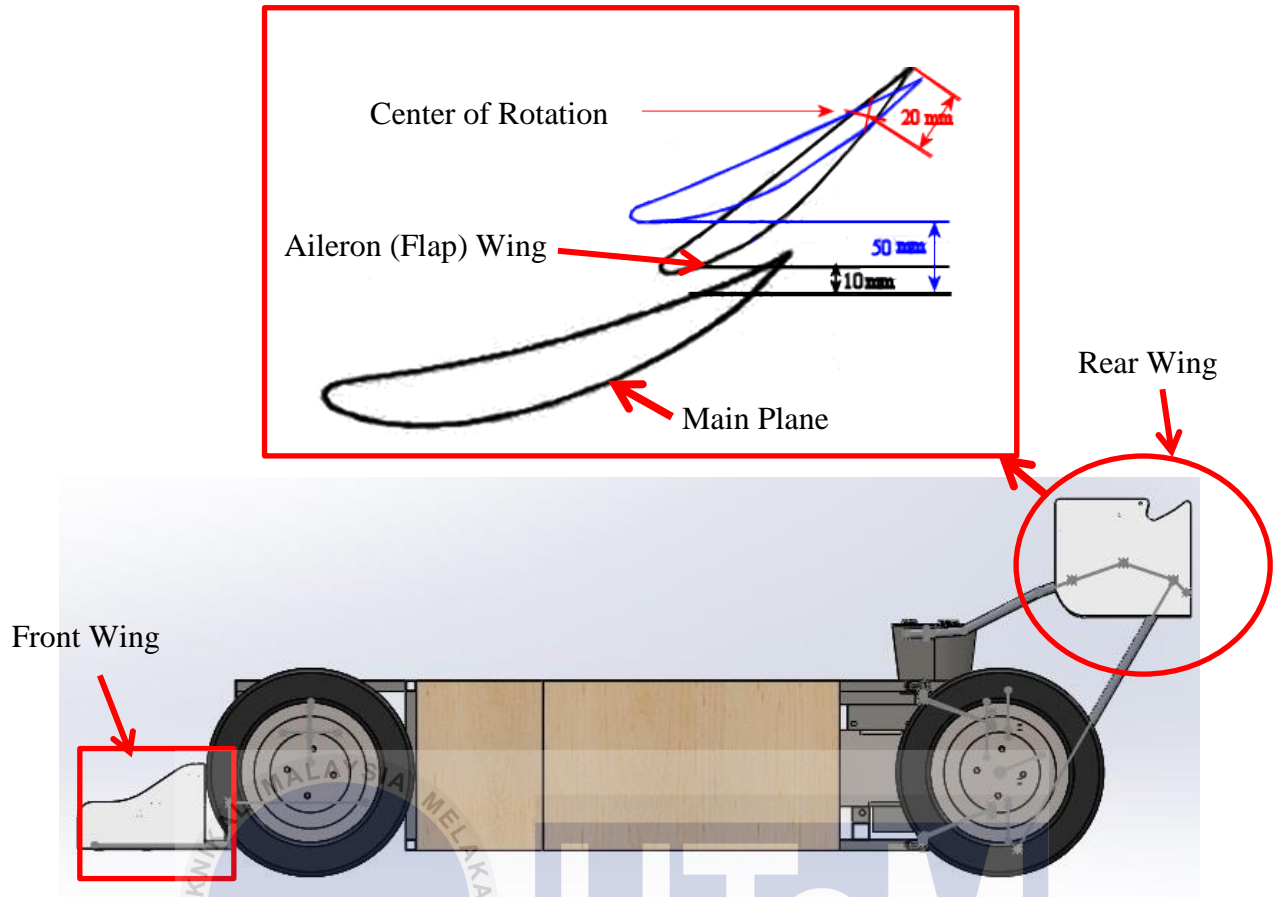


Figure 1.1: Drag Reduction System

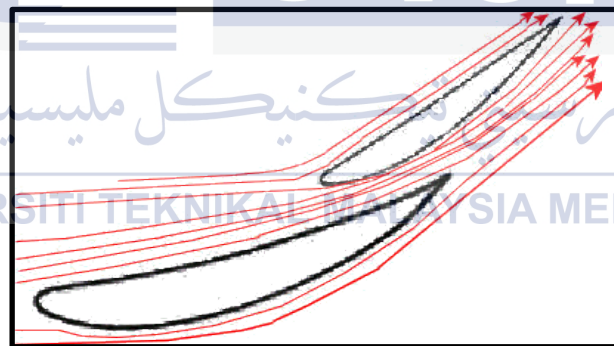


Figure 1.2: DRS deactivated [3]

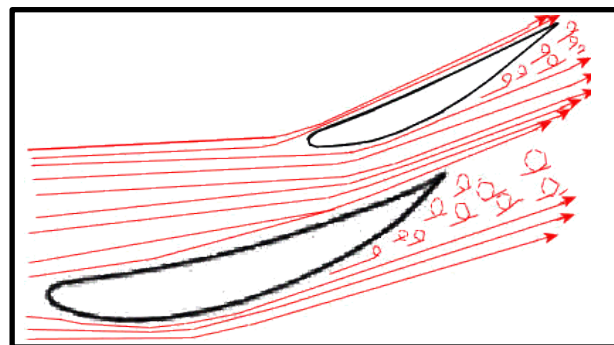


Figure 1.3: DRS activated [3]

This project is about a drag reduction system (DRS) for go-kart. The rear wing DRS capable to improve the straight line speed of race car. The front wing aerodynamic design allows increasing the downforce of the race car. This system capable to reduce the aerodynamic drag force to generate more stream line speed and improve car's handling stability. This DRS has two set of aerofoil (main plane and flap wing) connected to each other by the wing endplate and an actuator. The flap (aileron) wing can rotate only between 10mm to 50mm from the main plane. The flap rotate by using actuator that control by the driver. The front wing, which is responsible to produce downforce consist of deflector, fin, and main plane as shown in Figure 1.4.

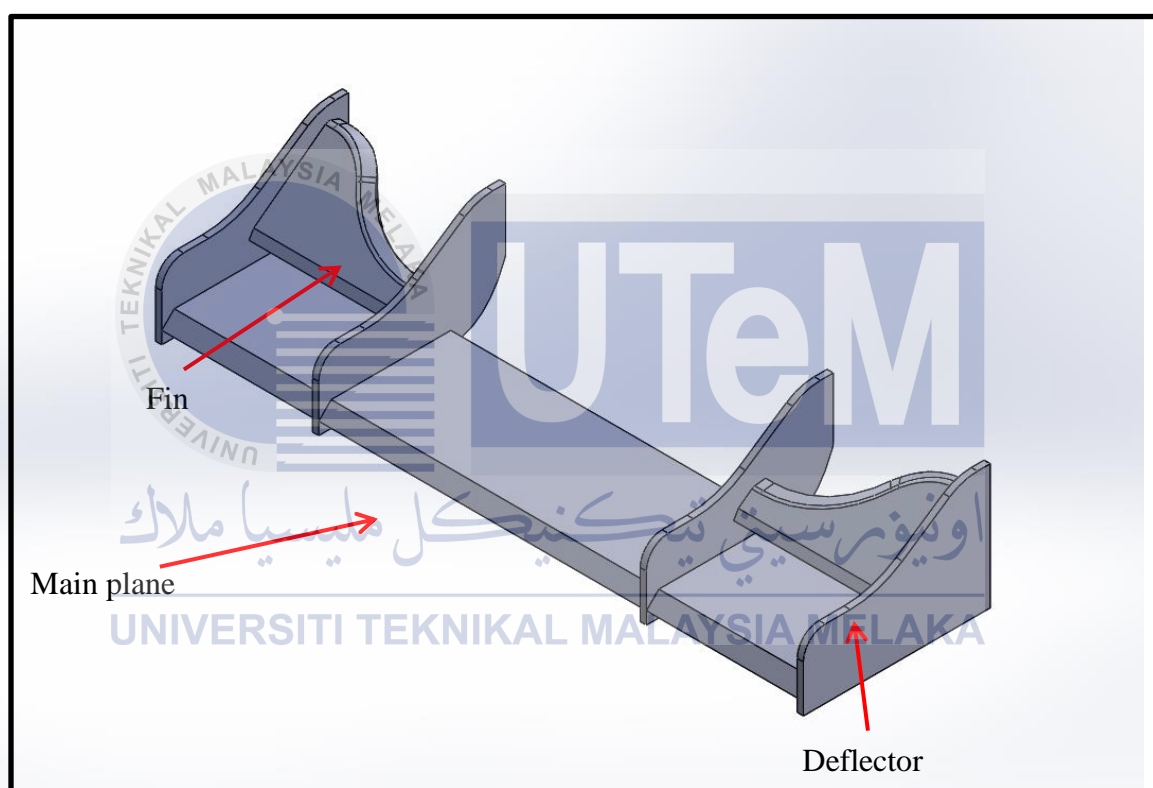


Figure 1.4: Front Wing

. The front and rear wing are designed by using Solidworks software. The aerodynamic flow motions of this wing are simulated by using Solidworks Flow Simulation software to yield aerodynamics forces and coefficients. These wings are built using PVC foam. The actuator to actuate the flap wing is controlled by using on/off control circuit.

## 1.2 Problem Statement

The purpose of DRS is to improve speed of a race car during overtaking situation. However, there are two enemies of speed in race car aerodynamics which is excess in drag force and lack of downforce. These two forces are the main constrain in every race car in order to achieve top speed. The drag is the resultant force in the direction of the upstream velocity [5], it opposes the forward motion of the vehicle. Excess in drag (wind resistance) reducing the effectiveness of the time and required more engine horsepower to achieve top speed. Lack of downforce can reduce the traction and road grip [3]. This reduction on tire traction can be very dangerous during the race car is braking or cornering. Oversteers will occurs if there is little grip at the rear of the car compare to the front. The main problem in aerodynamic design of a race car is how to provide sufficient downforce as well as minimum aerodynamic drag. Therefore, the current concern in this project is about on how to balance the downforce and aerodynamic drag. In order to balance these forces, a fundamental engineering knowledge of aerodynamics is essential as well as the downforce and drag force theories.

## 1.3 Objectives

The objectives of this project are listed as follows:

1. To study aerodynamic front and rear wings for go-kart in term drag force and downforce.
2. To develop the go-kart Drag Reduction System (DRS) and test its performance in term of aerodynamics element (drag force, downforce, drag coefficient, downforce coefficient) using simulation software and static test (real world test).
3. To develop and fabricate the front and rear wings for go-kart.

## 1.4 Scopes

The scopes of the project are summarized as follows:

1. This study concentrates on front and rear wings only and does not include study into other aerodynamic devices such as diffusers, venturies and body part.
2. Testing of the wings is limited to the analysis using Solidworks Flow simulation software and static test only.
3. The development of adjustable/actuated wing (DRS) only for the rear wing.
4. This study does not include material study or constructability analysis. Manufacturing consideration will be ignored in this study.
5. The controller to control DRS is by using Arduino controller.



## 1.5 Report Organization

This report is organized as follows:

### **Chapter 1 Introduction**

Chapter one explains the main idea of this project including the problem statement, objective and scopes of project.

### **Chapter 2 Literature Review**

This chapter discussed the published information in a particular subject from related journals or conferences papers.

### **Chapter 3 Methodology**

Chapter three is the part where the design and executed this project research. All relevant experimental and descriptive techniques used in the project outlined. In this chapter, literature divides to three parts such as front wing, rear wing and aerodynamic wing shape.

### **Chapter 4 Result and Discussion**

This chapter provide and show this project system design, system parameter, system simulation parameter and the simulation outcome. The finding presents in table, pictures and three-dimensional drawing.

### **Chapter 5 Conclusion and Recommendation**

In last chapter, contains a brief summary of this overall project including methods, results and major conclusions. The recommendation for future project also included.

## CHAPTER 2

### LITERATURE REVIEW

#### 2.1 Introduction

In the previous chapter, the main ideas for this project explained in detail in the introduction section which covers the objectives, problem statements and scopes of this project. In this chapter, the literature review will be discussed from journals or conference papers which related to this project. The important information on a particular subject will be extracted from these papers. In this literature review, the area that will be discussed focuses on parameter in aerodynamics.

As stated in paper [6], all of the moving vehicle components are in some way affected by the motion of air surrounding them. This creates a drag force which has a negative impact on the vehicle. On Figure 2.1, forces acting on a car are shown. Modifying of adding lifting surfaces onto the vehicle's body can generate aerodynamic downforce and reduce drag force.

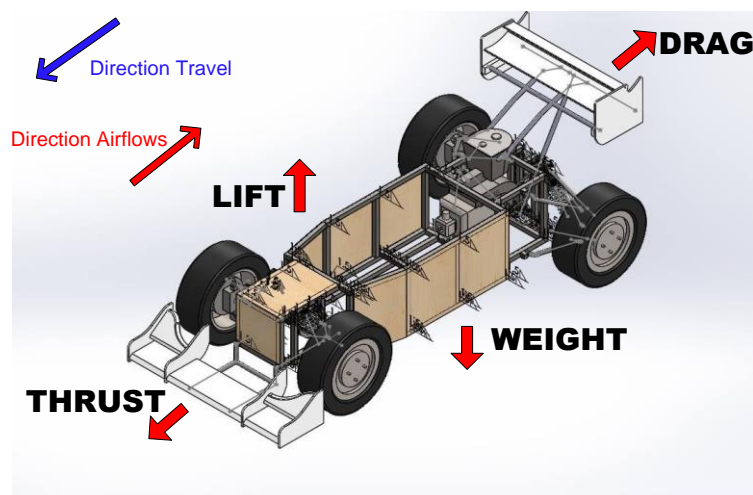


Figure 2.1: Forces acting on a car

## 2.2 Analysis of information

### 2.2.1 Rear Wing

In the paper made by [6], the rear wing is the most crucial and important parts of the aerodynamic platform of the race car to increase downforce at various road circumstance at high speed. In another paper done by [7], rear wing capable to reduce the lift of a car by improving the car rear flow field, supplying the right air pressure to the car and improving the downforce in the rear of the car. In this paper, the authors also stated that by installing rear wing to improve the distribution on the car surface pressure will reduce the aerodynamic lift effectively. In the next paper done by [8] described a maximum allowable wing plane area of 1.4m (span) by 0.65m (chord), or  $0.91\text{m}^2$ , with this parameter the performance range is categorised as “high lift and rely on multi-element design. In paper done by [9] explained that rear wing consists of two aerofoils connected each other by the wing endplate. The angle between this aerofoil will affect the performance of a car where more wing angle may result increasing in downforce and produce more drag, if the angle small, the drag force will decrease and increasing in speed of a car.

### 2.2.2 Front wing

In the paper done by [9], authors stated that the closer the front wing to the ground, the more downforce will be produced thus this phenomena will improve car stability during high speed cornering. In same paper, author claim that the front wing is designed to give the vehicle downforce directed at the front tires as well as to direct the airflow over the body, as it is the first thing that comes to contact with oncoming airflow. In another paper done by [10], when the height of front wing between 70-100mm, its will generate 20-30 percent of the car downforce. From the paper [11], the result from the performance of both single element and dual element of wings in ground effect experiment provides a good estimation of the lift and drag coefficient achievable. When the front wing operates in clean flow, the lift coefficient required about -3.4. In paper done by [12], an assumption has made that the desired aerodynamic centre of pressure location is 76mm behind the car centre of gravity.

### 2.2.3 Aerodynamic wing shape

In the paper done by [13], the authors study on the design optimization of the aerodynamic rear wing by using a fully automatic computer program to generate the shape of the rear wing. An optimization project determined which is 6.0% more downforce and 5.0% less aerodynamic drag. In paper done by [14], the authors study the airflow using Artificial Neural Network (ANN) method. This method proved to be effective and efficient. This method is effective because this method able to collect all earlier designs from an archive data and all data design results can strengthen the database, which is a beneficial experience for subsequent designs. Next, in paper done by [15], author studied the development of a Nonuniform Rational B-Spline (NURBS) based wing design optimization system. The optimization technique which combine computational fluid dynamic (CFD) and numerical optimization is very beneficial in generating optimum aerodynamic shapes. In same paper [15], authors discussed the drag minimization with a lift constraint for the design optimization problem where the initial design will undergo optimization method until generates the optimum aerodynamic shape. In addition, paper done by [16], this paper is study the computational method for aerodynamic shape design which is one of major application of high performance computing. The new formulations to solve the inverse problem for determining the shape of plural wings. This formulation concept provide the mathematical model which relates geometrical correction to pressure differences. Prandtl-Glauert transformation and Green's theorem formula is applied to solve inverse problems.



### 2.2.4 Downforce and drag force

In the paper done by [17], downforce generated by the wings give better traction to the car, but in the same time limit its top speed as the shapes of the wings generate more drag. Next, in paper done by [18], when the wings generate downforce, wings also create drag where drag force usually smaller than the downforce. In the same paper, downforce contributes to major improvements in race car performance, especially on tracks with numerous high-speed unbanked turns as well as increases the tires' cornering ability. Moreover, in paper done by [19], downforce (aerodynamic grip), works in conjunction with mechanical grip to improve the acceleration, cornering speed and braking of the car. In another paper done by [20], pressure drag is due to a net imbalanced of surface pressure acting in the streamwise direction. In the same paper, friction drag is due to the net effect of shear stress action on the surface of the object in the streamwise direction. Both can be influenced by Reynolds number, body geometry, and flow separation.

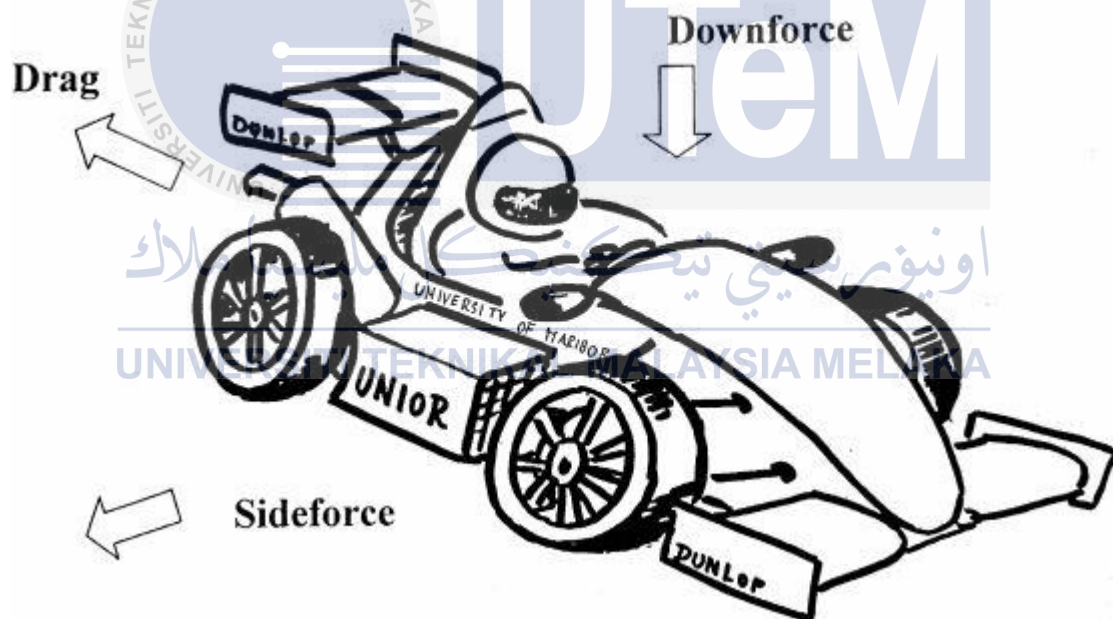


Figure 2.2: Three components of aerodynamic force [11]

## 2.3 Synthesis of information

### 2.3.1 Wing selection

There is a board range of designs, sizes, and shapes of the wings, a consequence of a lack design constraints. Studies have shown that the best aerofoil profile for racing application is with high lift to drag coefficient. There are several parameters need to be consider in order to identifying the wing's positions and orientations, these are as follows:

- a. The angle of attack and length of chord of both elements (for multi-element wing)
- b. The horizontal distance between the noses of each elements
- c. The vertical distance between the tail of the main element and the lower of the flap (between main plane and flap wing)

There are some approaches which can be taken at this point of the design process and the first is to find the main parameters and find their near-optimal values. By analyse the design using Computational Fluid Dynamic (CFD), these can produce clearer and more accurate results.

In aerodynamics package, there are two types of configuration; the single wing and double/dual wing configuration. The single wing configuration consists of only rear wing attached to the rear. These configurations are not suitable used in high speed condition. Double/dual wing configuration consists of a rear and front wing, thus providing a complex aerodynamics system to the race car

Table 2.1: Front and Rear Wing Comparison

	Front Wing	Rear Wing
Similarity	Improving downforce effect and reducing drag force	
Differences	<p>Front wing has the potential to operate in ground effect, a phenomena which is useful to the production of downforce with minimal drag. Front wing consist more component compare to rear wing. Front wing consist of base plate, diffuser, fins, winglet, and endplate. Base plate is designed to help in streamlining the flow of the under-body air away from front wheels. Deflectors also have same function of streamlining the air around the front wheels on the upper-body side [2].</p>	<p>Rear wing comprised of two sets of aerofoils connected each other by wing endplate. Upper aerofoil provides the most downforce, while the lower aerofoil provides some downforce. However, lower aerofoil creates a low-pressure region below the wing to help the diffuser create more downforce below the car [2].</p>
Relationship	<p>In order to produce aerodynamic balance to the race car, both of these wings is needed. If one of this wing absence, the car will be lost of balance and eventually effect car's manoeuvrability in term of speeding, turning and braking.</p>	

### 2.3.2 Drag force and downforce

Drag and downforce are generated perpendicularly to the direction of travel of every moving object. The drag is the resultant force in the direction of the upstream velocity [5], it opposes the forward motion of the vehicle. Downforce is net force acting on the moving object perpendicular to the motion of a fluid, which is created by different pressure.

Drag force formulae,  $f_D = \text{total drag force} = \frac{1}{2}\rho v^2 AC_d v$ . [18]

Downforce,  $f_L = \text{total downforce} = \frac{1}{2}\rho v^2 AC_d v$ . [18]

Where  $A$  is usually the frontal area, the projected area seen by a person looking toward the object from a direction parallel to the upstream velocity,  $v$ . Density of air,  $\rho$ . Coefficient of drag,  $C_d$ .

Table 2.2: Drag Force and Downforce Comparison

	Drag Force	Downforce
Similarity	The components of aerodynamic force acting on car	
Differences	Drag force is a resultant force in the direction of the upstream velocity and opposes the forward motion of the vehicle [5]. Drag force affects the power available to accelerate the car to top speed.	Downforce is a negative lift forces that acting against the gravity. Downforce contributes to major improvements in race car performance, especially on tracks with numerous high-speed unbanked turns as well as increases the tires' cornering ability.
Relationship	Change in amount of downforce also affecting the amount of drag force [2]. More wing angle increases the downforce as well as produce more drag, thus reducing the car's top speed.	

## 2.4 Evaluation of information

This chapter explained the important theory and information in aerodynamics. From these literature reviews, the studies from several papers proved that the front wing and rear wing help producing downforces on the race car. When one of these wings absence or destroyed, the vertical force distribution on the race car may change dramatically and will greatly affect its manoeuvrability particularly when speeding, cornering and braking. Reduce in drag force improve the acceleration of the race car. In the same time, race able to achieve the top speed and does not required addition horse power. The main objective and aim of race car aerodynamics is to generate enough downforce and least possible drag force. In my opinion, in order to reduce the drag force, the designs of the race car body have to be more streamlines and more aerodynamics. However, reducing in drag force must be compensated with a tremendous trade off in traction and road grip. By using Drag Reduction System (DRS), performance of a race car can be improved in term of acceleration especially in overtaking purpose. However, this system can be only used in certain condition and only in straight line track. Next chapter discuss the methodology of this study.

## CHAPTER 3

### METHODOLOGY

#### 3.1 Introduction

In previous chapter, the summary of journals explained based on particular subjects area such as front wing, rear wing, downforce and drag force, and aerodynamic shape of wing. This chapter will discuss and explain the project methodology in more detail and technically.

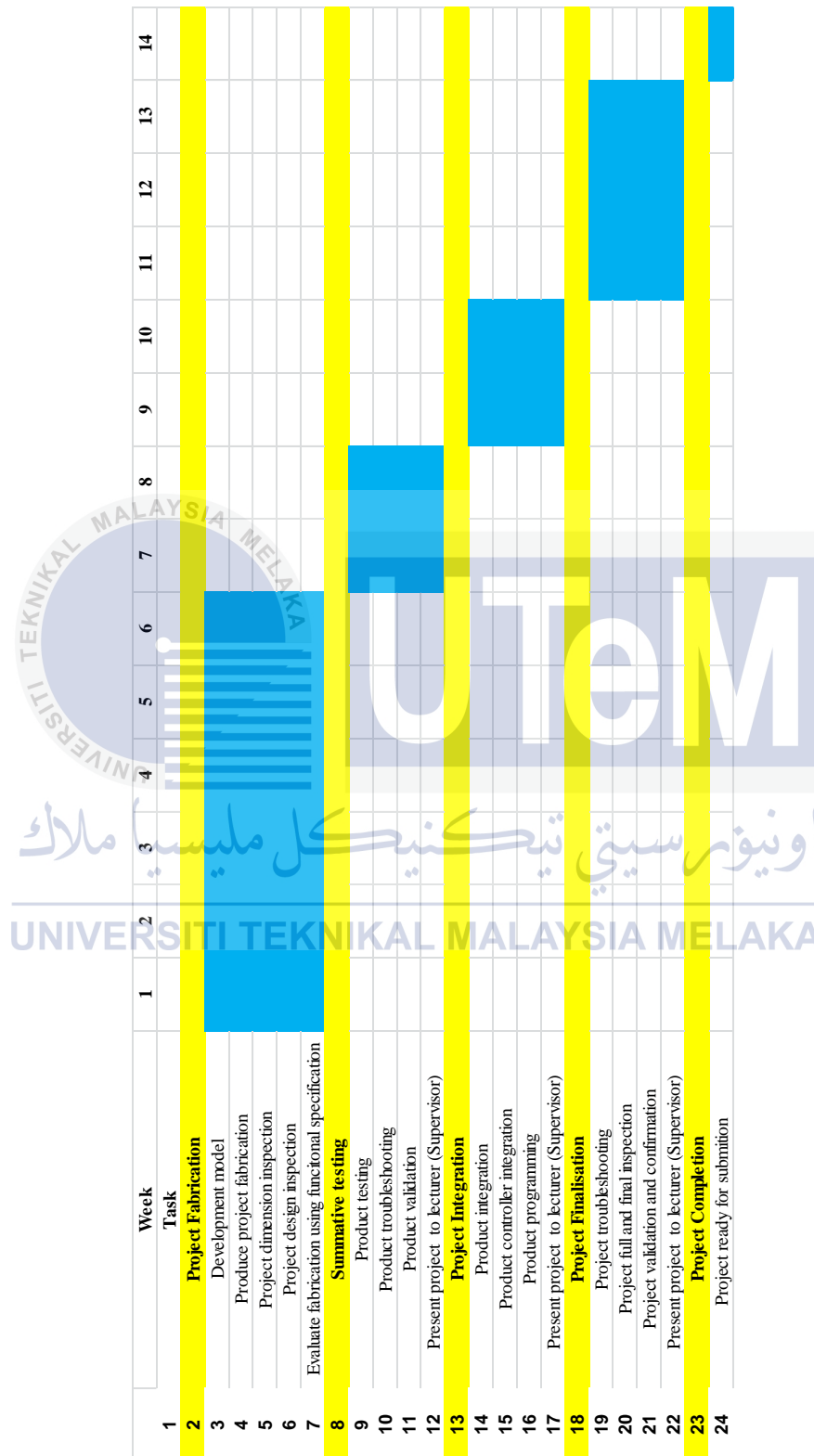
In this study, subjects that need to be measure is the drag force and the downforce produce by the wings. The lift (negative downforce) and drag force inversely proportional to each other [2]. In order to perform the measurement, the 3-Dimensional drawings of front and rear wing need to be draw as well as develop the wings actual model with DRS technology for this study. The outcomes of this study are measured in the open - loop system. Basically, there are three main research tools available for studying aerodynamics effect on a race car; full scale track tests, simulation and wind tunnel model tests. However, due to several constrain in term of high cost and other factors by using a wind tunnel, this method not be used in this project. Therefore, in this project the study on aerodynamic effect only will be done using simulation and static tests in real world. A tool to perform this measurement is by using Solidworks Flow Simulation to yield the values of the force in Newton (N) of drag as well as the drag force.

The measurement of this study will base on outcomes from the simulation. The experimental procedure shown in Figure 3.2 and procedure of the experiment briefly explained. The main purpose of adding aerodynamic external body work and DRS in the race car is to improve the car stability in high speed cornering as well as improve the straight line speed.



### 3.2 Project Gantt Chart

Table 3.1: Project Gantt Chart





### 3.3 Project Methodology Flow Chart

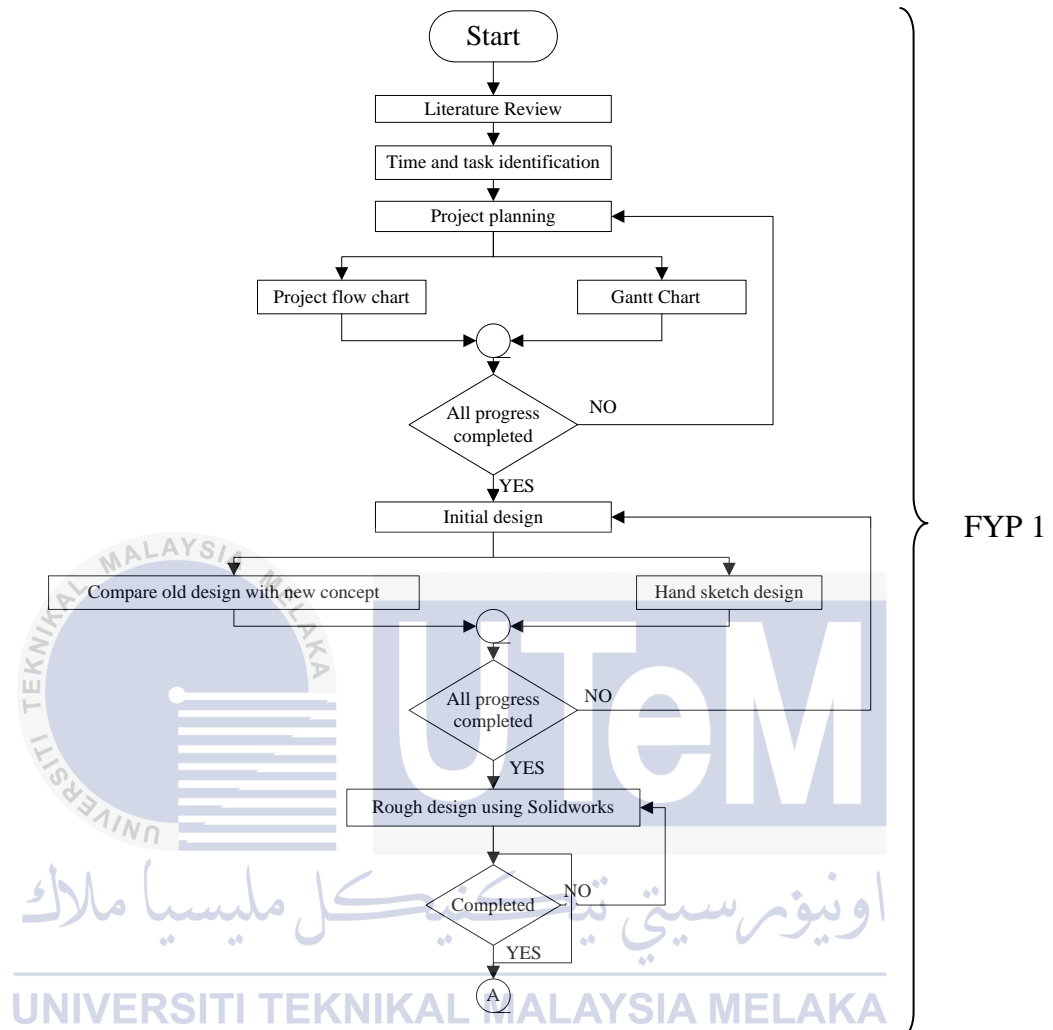


Figure 3.1(a): Project flow chart (part 1)

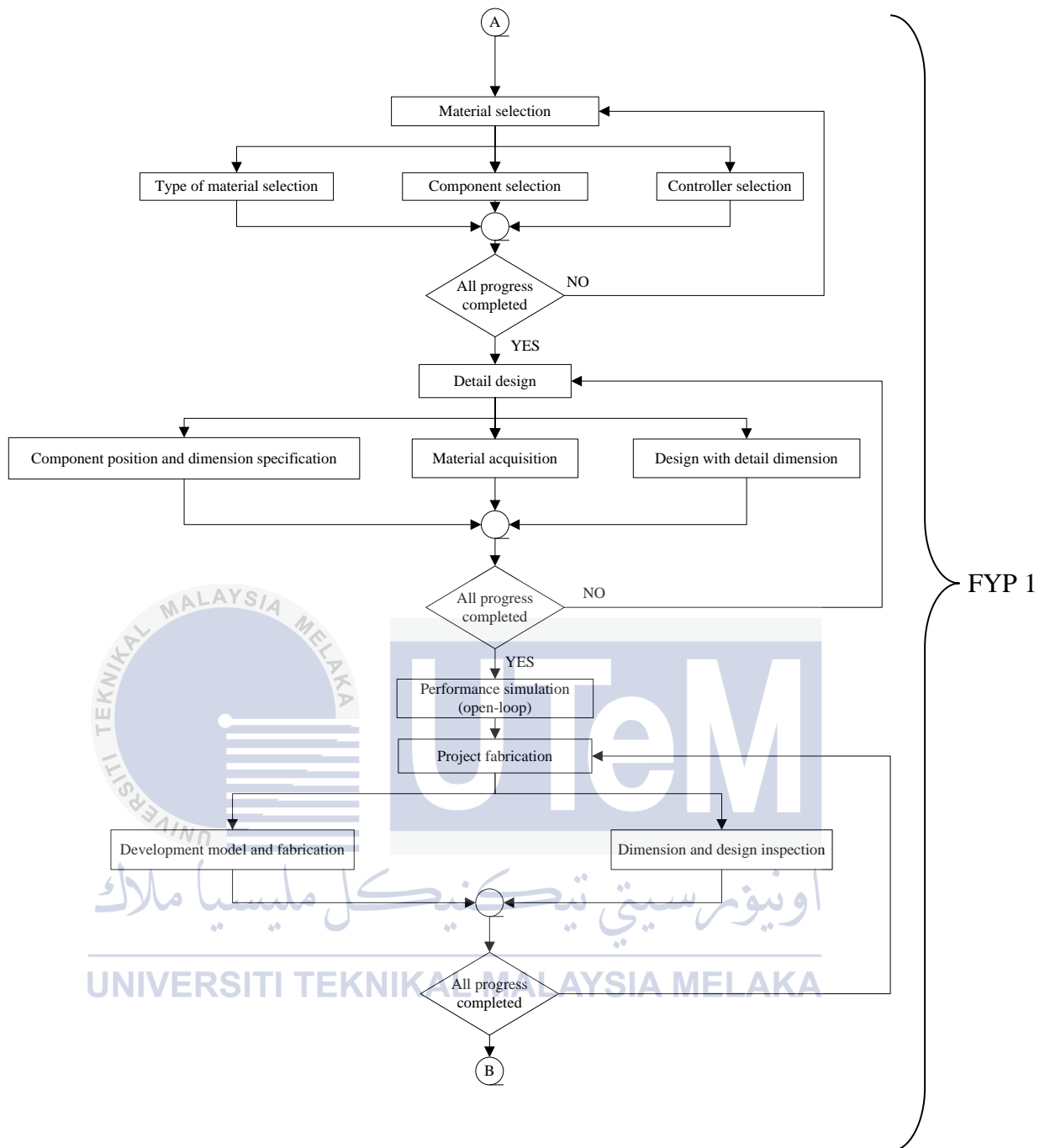


Figure 3.1 (b): Project flow chart (part 2)

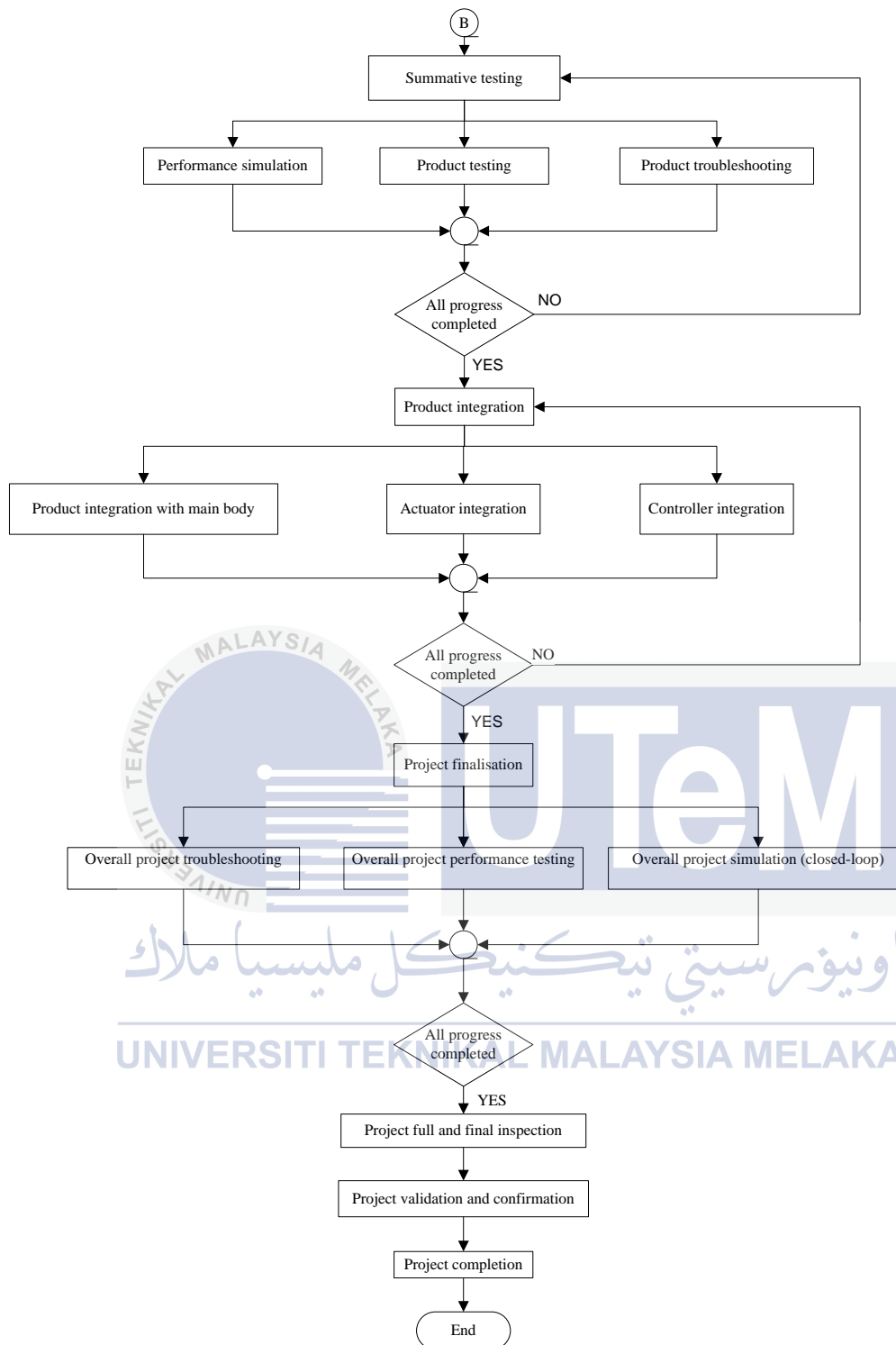


Figure 3.1 (c): Project flow chart (part 3)

Figure 3.1 (a) and 3.1 (b) shows the flow chart for the Final Year Project (FYP) 1. In the beginning, this project starts with literature review that focuses on parameter in aerodynamic. The purpose of the literature review is to summarize and synthesize the idea from others research. After literature review has been completed, task identification had been made to determine in detail the task and subtask that be performed. The goal and objective also determine in task identification. Then, after doing with task identification, project planning has been made to determine the project flow chart and Gantt chart. Project flow chart is to define the flow of task from beginning until the completion of this project, while Gantt chart is the time frame for this project. After the project planning has been completed, initial design of front and rear wings starts with doing hand sketching design of the project and at the same time comparing the old design with new concepts. Next, the process continues with doing rough design using Solidworks software to draw in 3-dimensional drawing. From the Solidworks drawing, the image of the front and rear wings can be seen more detail and ease to do material selection. Then, the process continued by selecting materials and components needed as well as to select the controller for this project. After all the selection completed, the process continues by detailing the design of the wings such as identifying the component position with detail dimension and material acquisition. After all the process completed, the final design is simulated to identify the performance of the both wings using Solidworks Flow Simulation software. In this simulation, performance only considered the open-loop parameter. After the performance fulfilled the objective and requirements of this project, a process continued by doing fabrication on the front and rear wings. After finishing the fabrication process, inspection in dimension and design has been done.

In Figure 3.1 (c) shows the progress in Final Year Project (FYP) 2. In FYP 2, it starts with summative testing of the wings. The test will include the performance simulation, test on the wings physical properties and troubleshooting the problem on the design of the wings. Next, after all the outcomes of the summative testing satisfies the objectives, the process continue to next process which is product integration, where the wings integrated with the main body of the go-kart as well as integration with the actuator and controller. Then, the whole go-kart undergoes project finalisation where full troubleshooting has been made. The performance of the go-kart also simulated in Solidworks Flow Trajectories simulation and also in static test run in real world environment. At final process, go-kart undergoes validation and confirmation process.



### 3.4 Fabrication Methodology Flow Chart

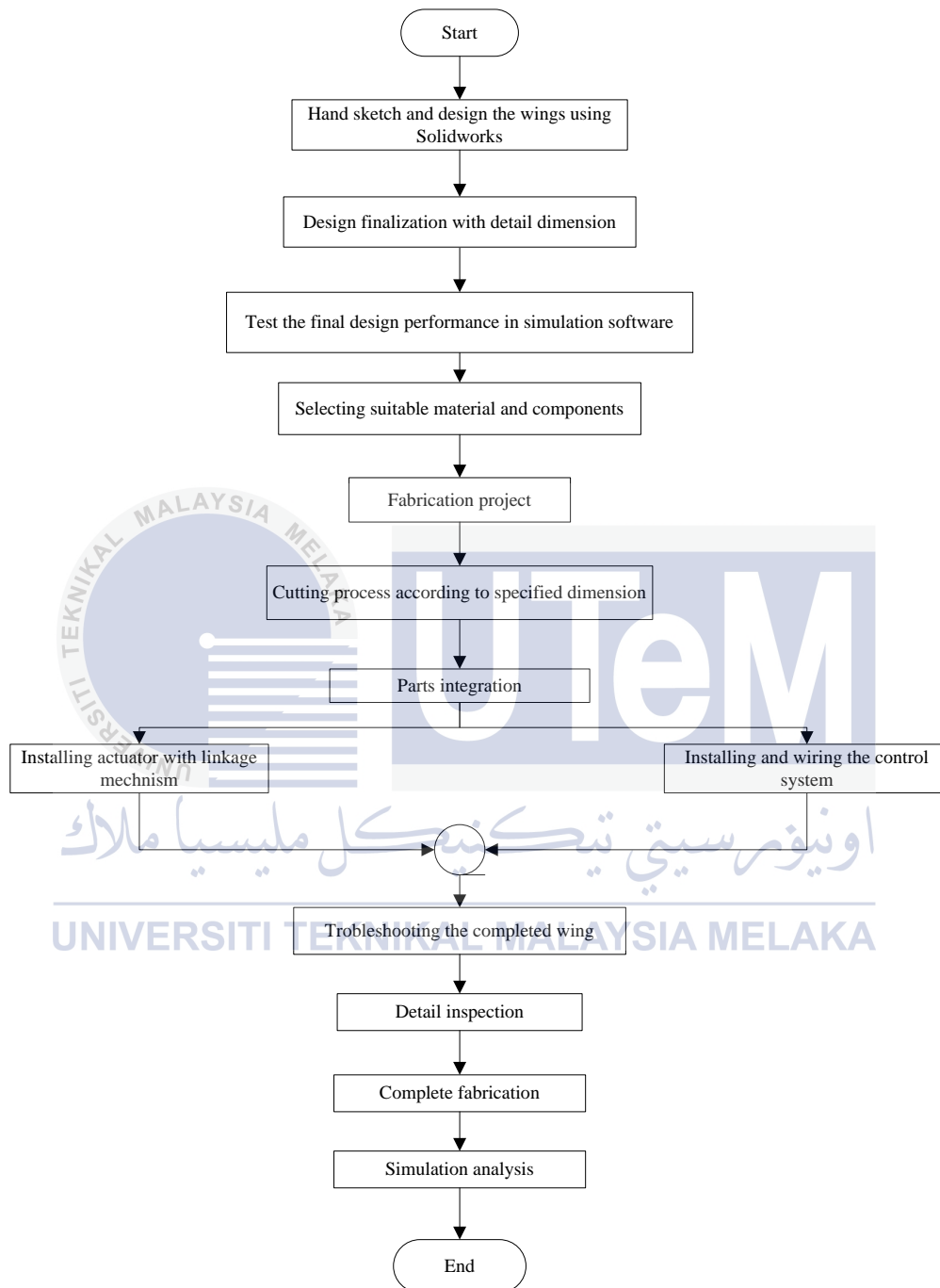
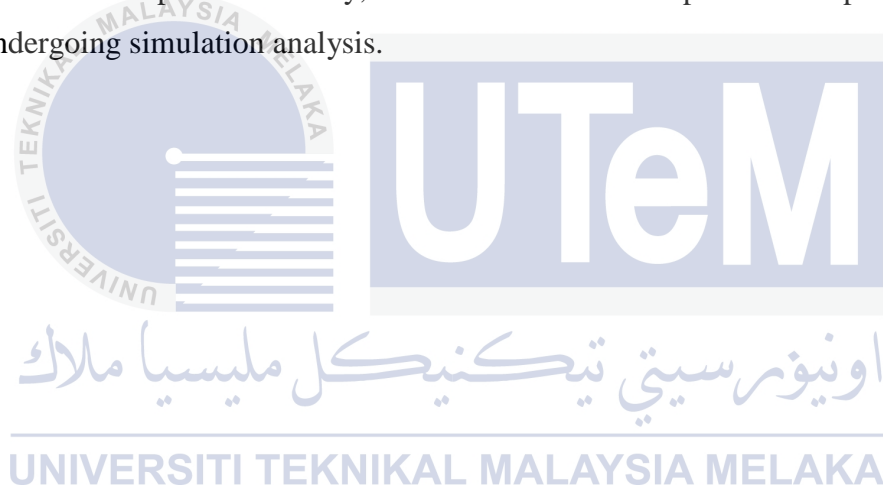


Figure 3.2: Experimental and setup flow chart

Figure 3.2 shows the experimental and setup flow chart for project fabrication. Setup starts with hand sketching then continue with a rough drawing in 3-dimensional using Solidworks software to view images in more detail. Second, the process continues with a final drawing with detail dimension. After that, the final design will simulate using Solidworks Flow Simulation software to test the performance whether it has satisfied the requirement and achieve the project objective. Next, the process proceeds with selecting the most suitable material and components for the fabrication process. After all the material and components has been finalized, the process continues with the project fabrication and the cutting process of the material will be cut according to the specified dimension. Then, after the fabrication process completed, parts integration will be take place. In parts integration, actuator will be installed with the linkage mechanism as well as the controller system. Process proceed with troubleshooting the completed wings and follow with detail inspection. Finally, after all the fabrication process complete, the wings will be undergoing simulation analysis.



### 3.5 System Block Diagram

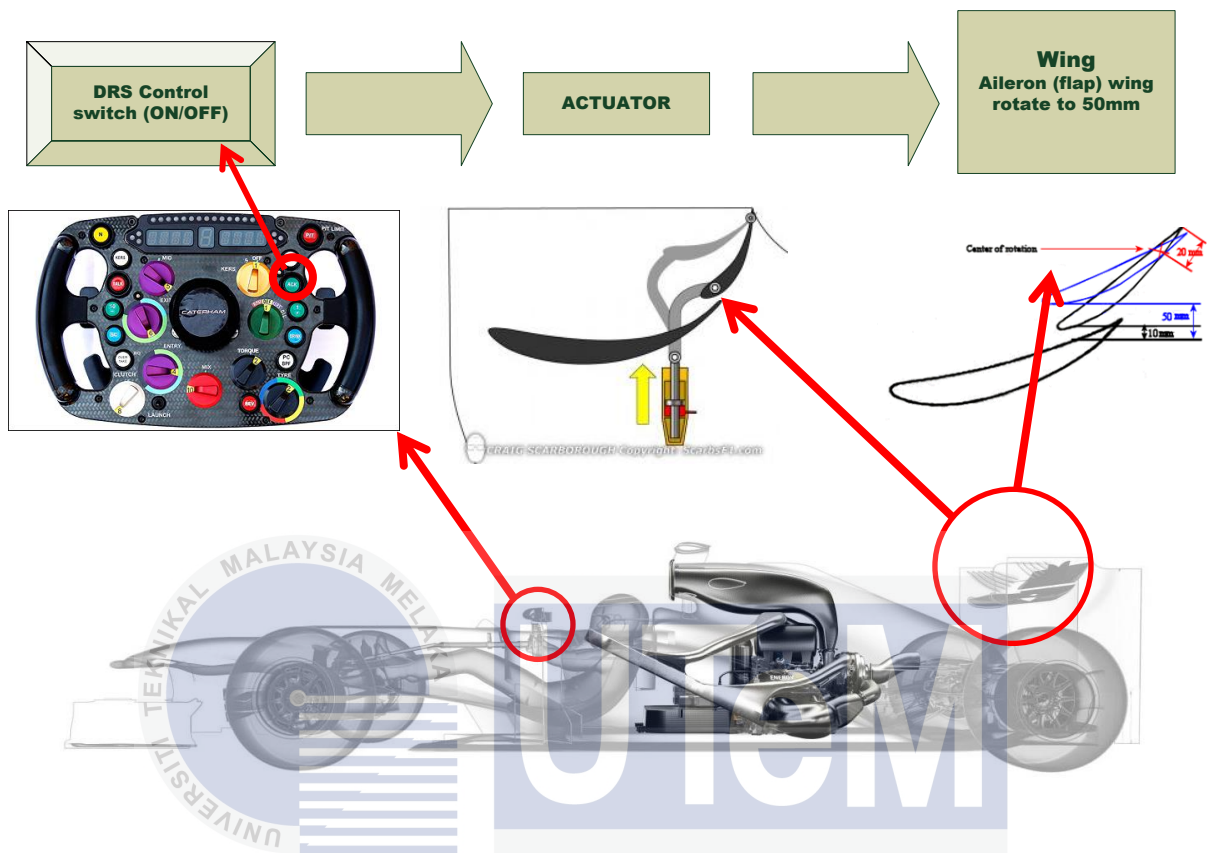


Figure 3.3: DRS Block Diagram

Figure 3.3 shows the DRS Block Diagram and how the system operates. A description of the project Block Diagram as follows:

- DRS control switch :** This control switch located on the steering wheel of a race car. The function of this control switch is to send signals either (ON/OFF) to the actuator.
- Actuator :** When actuator receives signal from input, actuator will actuate in predetermine position.
- Wing :** Initially, aileron (flap) wing at original position 10mm from main plane. When the actuator is activated, the wing will be move at the 50mm position of the main plane.



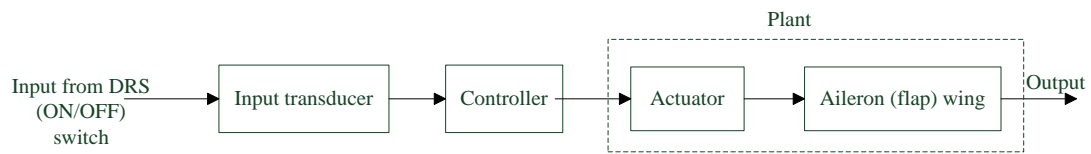


Figure 3.4: Open-Loop DRS Block Diagram

Figure 3.4 shows the generic open-loop DRS block diagram. It starts with an input from DRS (ON/OFF) control switch and the input goes to the input transducer to be converted in the form of the input to that used by the controller. The controller drives the actuator as well as the aileron (flap) wing. The controller uses electrical signal to operate the actuator. This open-loop DRS only for the FYP 1 analysis, since in this project the analysis only done by using the Solidworks Flow Simulation Software.



### 3.6 Process Flow Chart

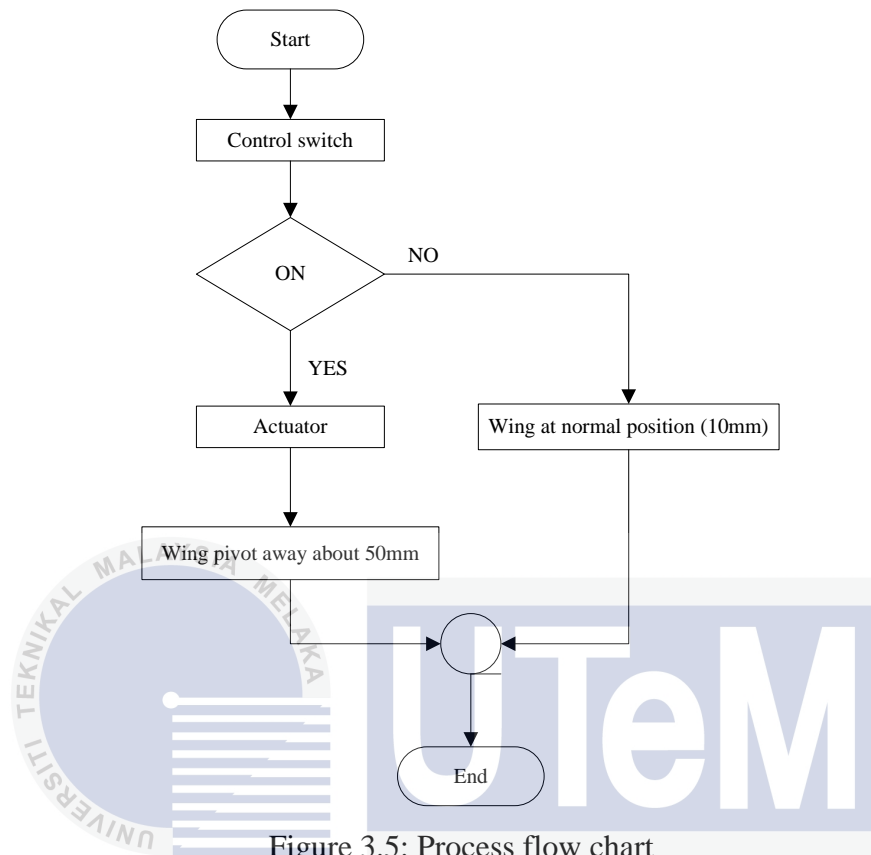


Figure 3.5: Process flow chart

A process flow chart is shown in Figure 3.5. It starts with a control switch which driving the actuator. Initially, control switches at OFF mode and wing at normal position, 10mm from the main plane. When control switches in ON condition, the controller sends signal to activate the actuator. When the actuator activated, the aileron wing moves to 50mm from main plane.

### 3.7 Components selection

Therefore, the final selection of actuator is a servo motor because of its precise control of angular position which is suitable for this project. Next, for the controller components, the most suitable is by using Arduino. Last but not least, the most suitable material for fabrication is PVC foam because this material is easy to fabricate, reasonable price compared to carbon fibre, high durability and robust compared to the FDM thermoplastic and high resistance to climate changes compared to wood.

### 3.8 Front and Rear Wings Design

The wing tiers must be able to withstand the aerodynamic forces exerted on them without significant deflection and of course without breaking. As low weight is a major concern, PVC Foam will be used. This material is enormously versatile in terms of usage, can be easily cut and fabricated, lightweight and strong.

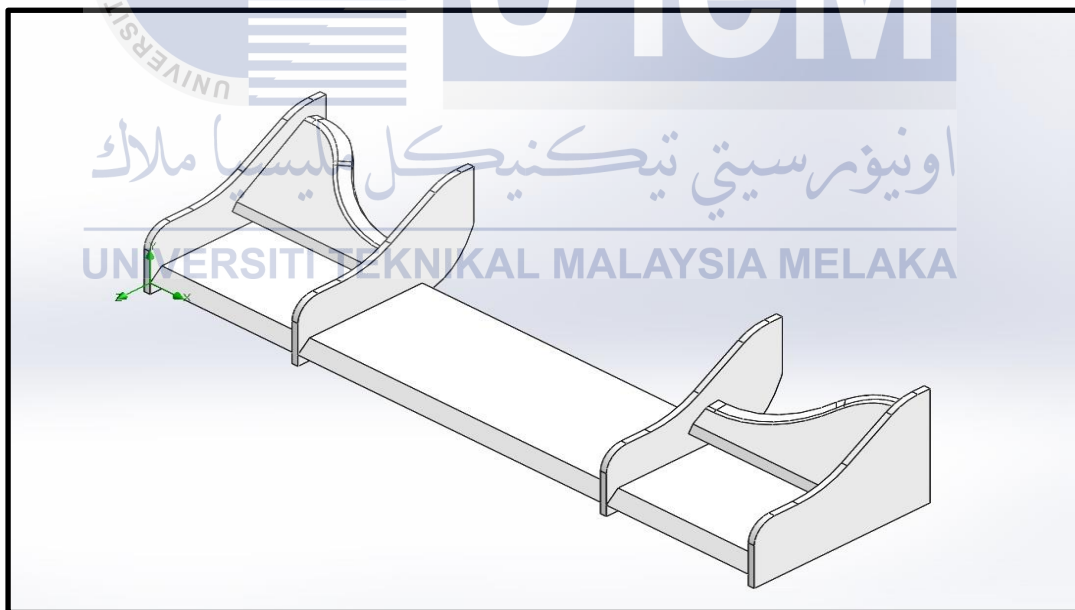


Figure 3.6: Front Wing Final Design

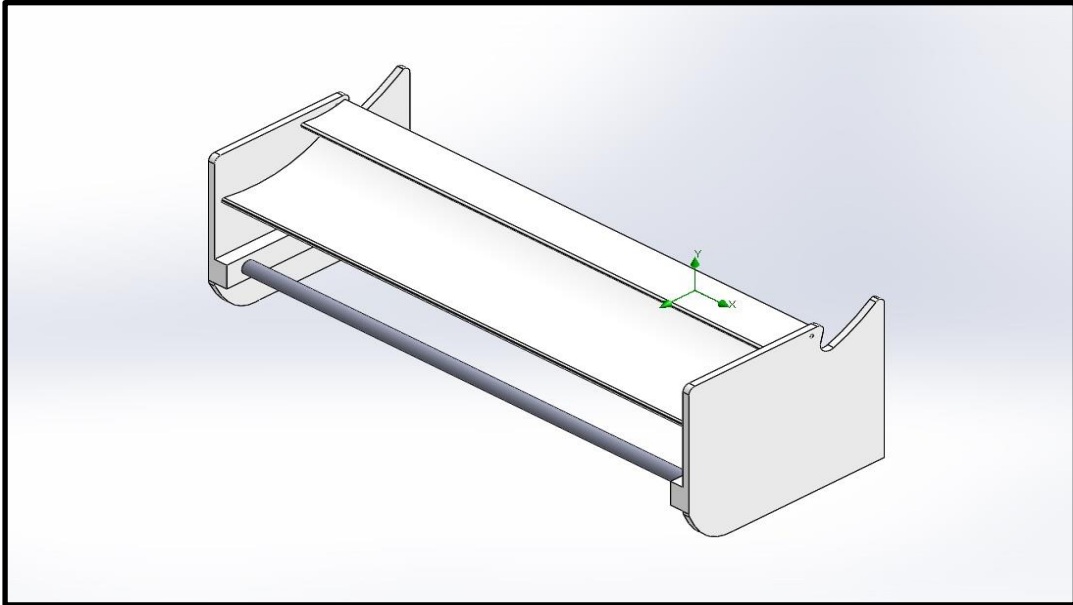


Figure 3.7: Rear Wing Final Design

### 3.9 Wings Fabrication

The wings fabricated using PVC Foam. Two dimension in thickness of PVC Form used in fabrication which is 20mm and 10mm in thickness. The main plane of both front and rear wing using 20mm PVC Form and other part of wing such as endplates using 10mm thickness.

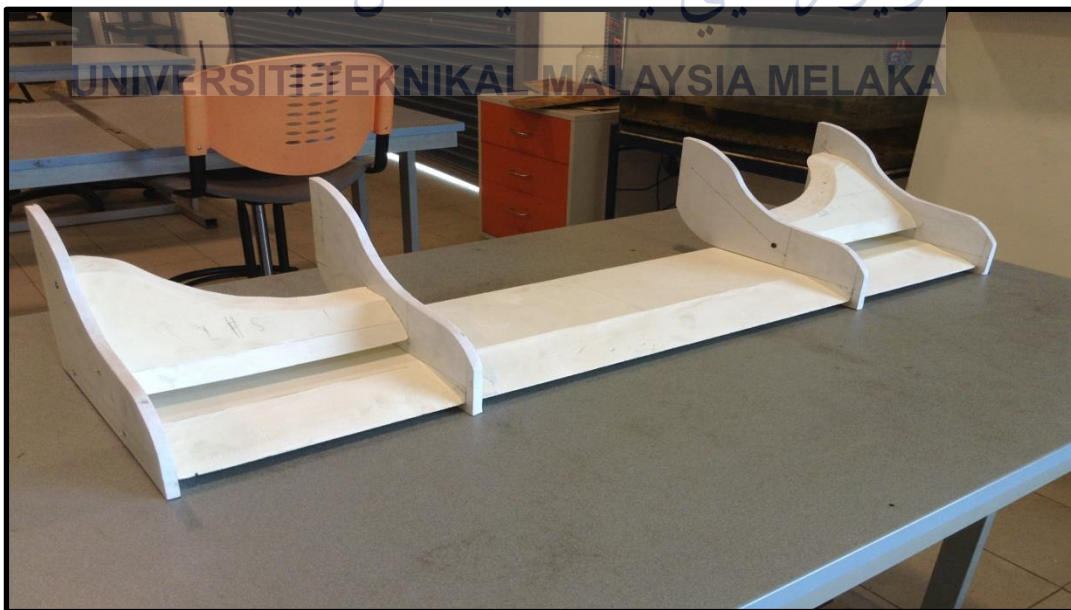


Figure 3.8: Front Wing Fabricated using PVC Foam

The links for the actuator to actuate the flap wing is using aluminium pipe 6mm in diameter. The link connected to the servo motor horn and flap wing mounting.



Figure 3.9: Linkage of Servo Motor

### 3.9.1 Tools and Equipment

Tools and equipment used in fabrications of wings are as follows:

- i. Jigsaw
- ii. Hand Grinder
- iii. Hand Driller
- iv. Pile
- v. Sand Paper
- vi. Measuring Tape
- vii. Meter Rule
- viii. L-Square
- ix. Glue Gun Kit
- x. Heavy Duty Glue
- xi. Mathematical Instruments

### 3.9.2 Controller

The controller to control DRS is by using Arduino controller. Arduino are used to control the specific angle of servo motor rotation. There are 3 input for the controller, DRS ON, DRS OFF and break. DRS ON will give signal to the servo motor rotate about  $90^\circ$  and DRS OFF about  $0^\circ$ . For break input, the flap wing will be pivot to normal position at 10mm. break input same with DRS OFF function.



Figure 3.10:

UNIVERSITI TEKNIKAL MALAYSIA MELAKA

### 3.10 Validity of Data

#### 3.10.1 Design of Experiment

##### Simulation (Solidworks Flow Simulation)

As all flow analysis is done using Solidworks Flow Simulation and design decisions will be made by utilizing its results, the model must be validated. This can be done many ways, the first of which involves configuring the model to match known experimental data, the second and third of which are real-world validation with the full scale assembly. The aims of these simulations are to obtain the drag and lift force as well as the coefficient of drag and lift. The simulation input data parameter shown as follows;

##### Input Data

##### Initial Mesh Settings

Automatic initial mesh: On

Result resolution level: 5

Advanced narrow channel refinement: Off

Refinement in solid region: Off

##### Geometry Resolution

Evaluation of minimum gap size: Automatic

Evaluation of minimum wall thickness: Automatic

##### Ambient Conditions

Table 3.2: Input Data Table

Thermodynamic parameters	Static Pressure: 101325.00 Pa Temperature: 293.20 K
Velocity parameters	Velocity vector Velocity in X direction: 0 m/s Velocity in Y direction: 0 m/s Velocity in Z direction: 33.333 m/s
Turbulence parameters	Turbulence intensity and length Intensity: 0.10 % Length: 0.009 m



## Material Settings

### Fluids

Air

### Computational Domain

Size Parameter

Table 3.3: Rear Wing Size Parameter

X min	-0.160 m
X max	1.000 m
Y min	0.170 m
Y max	0.800 m
Z min	0 m
Z max	1.000 m

Table 3.4: Front Wing Size Parameter

X min	-0.120 m
X max	1.200 m
Y min	-0.080 m
Y max	0.270 m
Z min	-0.460 m
Z max	0.170 m

Table 3.5: Full Scale Size Parameter

X min	0.110 m
X max	1.580 m
Y min	0.900 m
Y max	1.900 m
Z min	0.300 m
Z max	3.300 m

### Specifying a Global Goal

In this simulation the engineering goals are set to determine the drag force and downforce. Downforce are set to parameter Force (Y) and drag force to parameter Force (Z). Downforce are set to z-axis due to the direction of drag force are respect to z-axis. Downforce are set to y-axis due to the direction of downforce are respect to y-axis.



## Specifying an Equation Goal

Specifying equation goal is to yield the both coefficient of drag and coefficient of lift. The equations of drag and lift coefficient are as follows;

The dimensionless Drag coefficient is given by:

$$C_D = \frac{\text{Drag Force}}{\frac{1}{2}\rho v A} \quad [17] \quad (3.1)$$

The dimensionless Lift coefficient is given by:

$$C_L = \frac{\text{Lift Force}}{\frac{1}{2}\rho v A} \quad [17] \quad (3.2)$$

Where  $A$  is usually the frontal area, the projected area seen by a person looking toward the object from a direction parallel to the upstream velocity,  $v$ . Lift force and drag force can be obtained from the simulation. Density of air,  $\rho$ .

The following two equation goals were imposed in Solidworks Equation Goal:

$$(2 * \{\text{Drag Force (Z)}\}) / (1.293 * (33.3333^2) * A)$$

$$(2 * \{\text{Down Force (Y)}\}) / (1.293 * (33.3333^2) * A)$$

to obtain the numerical values of the drag and lift coefficient at the end calculation. The expressions were obtained by extraction of the  $C_D$  and  $C_L$  coefficients from relations (3.1) and (3.2), with the following values:

- 1.2930 kg/m<sup>3</sup> : the water density;
- 33.3333 m/s : the fluid velocity in Z direction;
- 0.2080 m<sup>2</sup> : the front wing area;
- 0.2124 m<sup>2</sup> : the rear wing area;
- 0.2200 m<sup>2</sup> : the full scale frontal area

### Full scale static tests

Full scale static test is to validate the result from simulation. The test conducted in lab environment with controlling the flow of air by placing the full scale Go-kart in confined space. Due to no wind tunnel to conduct this test, an alternative method has been used by using canopy tent. For generating the air flow, a fan with 1400rpm has been used. Go-kart will be placed inside the tent and applying air flow to the car.

As a matter of fact, there is existing several weaknesses in this static test, where drag and lift force cannot be obtained in this real world test. Furthermore, the coefficient of drag and lift also cannot be obtained. Therefore, results from this test only to compare the flow trajectories for rear and front wings with simulations results.

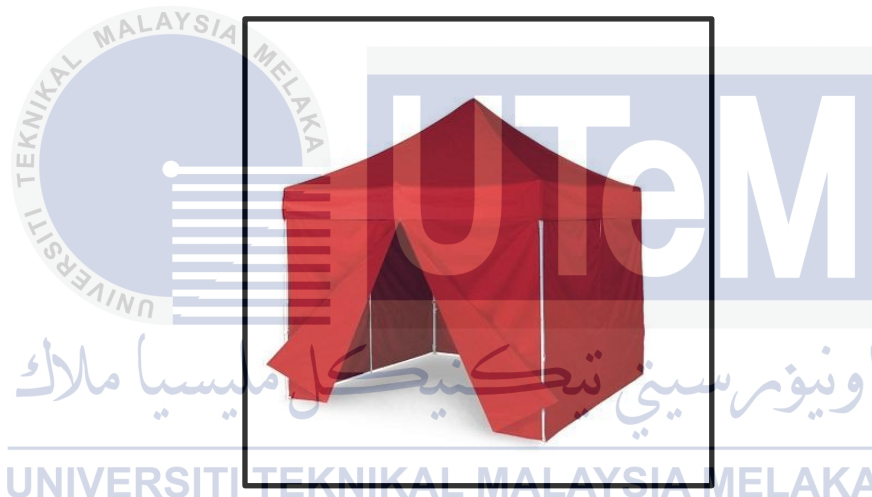


Figure 3.11: Canopy Tent



Figure 3.12: Go-kart under Static Test

### 3.10.2 Measurement

The unit measurements used in wings design are in millimetre (mm). The dimensions of front and rear wing shown in Figure 3.13 and Figure 3.14 below. The detail dimension for wing design shown in Appendix A.

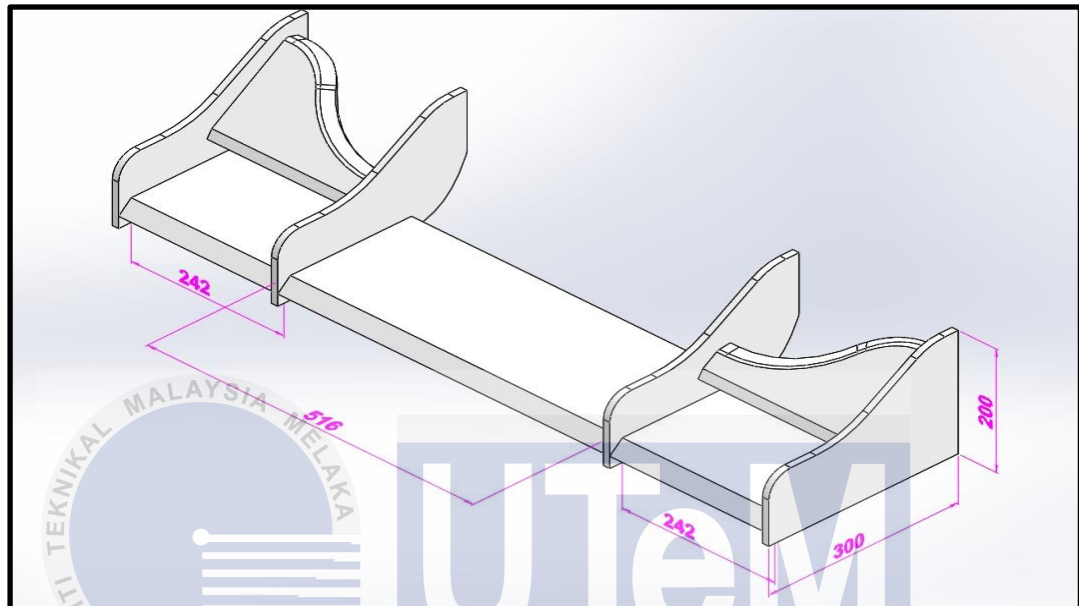


Figure 3.13: Front Wing Dimension in millimetre (mm)

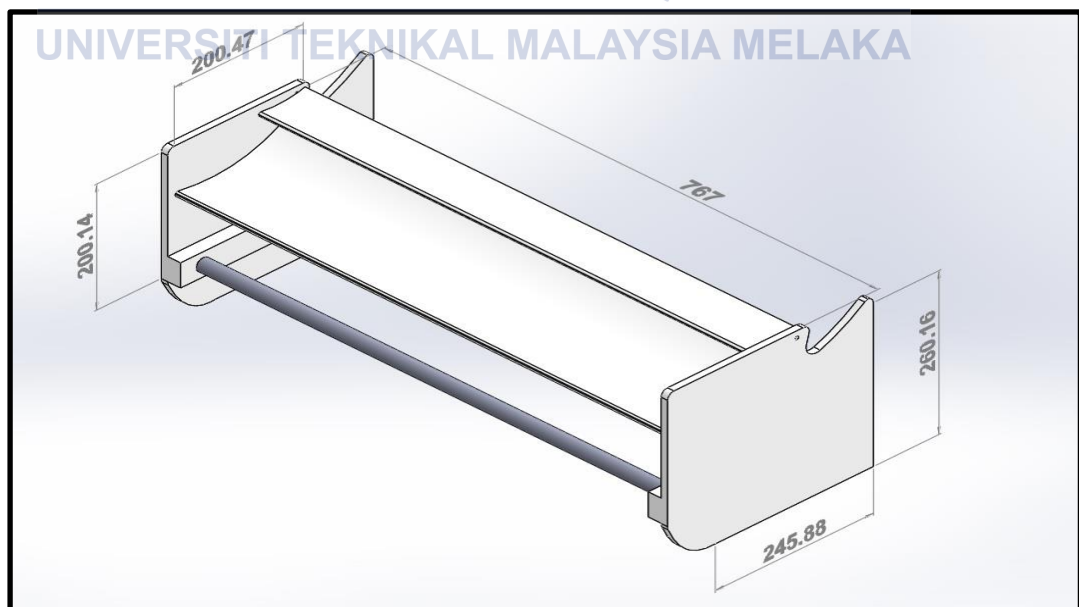


Figure 3.14: Rear Wing Dimension in millimetre (mm)

### 3.10.3 Presentation of Result

The result from the simulation shows by using figures and tables. The simulation results figures shown in four different of orientation such as isometric view, front view, side view, and top view. There are two table of result which is minimum and maximum table and goal plot table. Minimum and maximum table shows the values of pressure, temperature, density, velocity, shear stress, and relative pressure. For the goal plot table, the result shows the surface goal normal to respective force (y-axis and z-axis). The result divided in several parameter such as drag force, downforce, DRS ON and DRS OFF. For drag force simulation, reference axis is set respect to z-axis and downforce is set respect to y-axis. In DRS simulation, during DRS ON, flap wing pivot away from main plane about 50mm. For DRS OFF, flap wing in normal position at 10mm distance from main plane.

### 3.10.4 Interpretation of Result

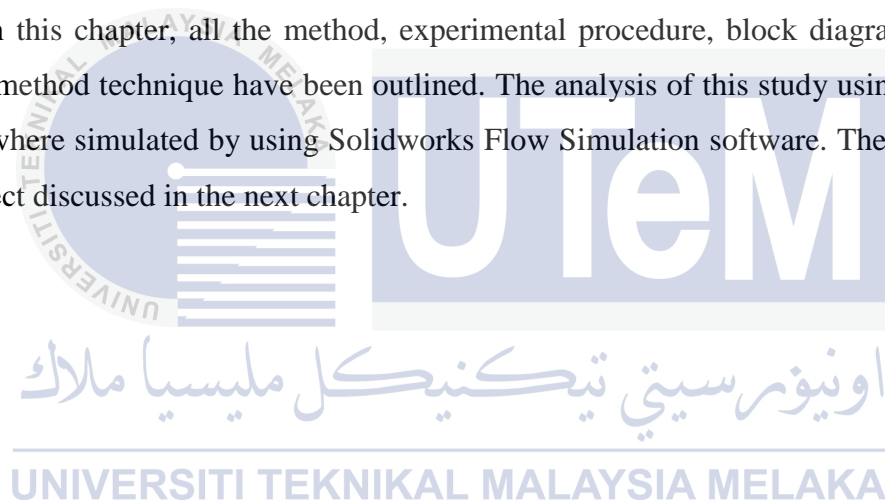
The interpretation of result shows by comparing the result from simulation and static test. There are four comparison result shown in analysis part. The comparison is based on the flow trajectories and the average force acting in respective axis (y-axis and z-axis).

### 3.11 Reliability of Data

In order to improve the accuracy of the simulation tests on the front and rear wings, the tests repeated in three-dimensional simulation. The final validation of the wing's performance will be done in full scale static tests. Due to the probability in influencing factors during fabrication process is high, thus the result might be slightly different from the simulation result. The most influential factor is the shape of the fabricated wing does not exactly the same with the drawing in the Solidworks. Besides that, the uncertainties in making measurements during fabrication are one of the factors.

### 3.12 Summary

In this chapter, all the method, experimental procedure, block diagram and other relevant method technique have been outlined. The analysis of this study using simulation process where simulated by using Solidworks Flow Simulation software. The results from this project discussed in the next chapter.



## CHAPTER 4

### RESULTS AND DISCUSSION

#### 4.1 Introduction

In the previous chapter, the research methodology has been discussed in terms of design method of this study and all the related experimental and descriptive techniques used in this study. The methodology part has been explained in the form of flow chart as well as block diagrams with clear explanations. In this chapter, the results of this project, explained in more detail. As mentions in previous chapters, aerodynamics plays a critical role in modern race cars. Figure 4.1 below shows the summary of the essential elements in aerodynamics.

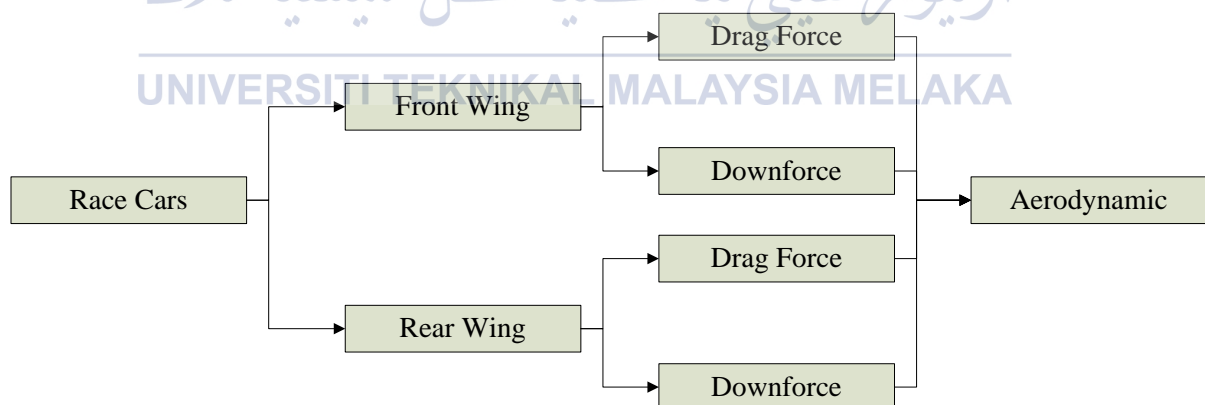


Figure 4.1: Element in Aerodynamics

As can be seen in Figure 4.1, there are two main aerodynamics elements in a race car which is front wing and rear wing. These elements play a critical role in order to reduce the drag force and increasing downforce of a race car. In this chapter, CFD analysis using Flow Trajectories Solidworks Simulation used to simulate of both front wing and rear wing performance in term of drag force and downforce. Simulation result validate by conducting static testing in real world environment. Results obtained from simulation were configured using methods described in Chapter 3.

## 4.2 Solidworks Simulation

Simulation has been done to obtain the drag force and downforce in Newton (N) unit. Then the coefficient of drag and lift can yield by inserting the equations in equation goal in Solidworks. This section presents the results from the simulations and divided into three parts. Each part of simulations presents the results in table of goals plot, three-dimensional of pressure flow trajectories and three-dimensional of pressure surface plot. The results and outcome from these simulations will be discussed in analysis section.

### 4.2.1 Front wing Simulation

In this part, results show the simulation of front wing only without attached to go-kart. The table of result shows the drag and lift force acting on the front wing. Then numerical values of drag and lift coefficient obtained at the end of the simulation calculation and presented in Table 4.1. Three-dimensional figures are presented to shows the behaviour pressure acting on the front wing.



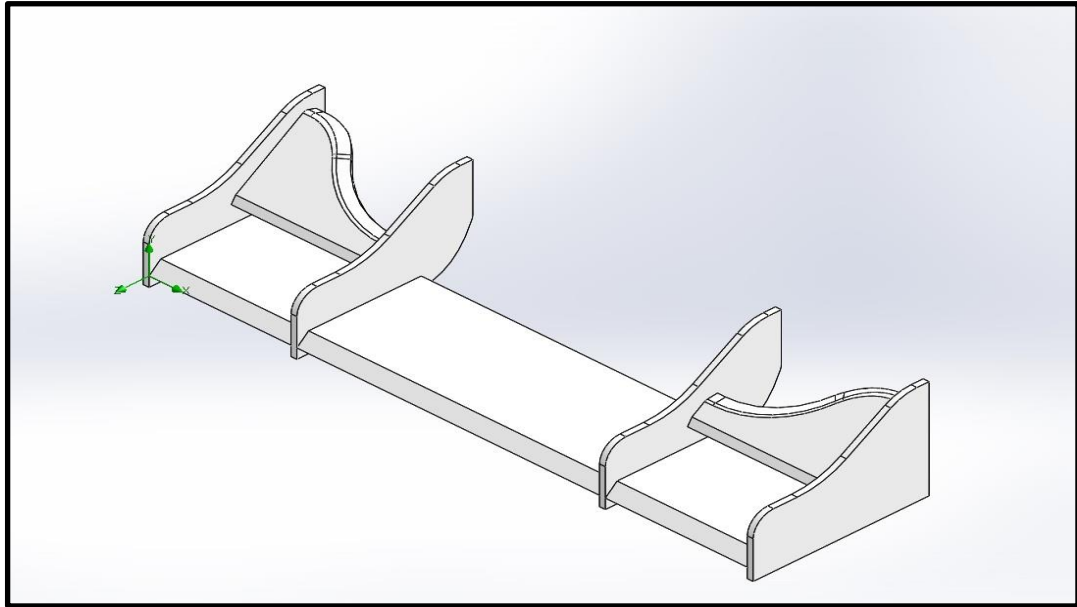


Figure 4.2: Front Wing

Table 4.1: Front Wing Goal Plot Table Result

Goal Name	Unit	Value	Averaged Value	Minimum Value	Maximum Value
Drag Force (Z)	[N]	28.86750081	29.71754524	30.59570871	28.30823161
Drag Coefficient		0.193206041	0.198895266	0.204772688	0.189462932
Lift Force (Y)	[N]	-33.67683727	-34.51848225	-36.4789277	-31.95507845
Lift Coefficient		-0.225394239	-0.231027248	-0.244148229	-0.213870755

UNIVERSITI TEKNIKAL MALAYSIA MELAKA

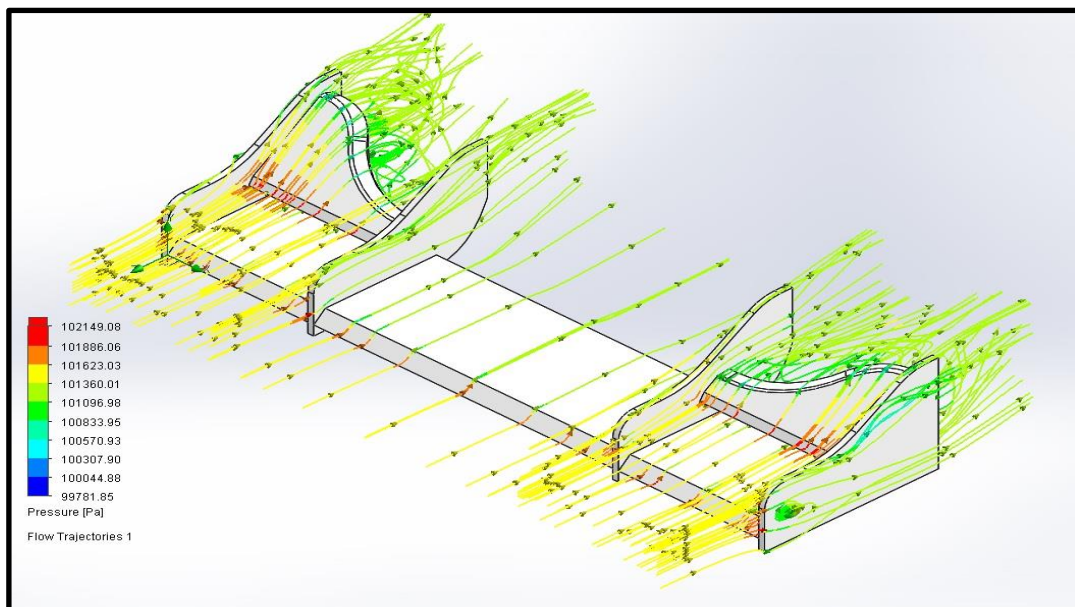


Figure 4.3: Isometric View for Pressure Flow Trajectories



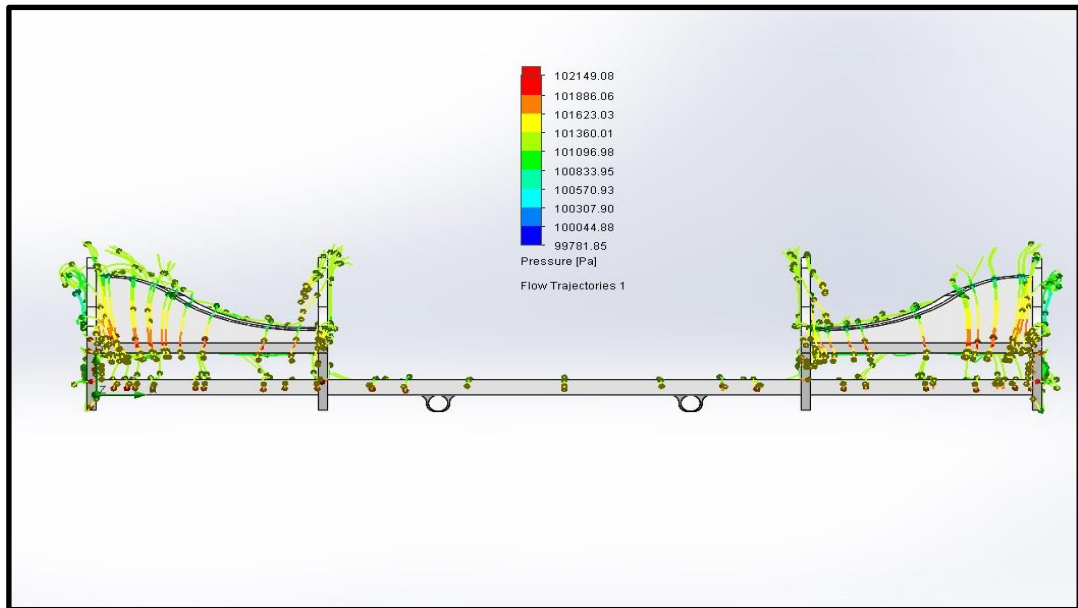


Figure 4.4: Front View for Pressure Flow Trajectories

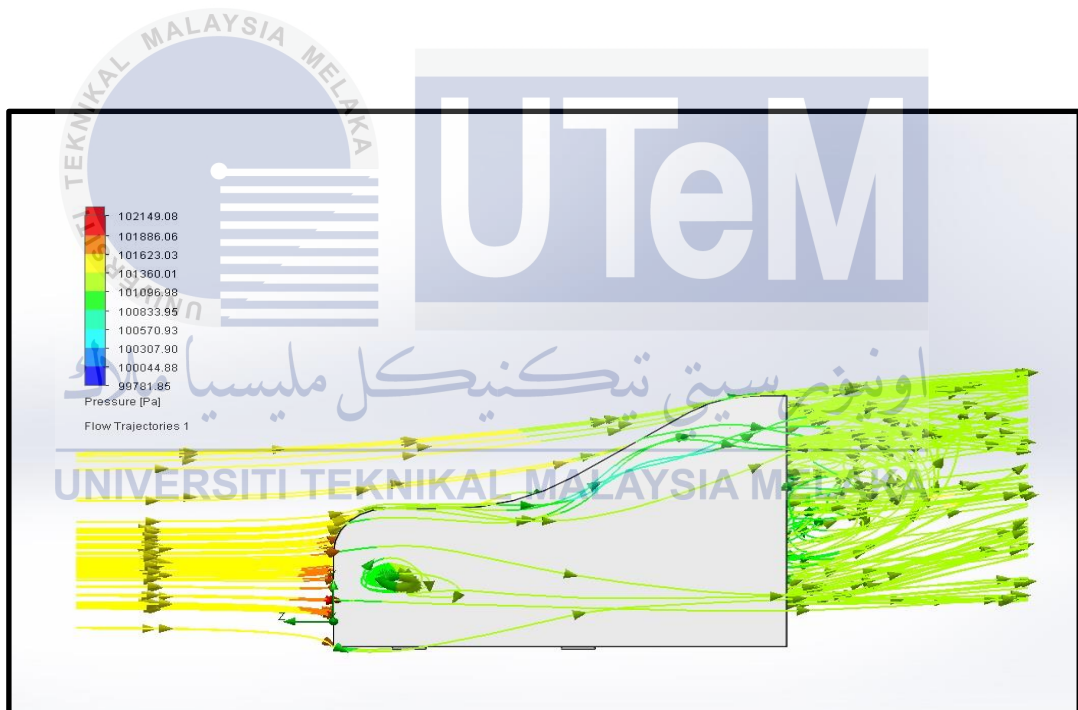


Figure 4.5: Side View for Pressure Flow Trajectories

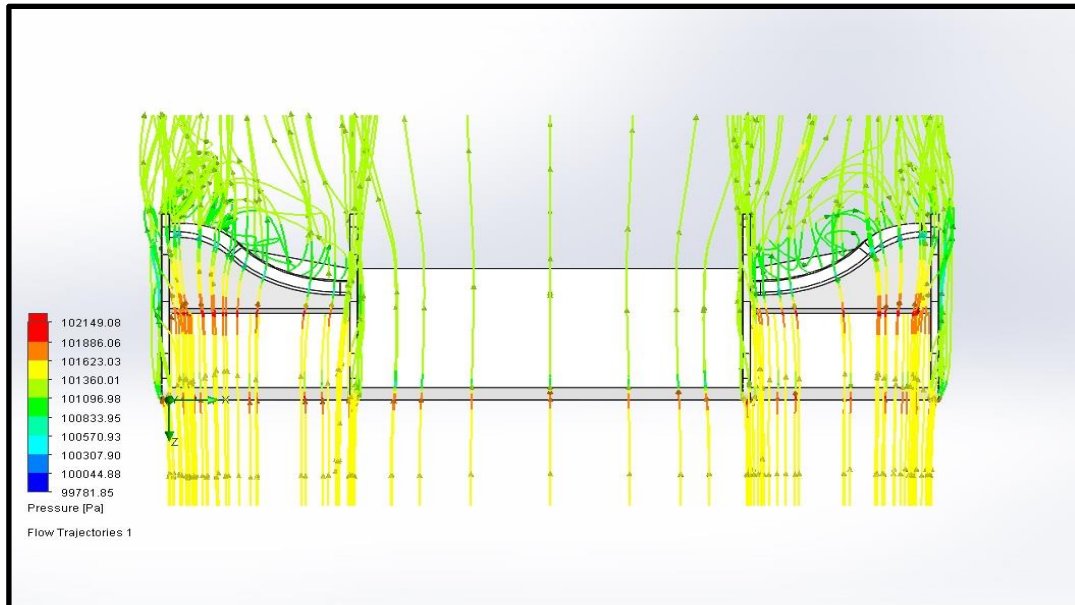


Figure 4.6: Top View for Pressure Flow Trajectories

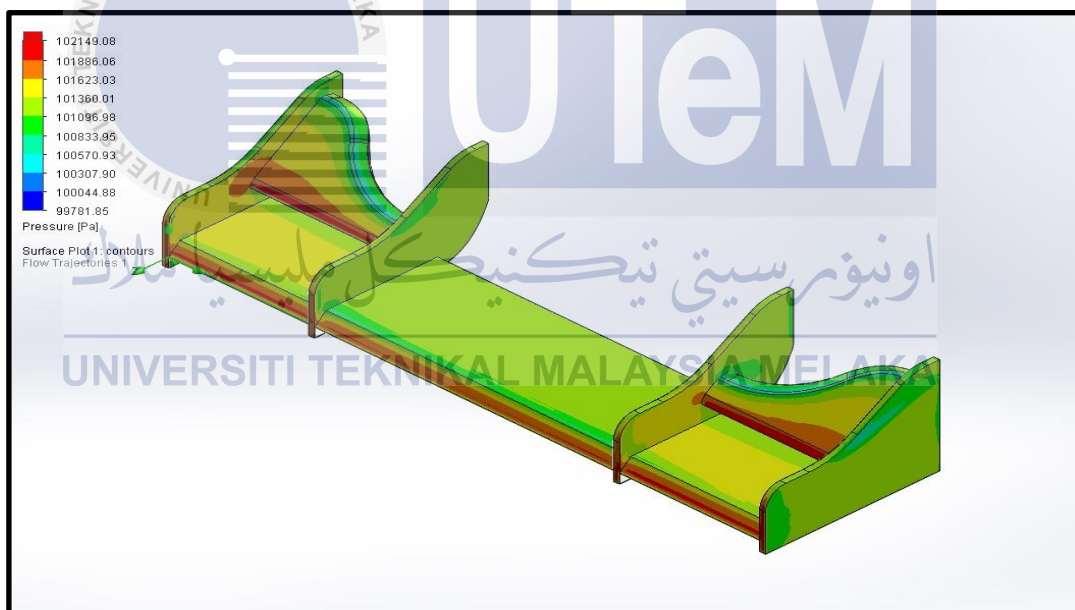


Figure 4.7: Isometric View for Surface Plot Pressure

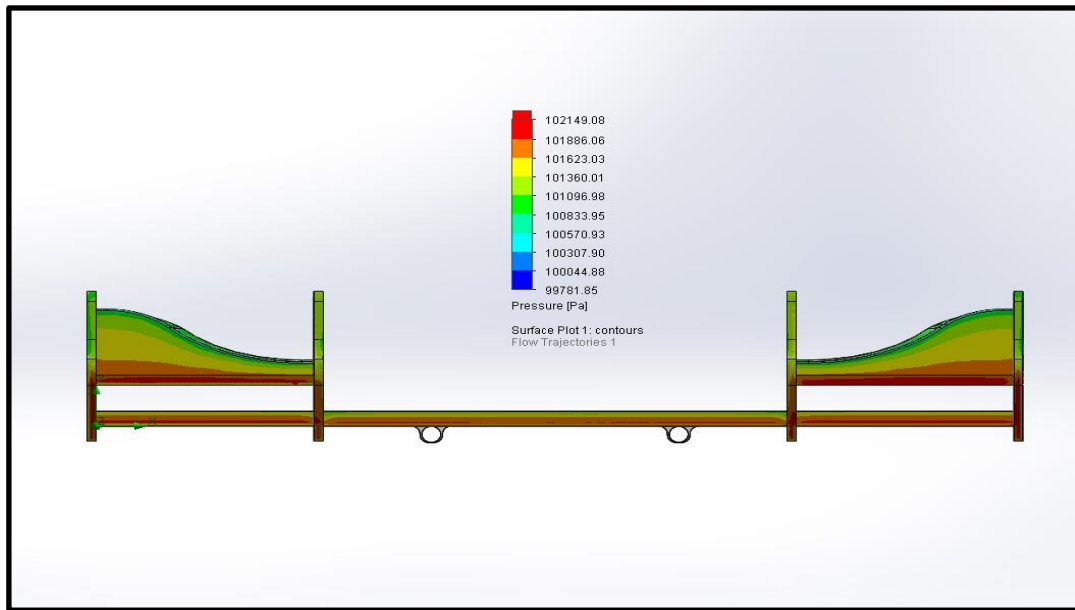


Figure 4.8: Front View for Surface Plot Pressure



Figure 4.9: Side View for Surface Plot Pressure

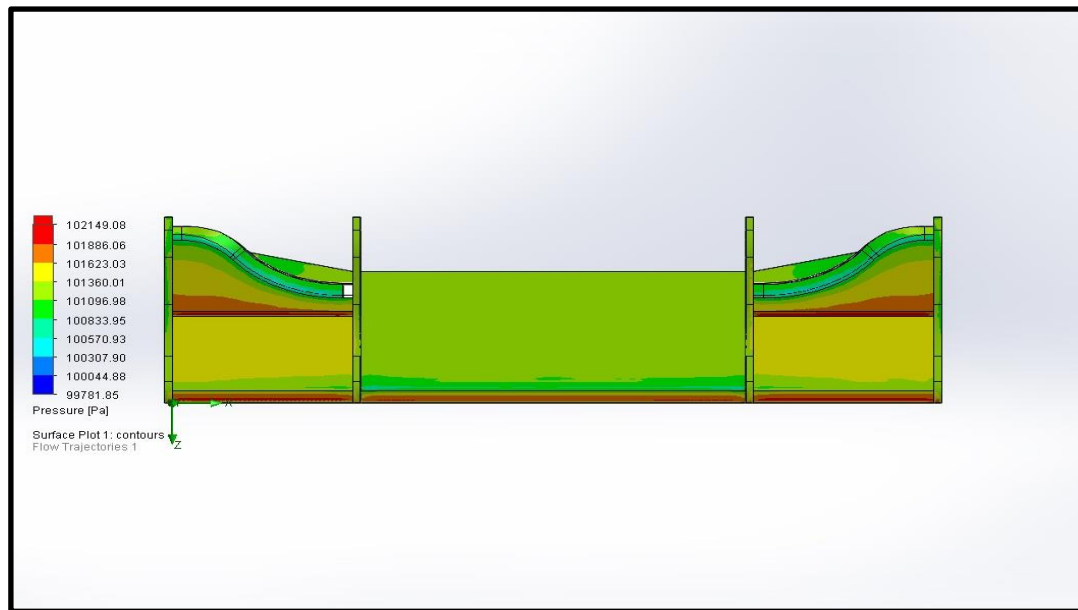


Figure 4.10: Top View for Surface Plot Pressure

## 4.2.2 Rear Wing Simulation

In this part, results show the simulation of rear wing only without attached to go-kart. The simulation divided in two conditions, during DRS activated (DRS ON) and during DRS OFF. The table of result shows the drag and lift force acting on the front wing. Then numerical values of drag and lift coefficient obtained at the end of the simulation calculation and presented in Table 4.2 and Table 4.3. Three-dimensional figures are presented to shows the behaviour pressure acting on the rear wing.

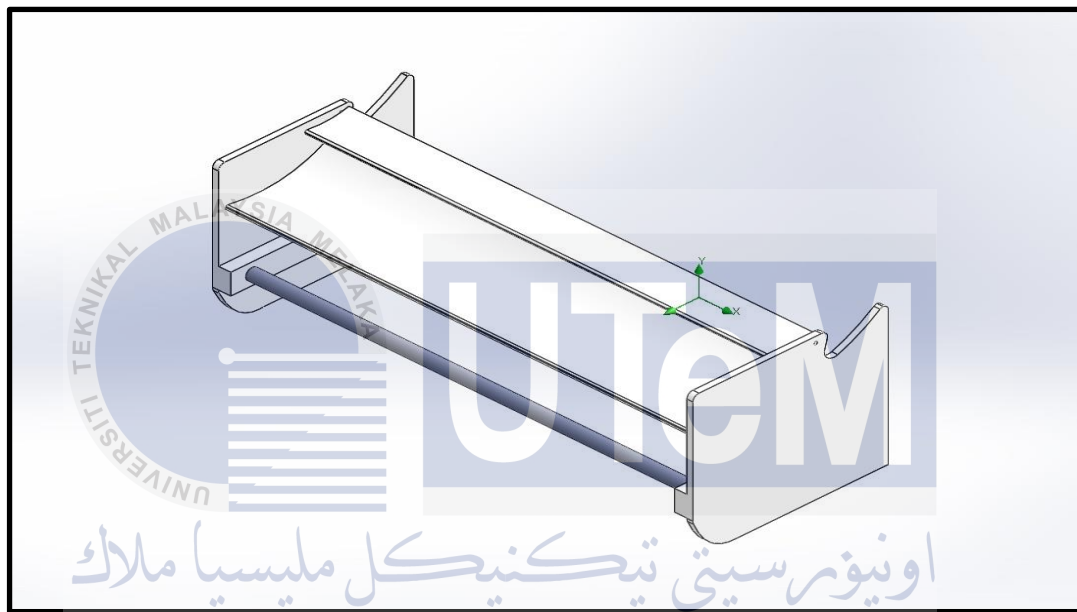


Figure 4.11: Rear Wing

### 4.2.2.1 Rear Wing (DRS OFF) Simulation Result

Table 4.2: Rear Wing (DRS OFF) Goal Plot Table Result

Goal Name	Unit	Value	Averaged Value	Minimum Value	Maximum Value
Drag Force (Z)	[N]	43.09434726	55.23042715	43.09434726	60.85225584
Drag Coefficient		0.28232976	0.361838483	0.28232976	0.398669521
Lift Force (Y)	[N]	-72.04246262	-105.2466044	-72.04246262	-117.190273
Lift Coefficient		-0.47198142	-0.689516154	-0.47198142	-0.767764308

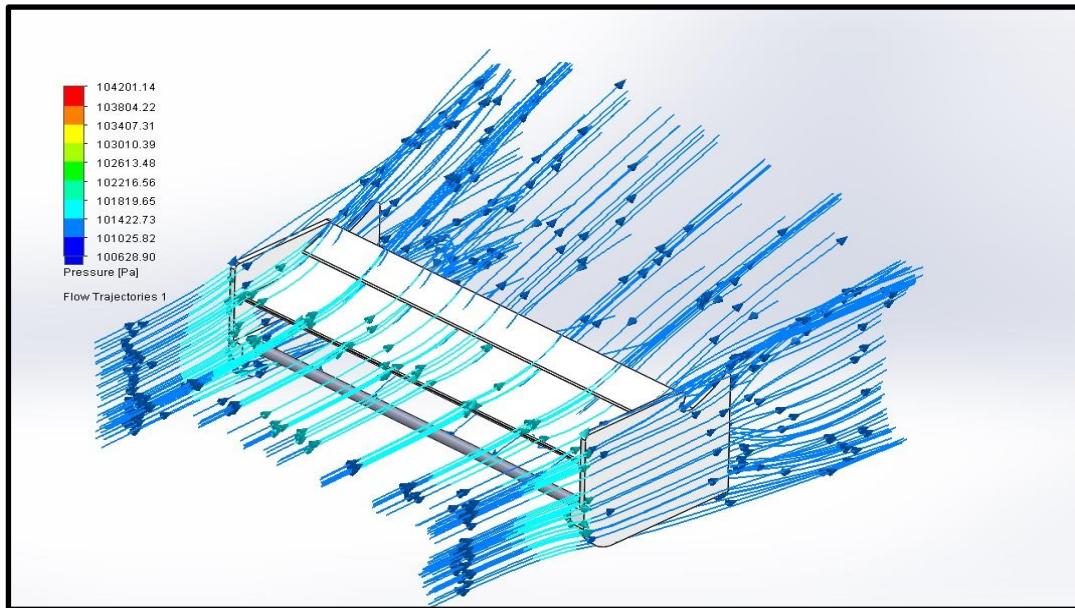


Figure 4.12: Isometric View for Pressure Flow Trajectories (DRS OFF)

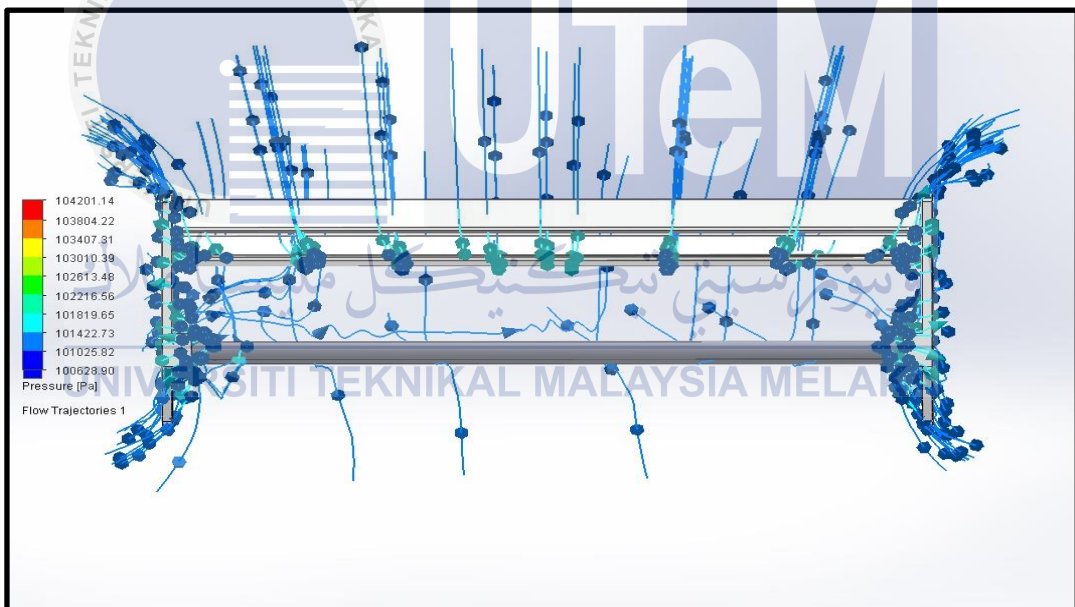


Figure 4.13: Front View for Pressure Flow Trajectories (DRS OFF)



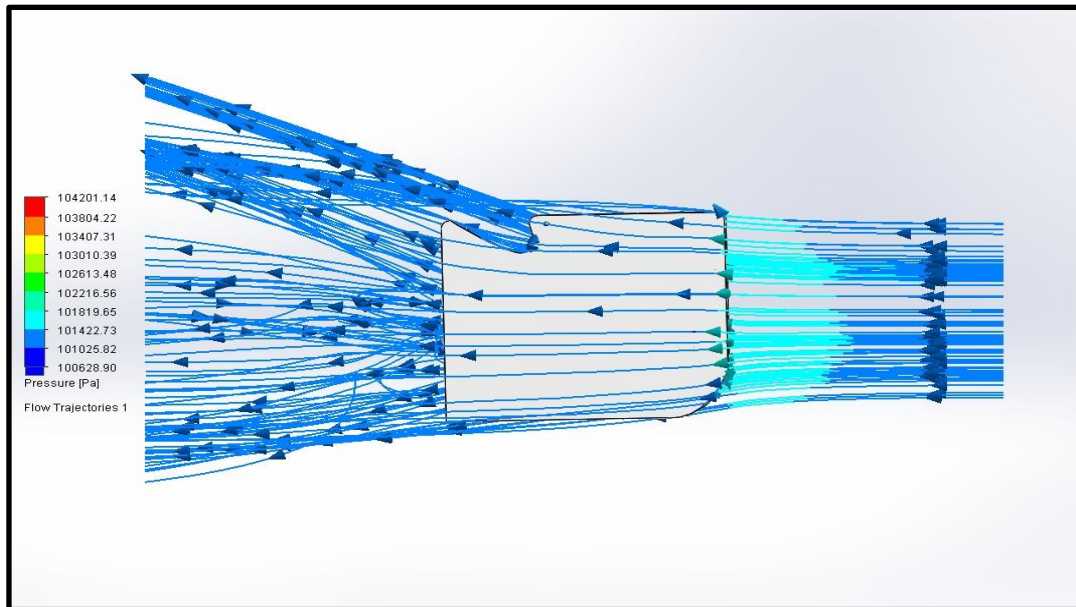


Figure 4.14: Top View for Pressure Flow Trajectories (DRS OFF)

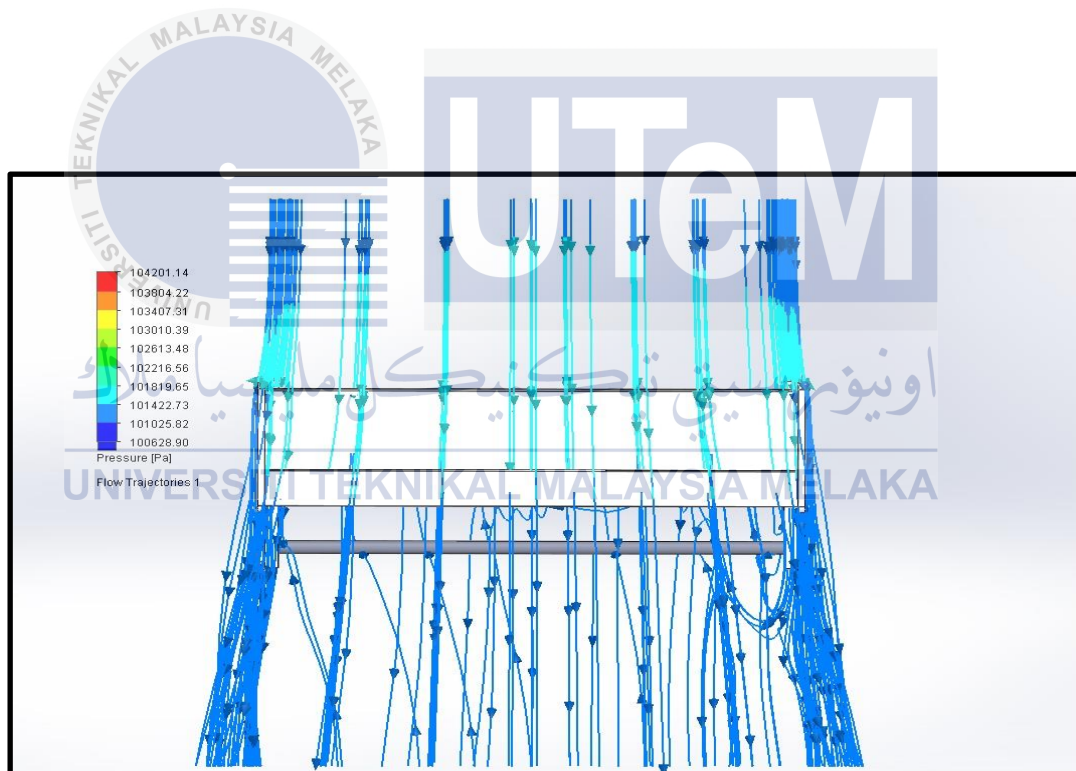


Figure 4.15: Top View for Pressure Flow Trajectories (DRS OFF)

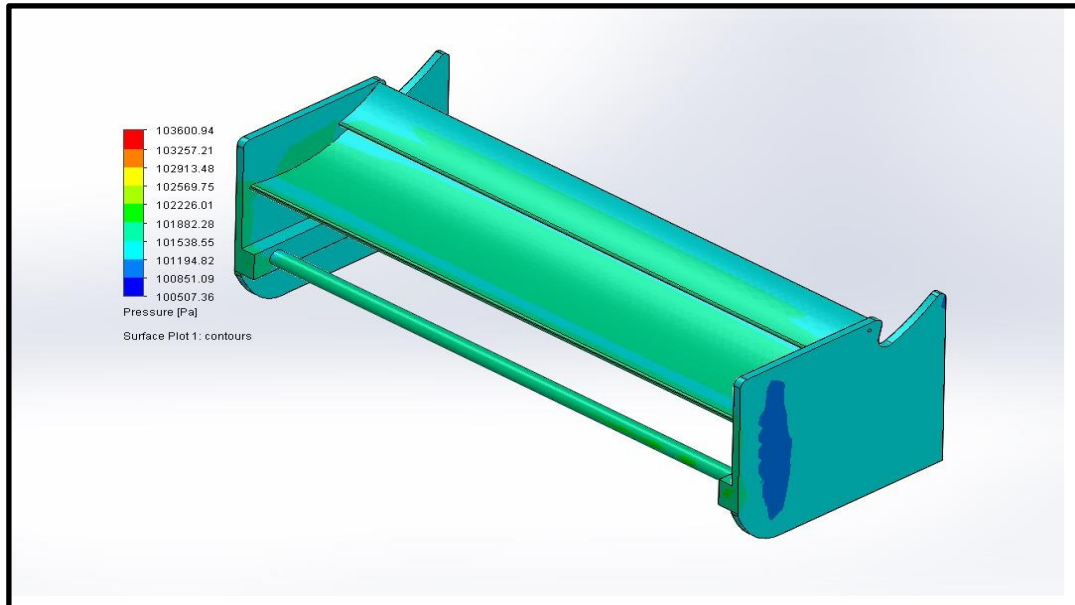


Figure 4.16: Isometric View for Pressure Surface Plot (DRS OFF)

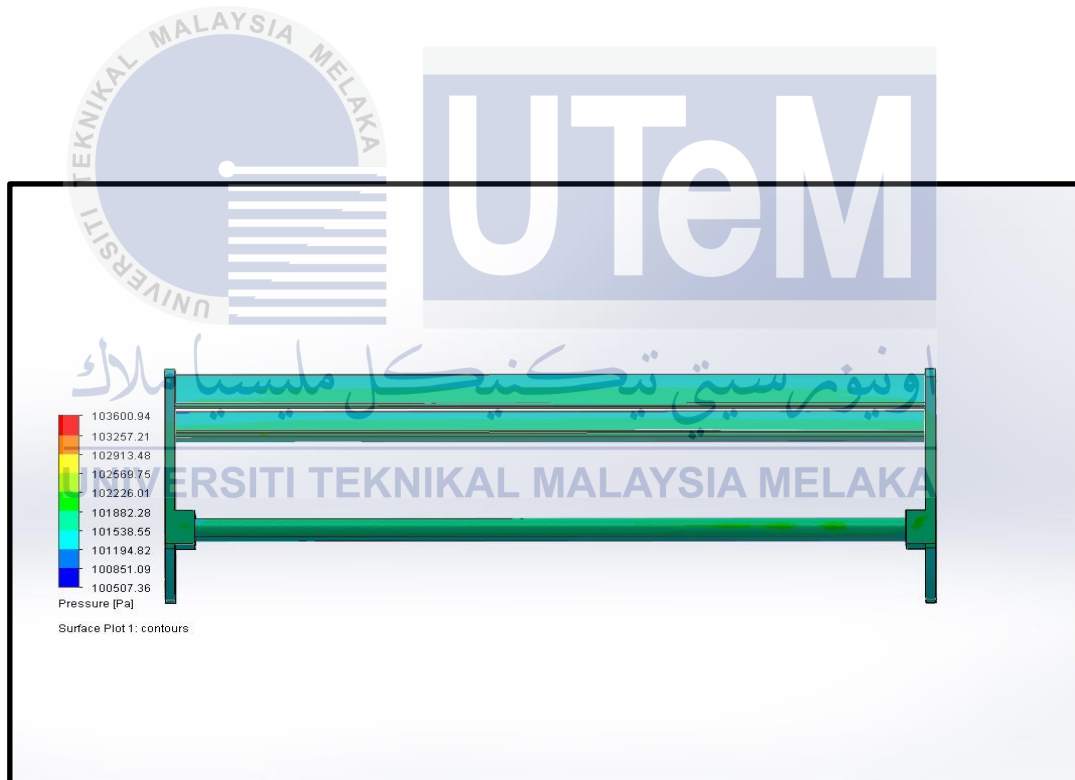


Figure 4.17: Front View for Pressure Surface Plot (DRS OFF)



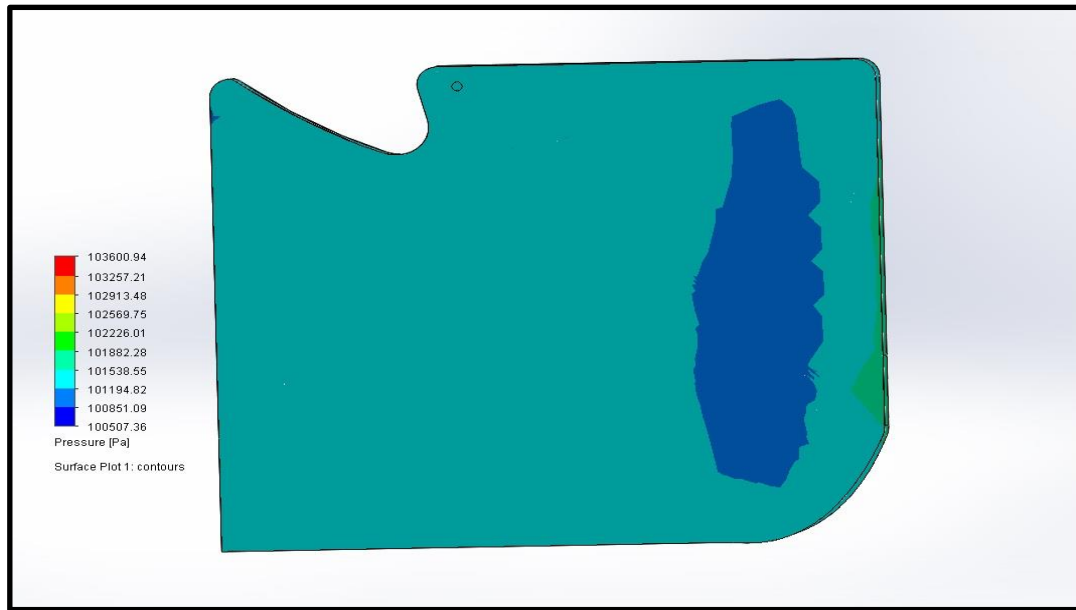


Figure 4.18: Side View for Pressure Surface Plot (DRS OFF)



Figure 4.19: Top View for Pressure Surface Plot (DRS OFF)

#### 4.2.2.2 Rear Wing (DRS ON) Simulation Result

Table 4.3: Rear Wing (DRS ON) Goal Plot Table Result

Goal Name	Unit	Value	Averaged Value	Minimum Value	Maximum Value
Drag Force (Z)	[N]	29.27609195	29.28886545	29.15813664	29.51081491
Drag Coefficient		0.191800376	0.191884061	0.1910276	0.193338148
Lift Force (Y)	[N]	-68.03264103	-67.99033602	-67.63386411	-68.43785184
Lift Coefficient		-0.445711339	-0.445434181	-0.443098779	-0.448366051

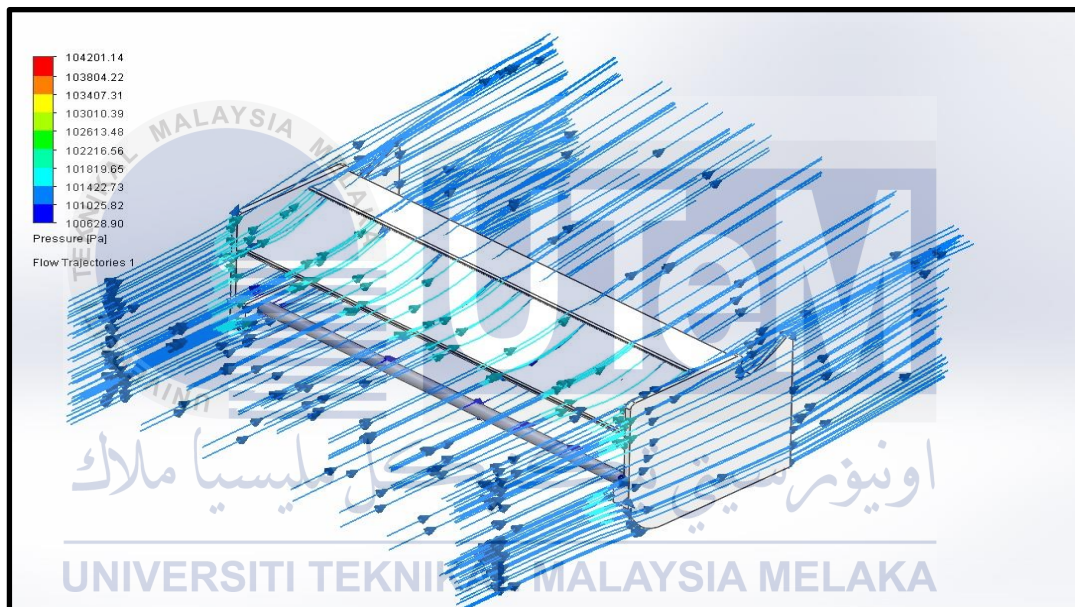


Figure 4.20: Isometric View for Pressure Flow Trajectories (DRS ON)

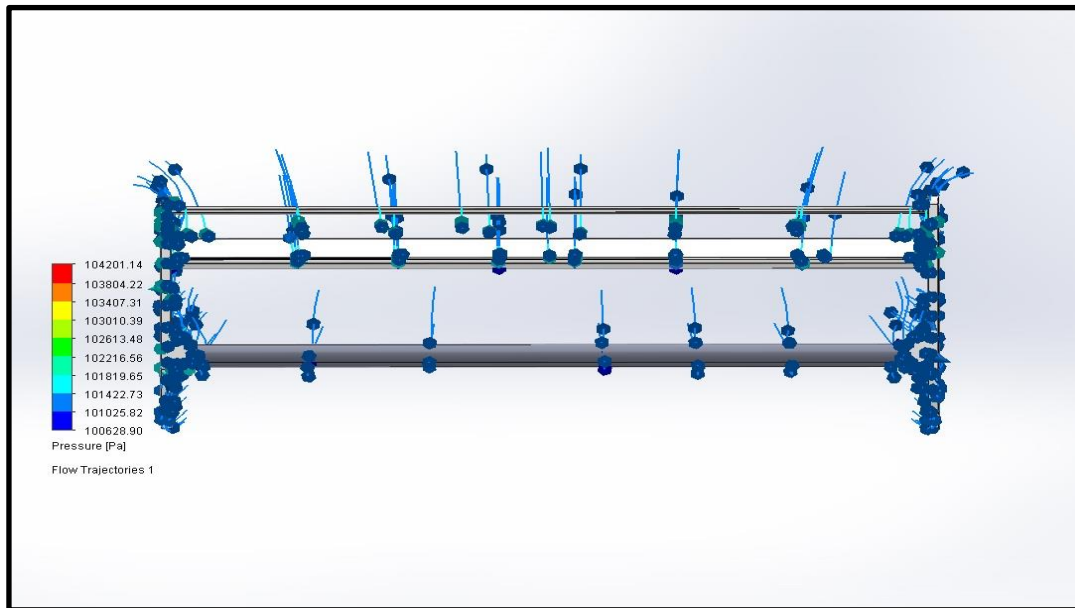


Figure 4.21: Front View for Pressure Flow Trajectories (DRS ON)

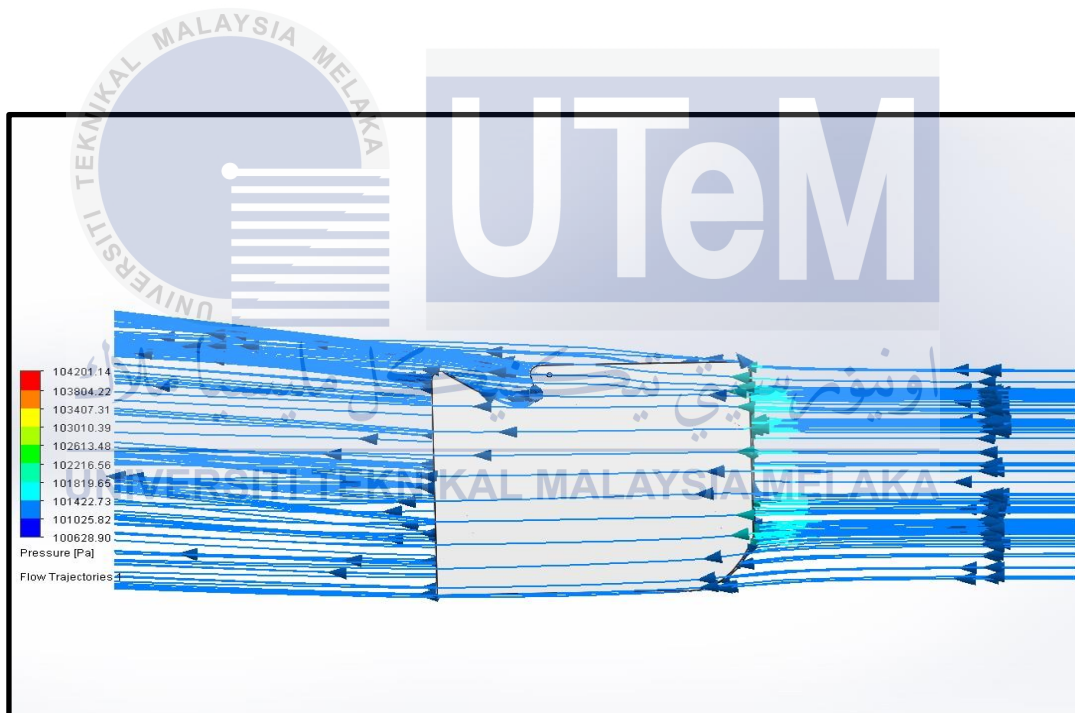


Figure 4.22: Top View for Pressure Flow Trajectories (DRS ON)

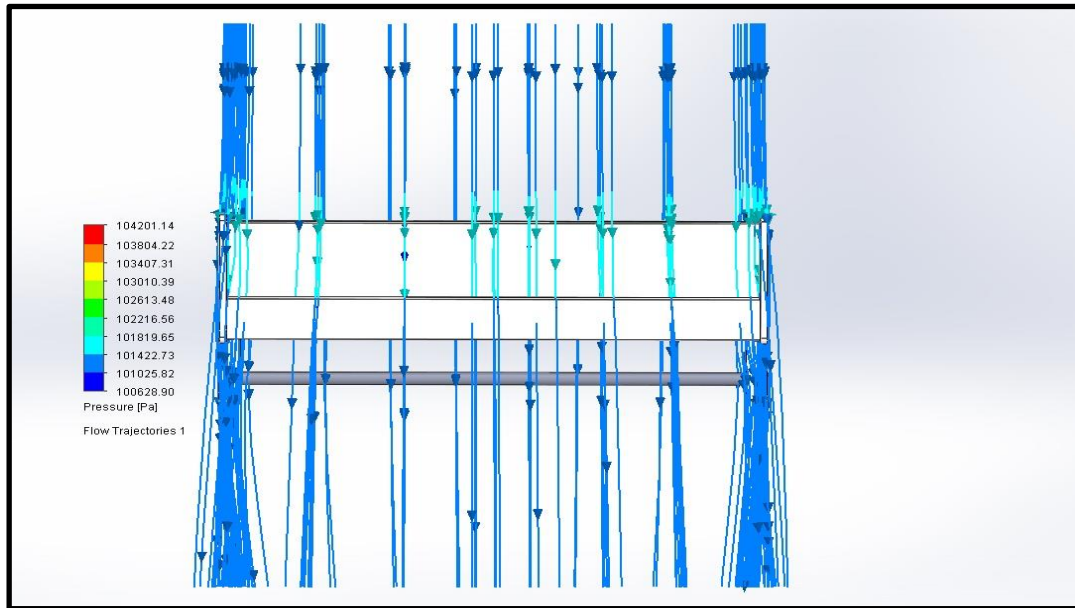


Figure 4.23: Top View for Pressure Flow Trajectories (DRS ON)

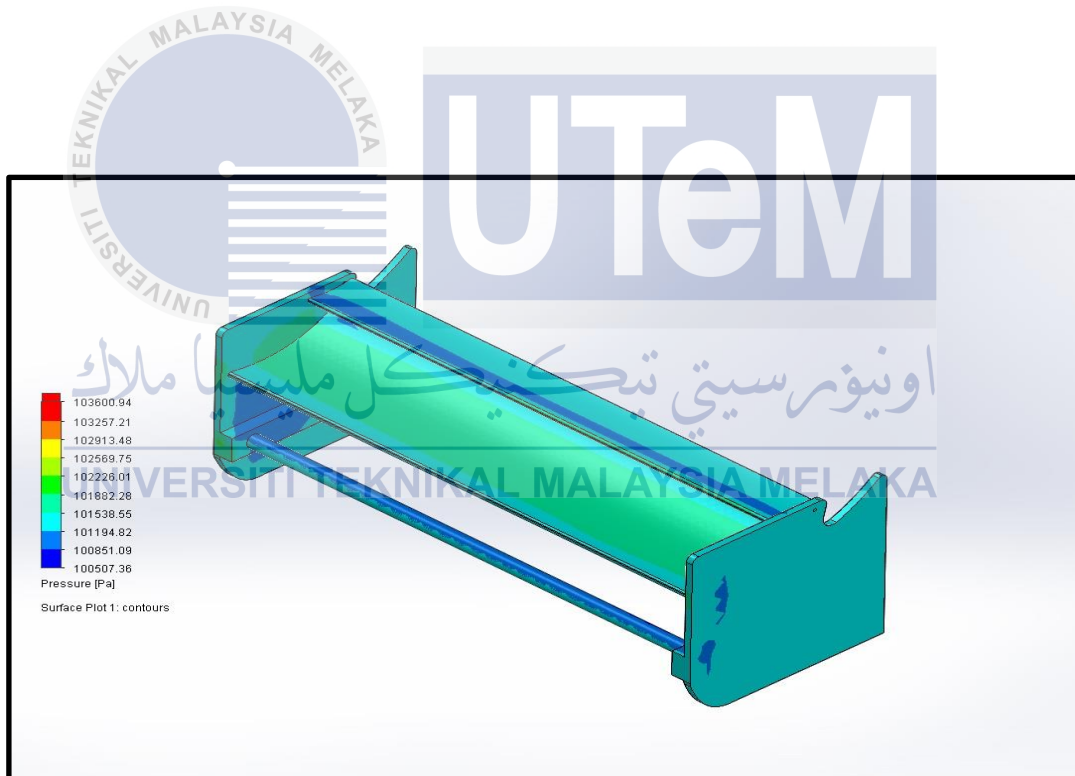


Figure 4.24: Isometric View for Pressure Surface Plot (DRS ON)



Figure 4.25: Front View for Pressure Surface Plot (DRS ON)

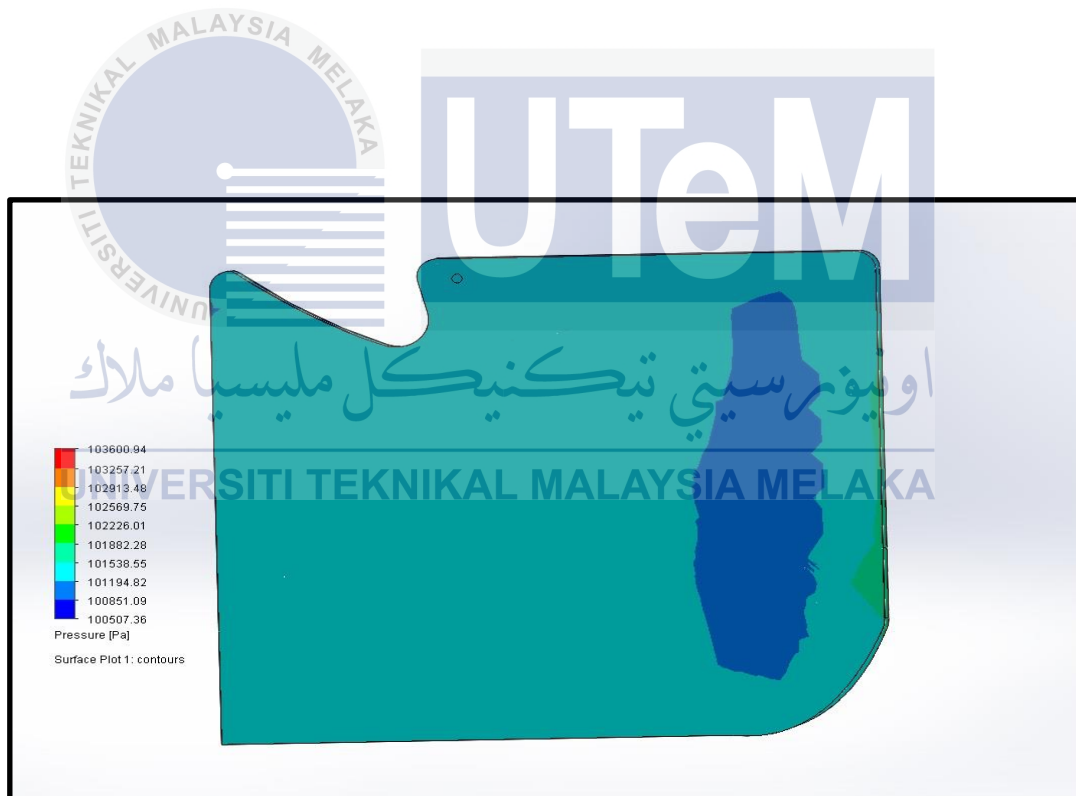


Figure 4.26: Side View for Pressure Surface Plot (DRS ON)

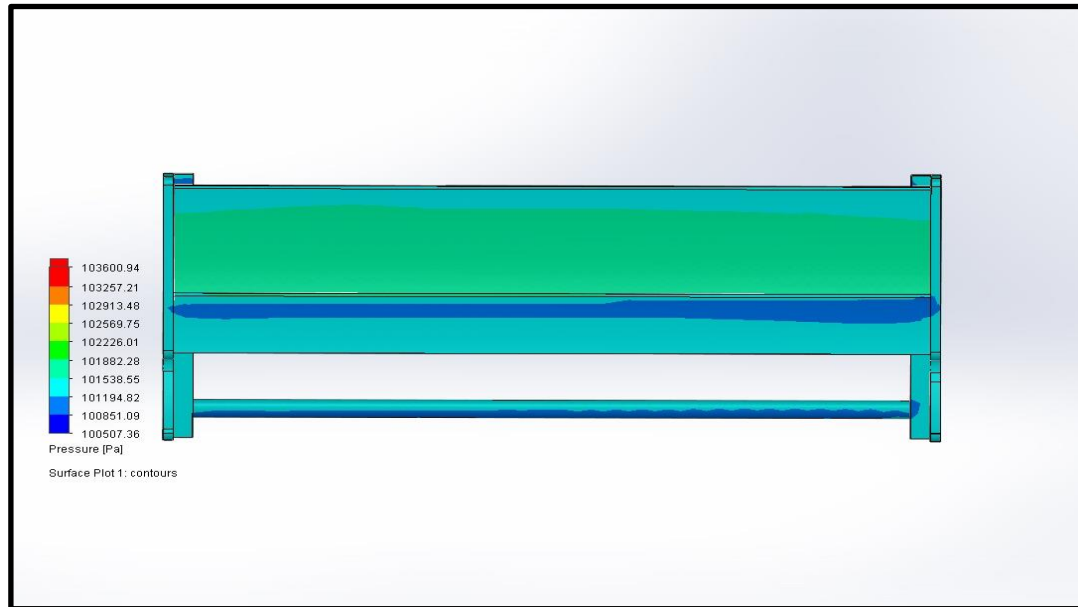


Figure 4.27: Top View for Pressure Surface Plot (DRS ON)



### 4.2.3 Full Scale Go-kart Simulation

In this part, results show the simulation of full scale of Go-kart with front and rear wing attached. The simulation divided in two conditions, during DRS activated (DRS ON) and during DRS OFF. The table of result shows the drag and lift force acting on the front wing. Then numerical values of drag and lift coefficient obtained at the end of the simulation calculation and presented in Table 4.4 and Table 4.5. Three-dimensional figures are presented to shows the behaviour pressure acting on the rear wing.

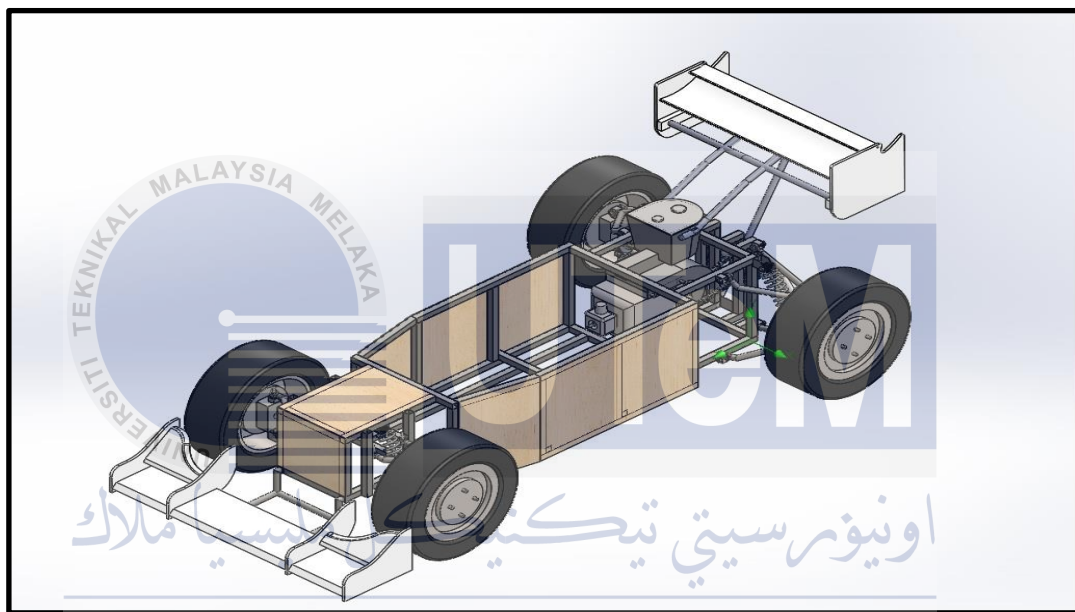


Figure 4.28: Full Scale Go-kart Solidworks Drawing

#### 4.2.3.1 Go-Kart Full Scale (DRS OFF) Simulation Result

Table 4.4: Full Scale (DRS OFF) Goal Plot Table Result

Goal Name	Unit	Value	Averaged Value	Minimum Value	Maximum Value
Drag Force (Z)	[N]	255.277854	253.2919693	249.7055744	255.277854
Drag Coefficient		1.615345061	1.602778797	1.580084838	1.615345061
Lift Force (Y)	[N]	-55.03018996	-56.04434086	-54.84792629	-59.41734485
Lift Coefficient		-0.348219574	-0.35463691	-0.347066248	-0.375980576



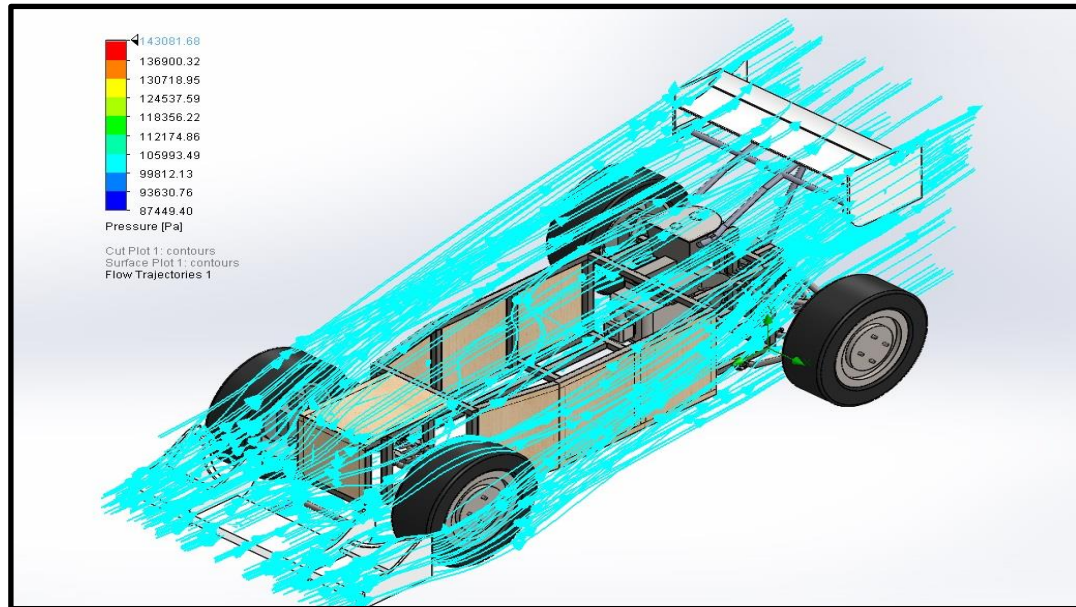


Figure 4.29: Isometric View for Pressure Flow Trajectories (DRS OFF)

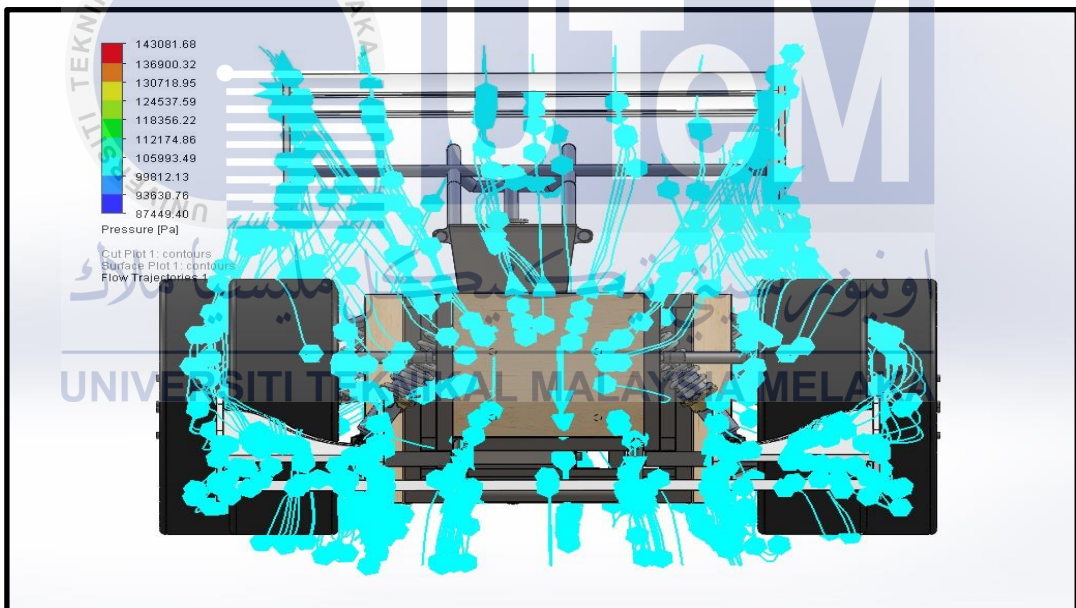


Figure 4.30: Front View for Pressure Flow Trajectories (DRS OFF)



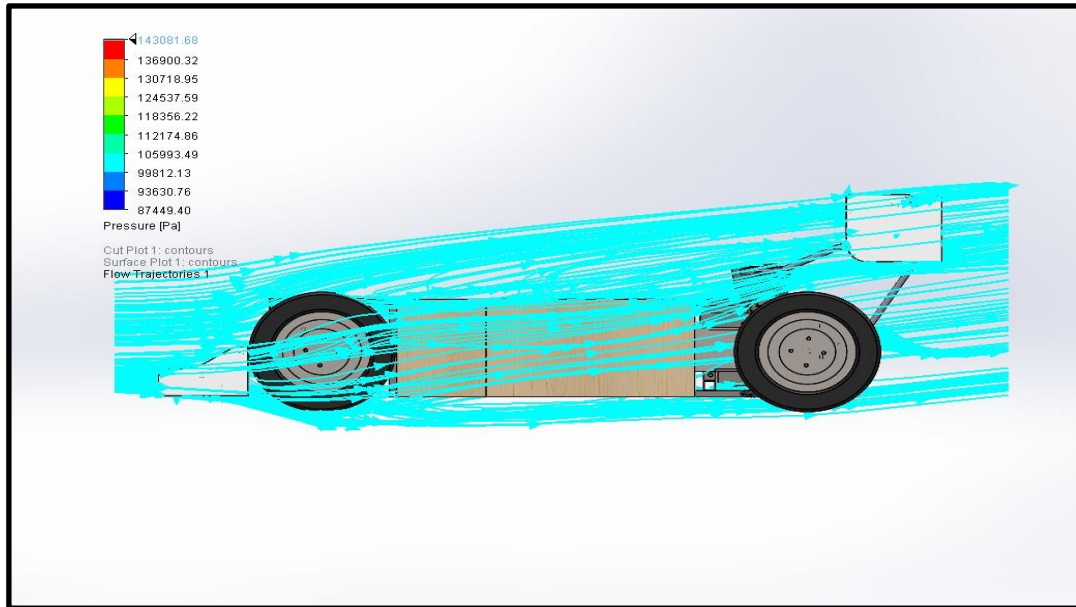


Figure 4.30: Side View for Pressure Flow Trajectories (DRS OFF)

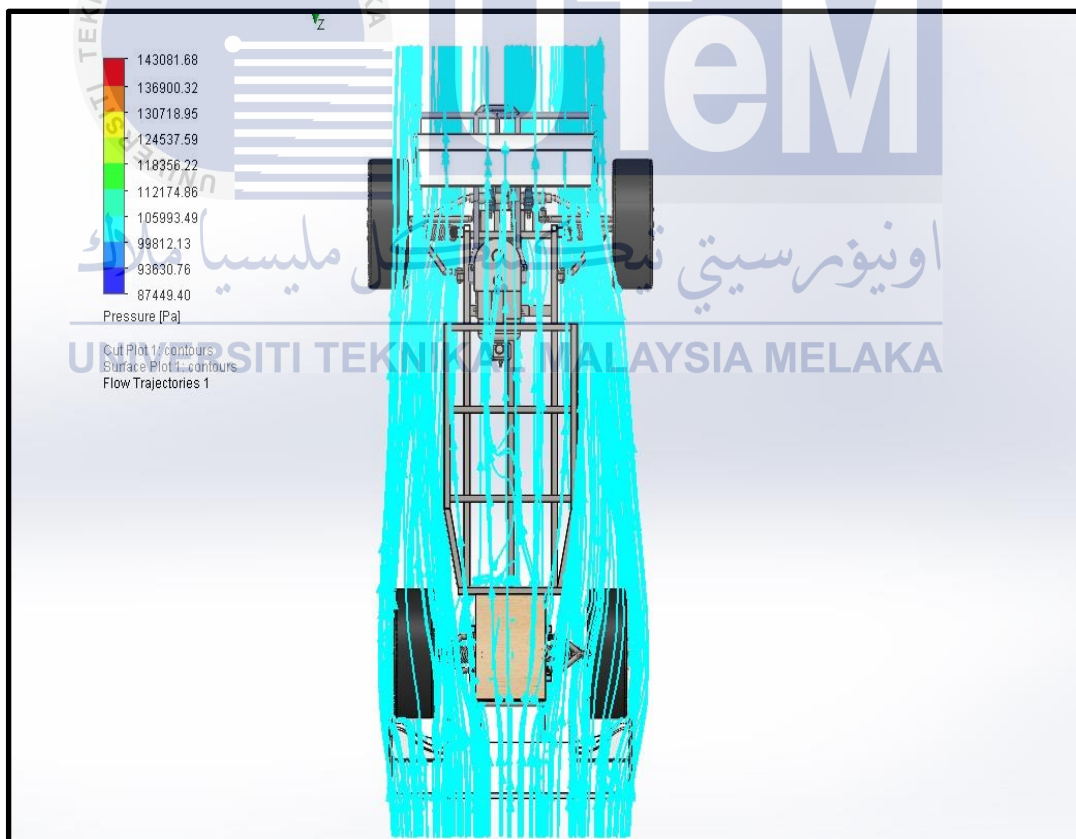


Figure 4.31: Top View for Pressure Flow Trajectories (DRS OFF)

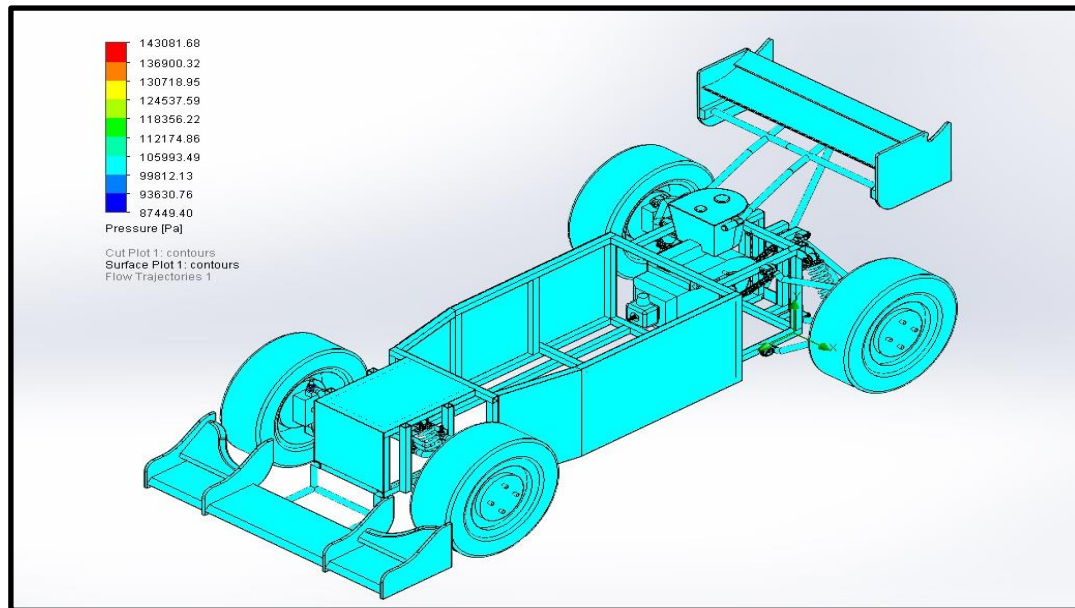


Figure 4.32: Isometric View for Pressure Surface Plot (DRS OFF)

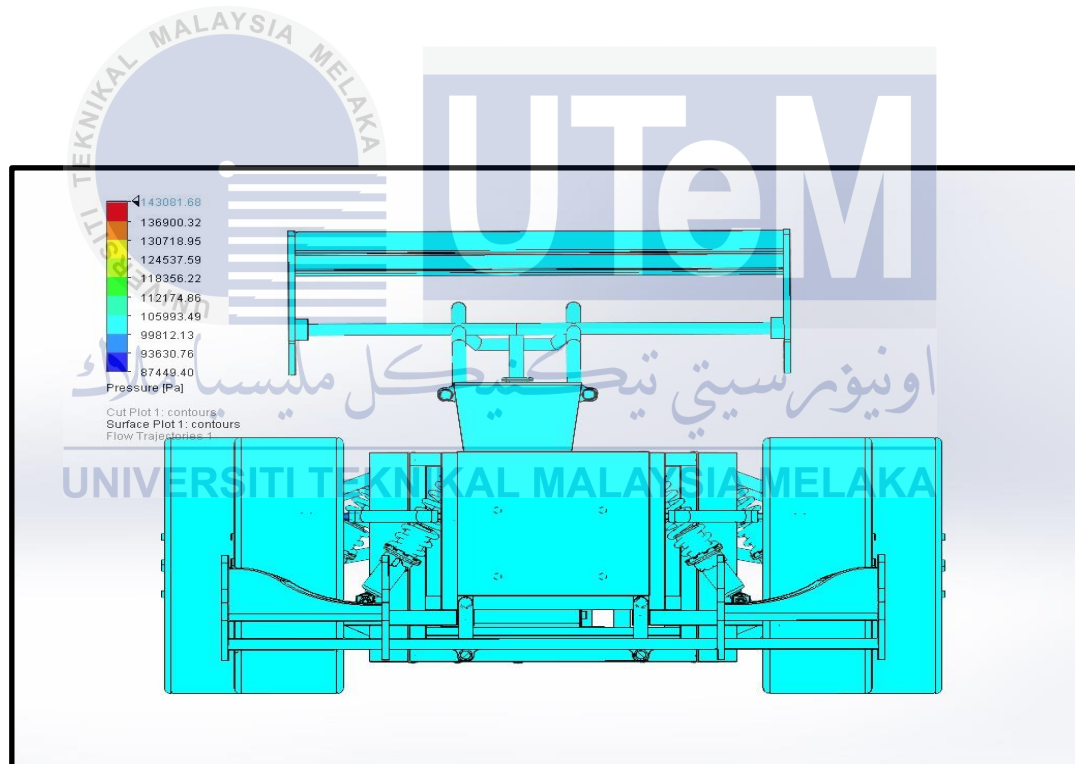


Figure 4.33: Front View for Pressure Surface Plot (DRS OFF)

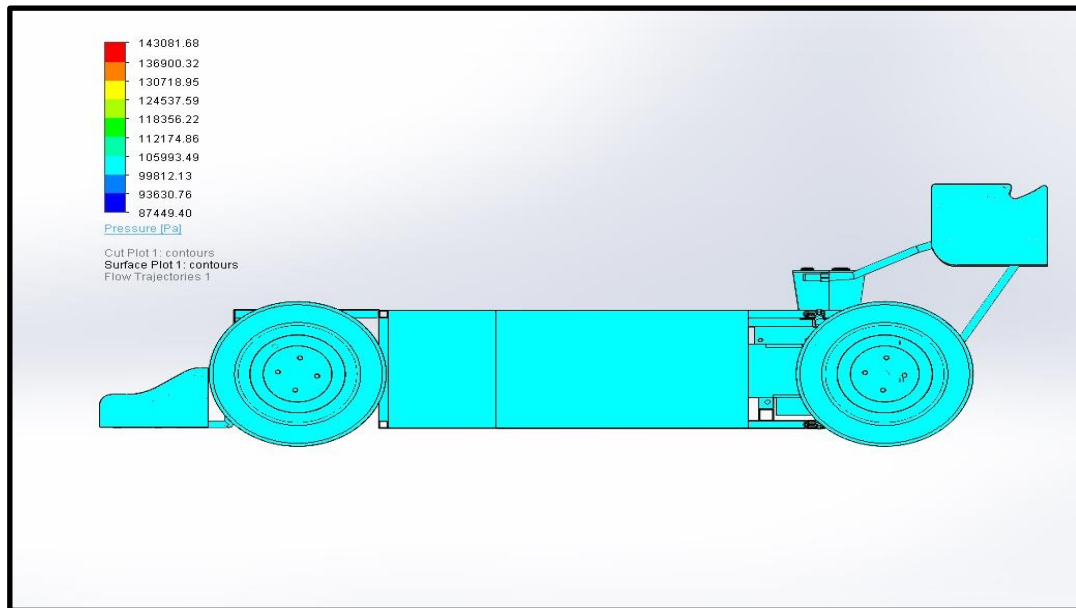


Figure 4.34: Side View for Pressure Surface Plot (DRS OFF)

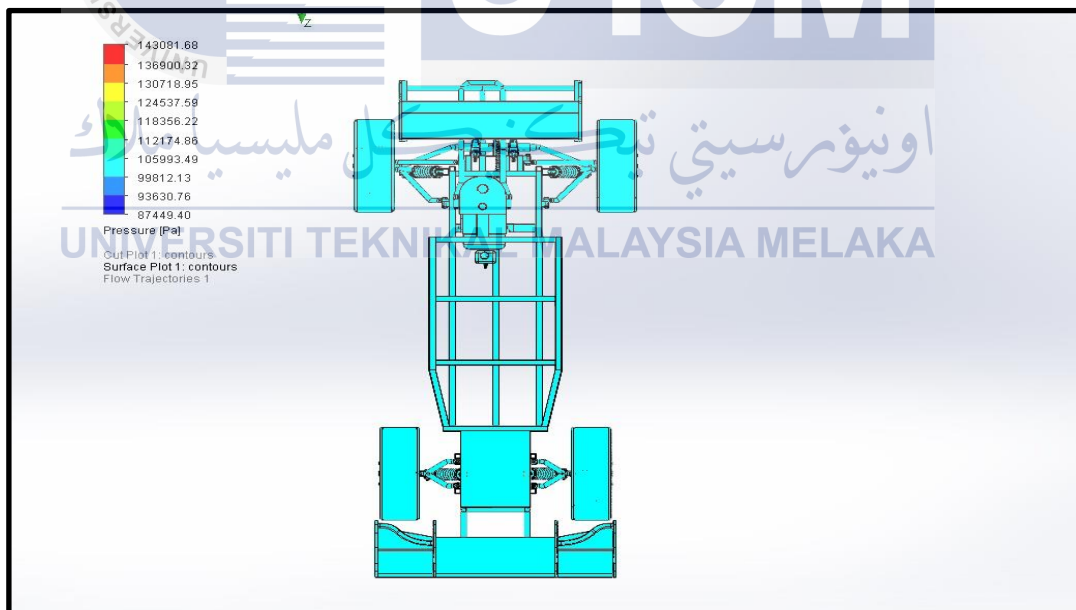


Figure 4.35: Top View for Pressure Surface Plot (DRS OFF)

#### 4.2.3.2 Go-Kart Full Scale (DRS ON) Simulation Result

Table 4.5: Full Scale (DRS ON) Goal Plot Table Result

Goal Name	Unit	Value	Averaged Value	Minimum Value	Maximum Value
Drag Force (Z)	[N]	254.4428811	252.7436586	249.5498352	254.7979508
Drag Coefficient		1.610061527	1.599309201	1.579099352	1.612308334
Lift Force (Y)	[N]	-55.70474255	-55.94515108	-54.9912329	-60.00904916
Lift Coefficient		-0.352488002	-0.354009257	-0.347973062	-0.379724757

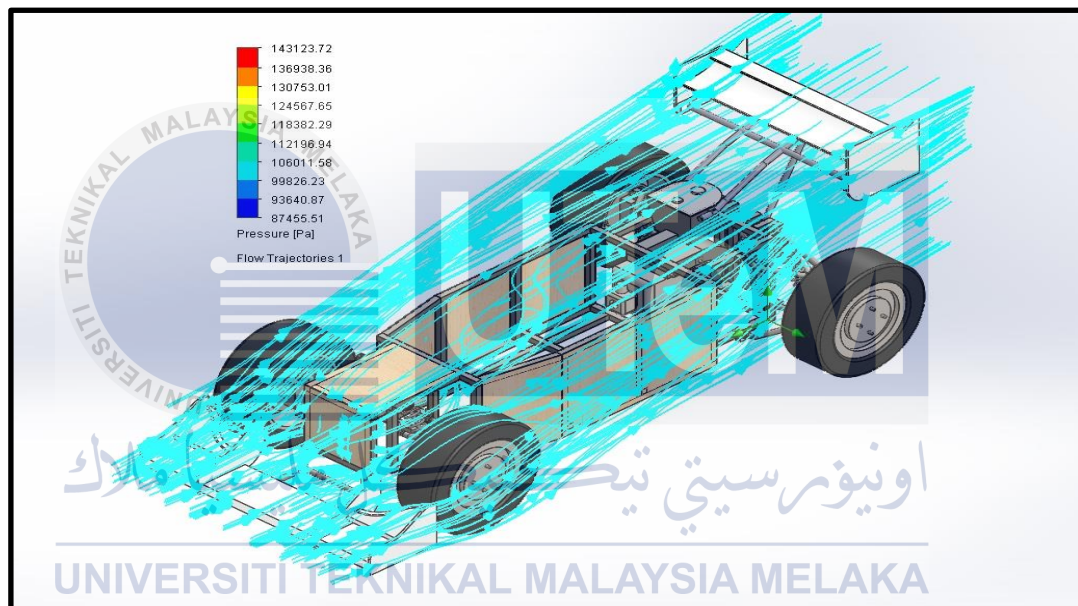


Figure 4.36: Isometric View for Pressure Flow Trajectories (DRS ON)



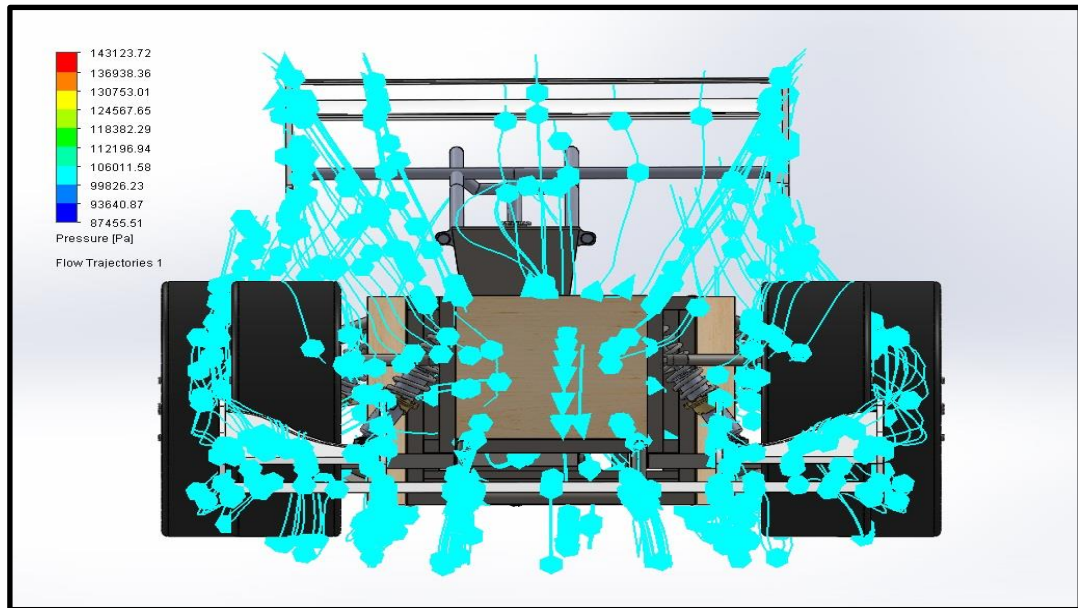


Figure 4.37: Front View for Pressure Flow Trajectories (DRS ON)

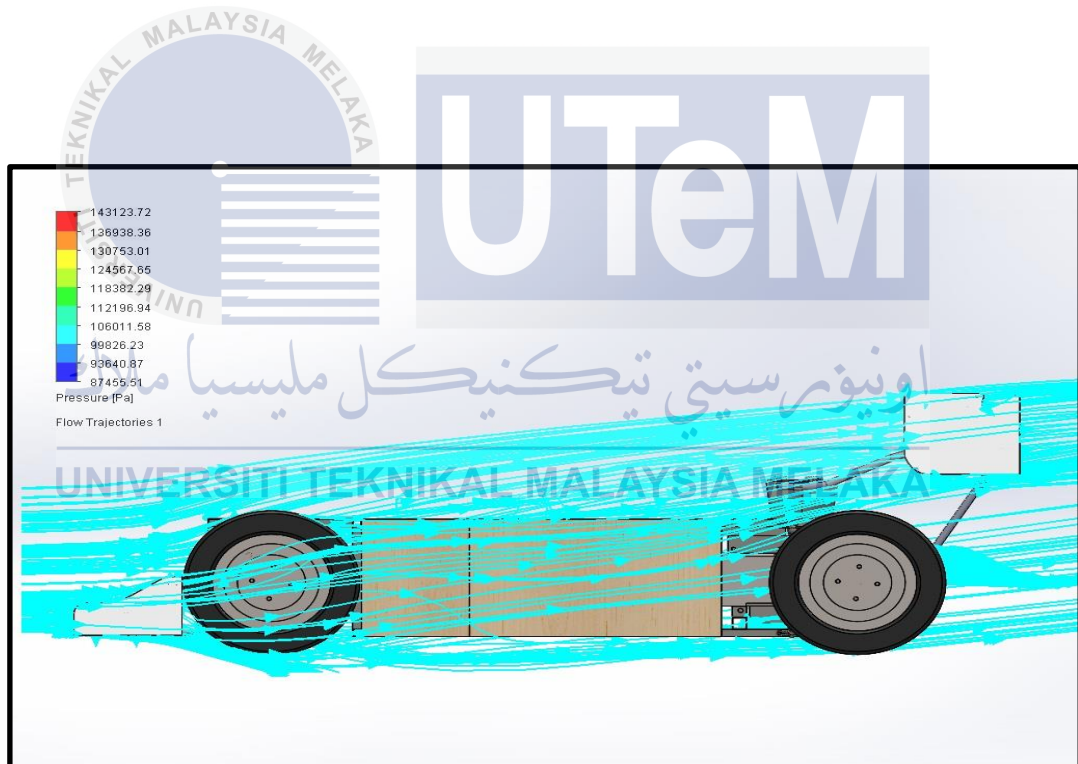


Figure 3.38: Side View for Pressure Flow Trajectories (DRS ON)

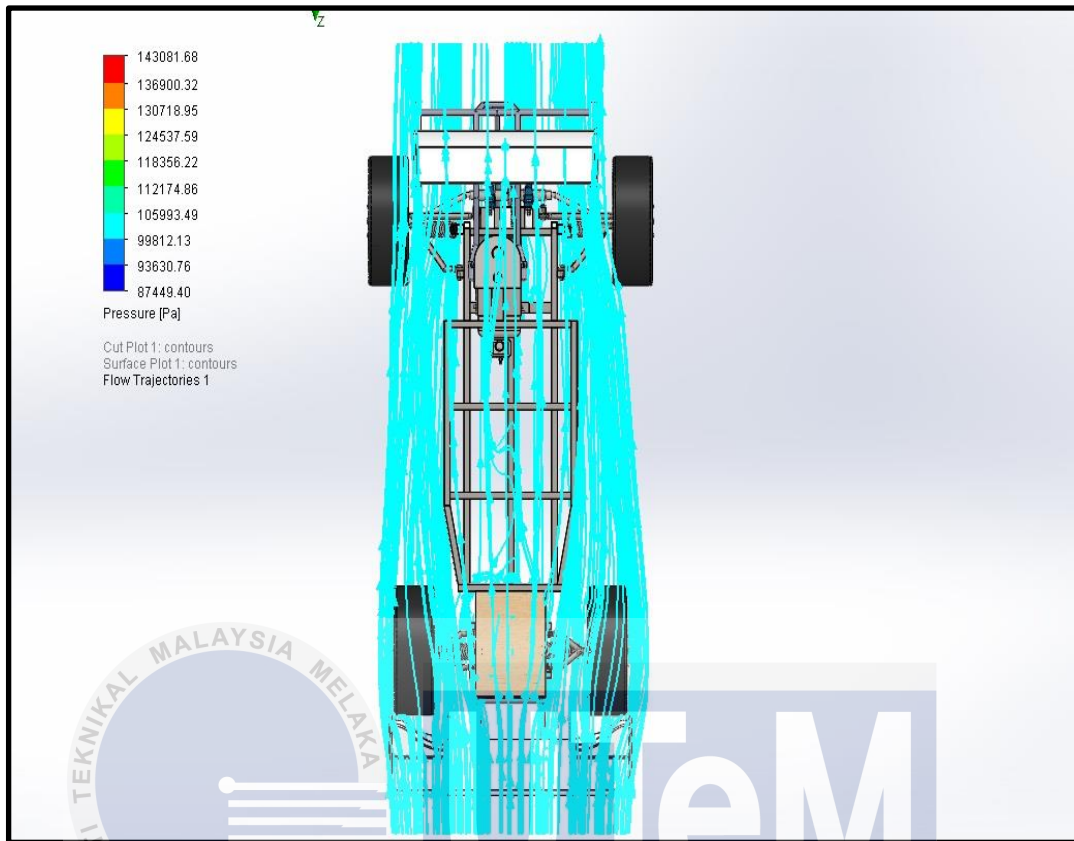


Figure 4.39: Top View for Pressure Flow Trajectories (DRS ON)

اونيورسيتي تیکنیکل ملیسیا ملاک

UNIVERSITI TEKNIKAL MALAYSIA MELAKA

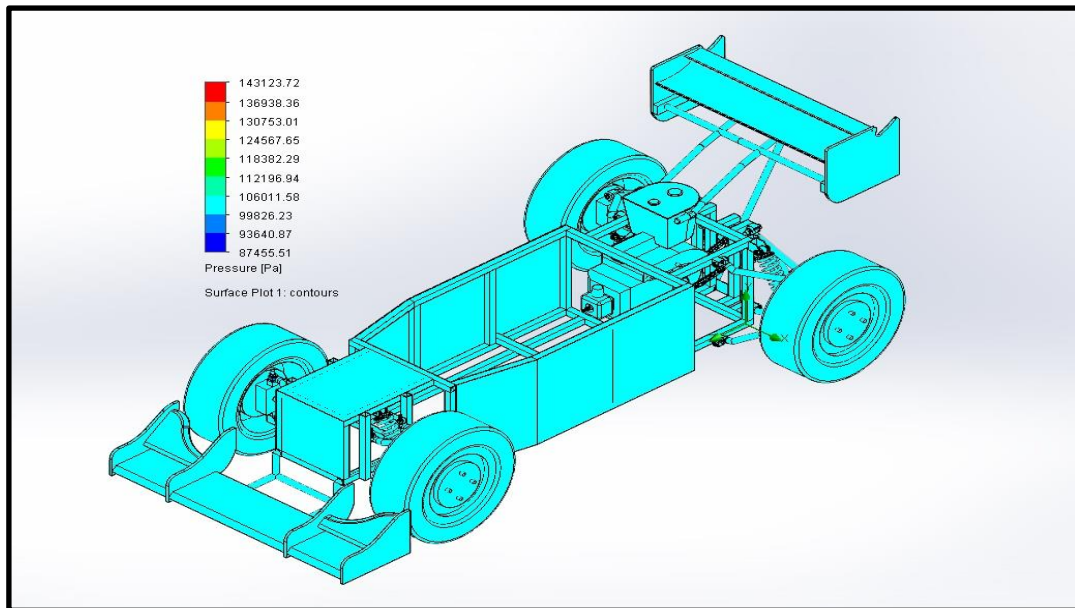


Figure 4.40: Isometric View for Pressure Surface Plot (DRS ON)

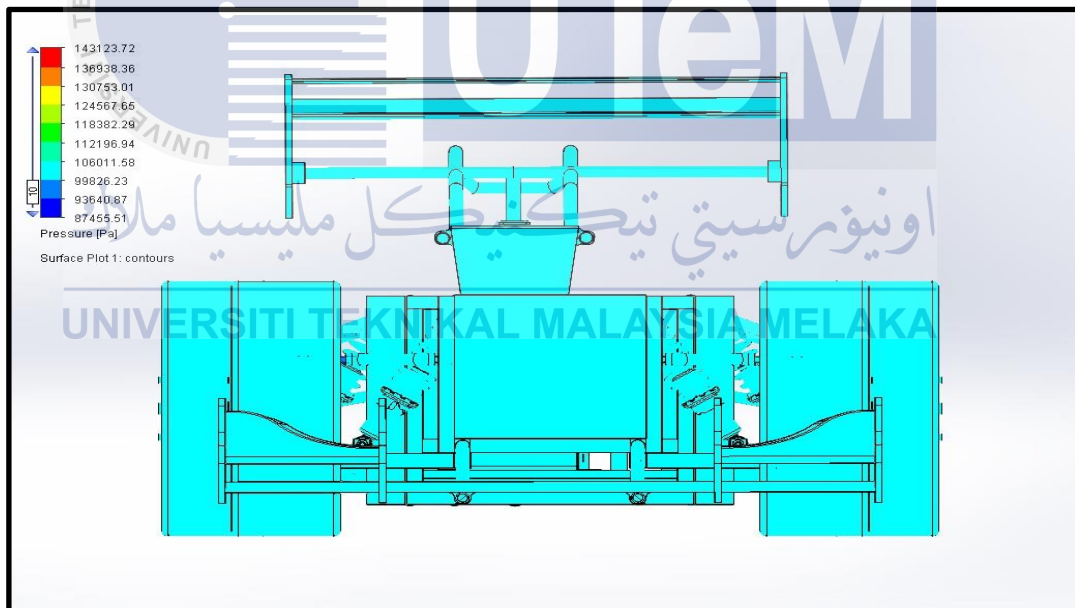


Figure 4.41: Front View for Pressure Surface Plot (DRS ON)

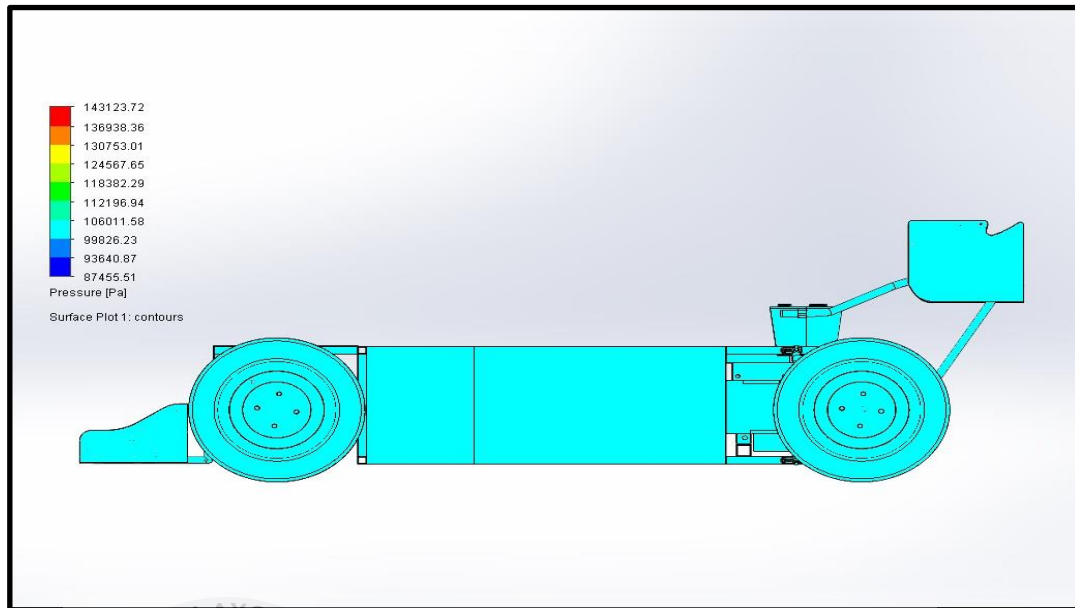


Figure 4.42: Side View for Pressure Surface Plot (DRS ON)

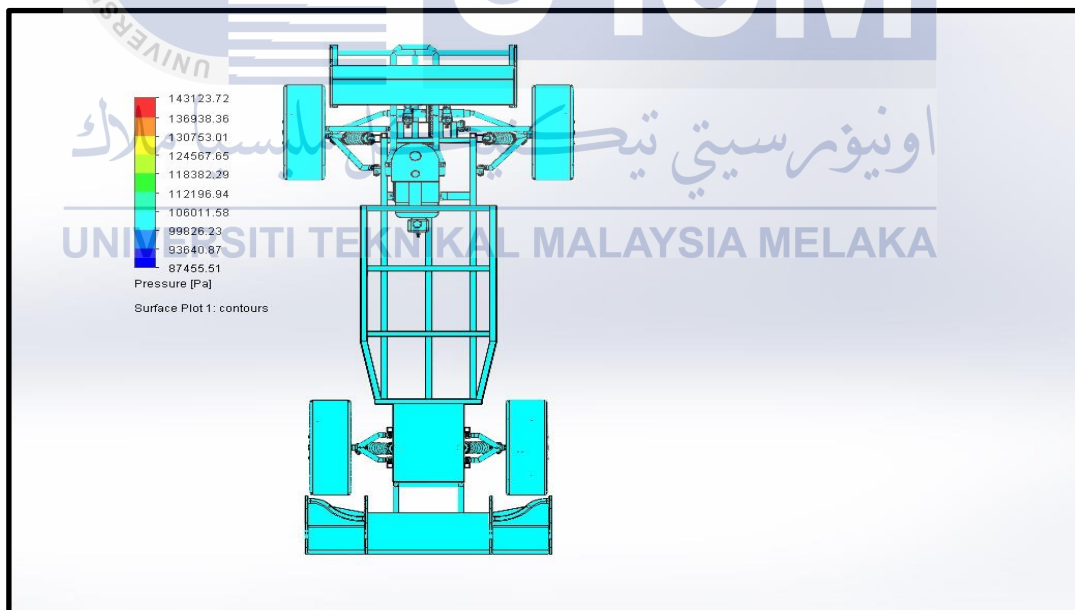


Figure 4.43: Top View for Pressure Surface Plot (DRS ON)



#### 4.3 Static Test (Real World Test)

In this part, results show the static in real world environment of full scale of Go-kart with front and rear wing attached. The simulation divided in two conditions, during DRS activated (DRS ON) and during DRS OFF.



Figure 4.44: Go-kart



4.3.1 Front Wing Test

Figure 4.45: Go-kart's Front Wing

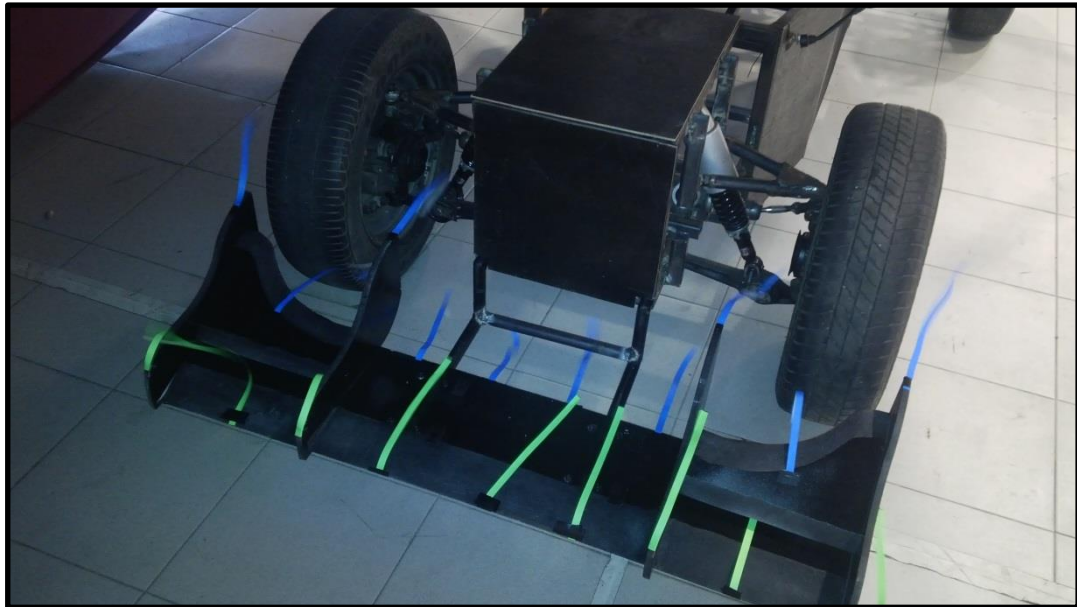


Figure 4.46: Go-kart's Front Wing Testing (a)



Figure 4.47: Go-kart's Front Wing Testing (b)



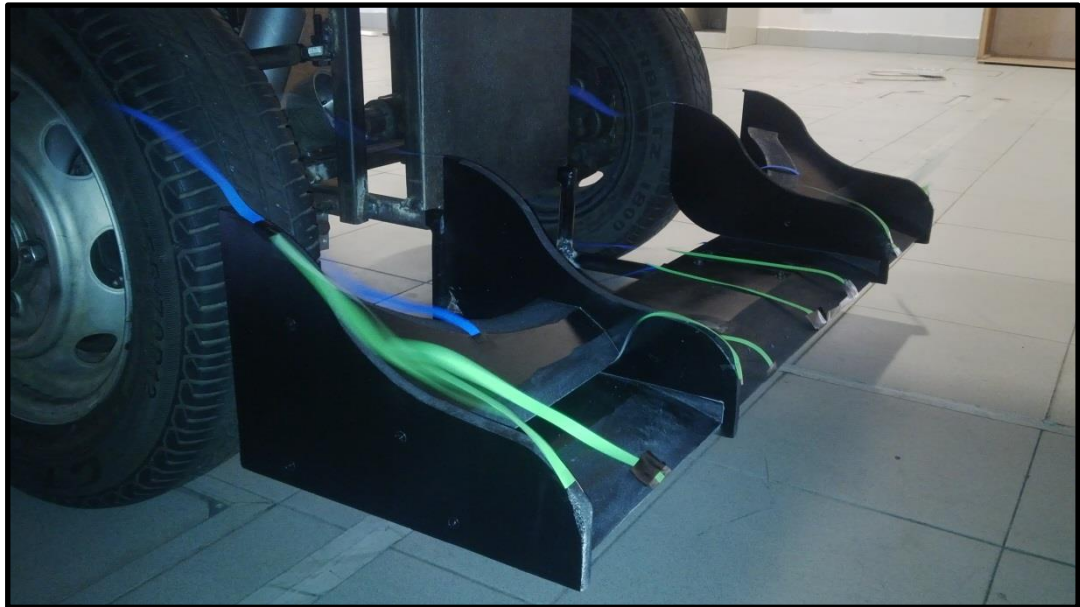


Figure 4.48: Go-kart's Front Wing Testing (c)

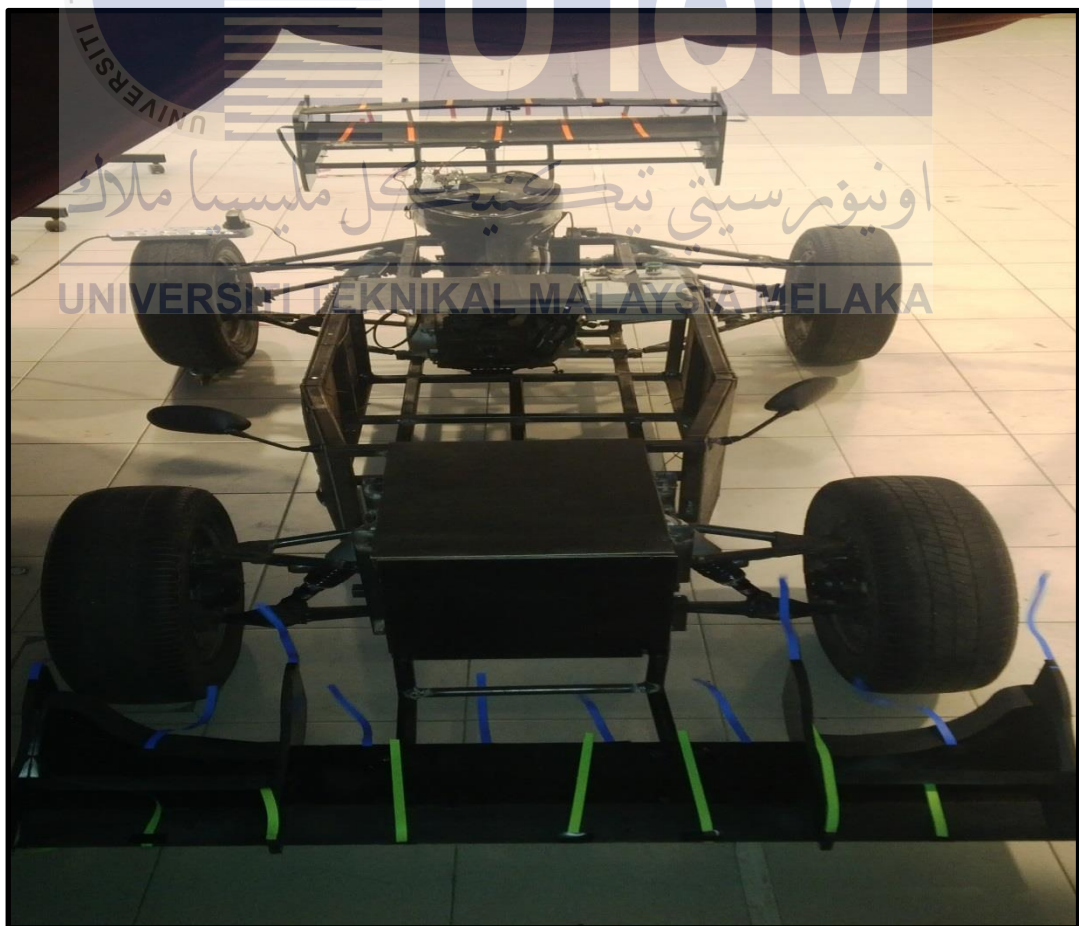


Figure 4.49: Go-kart's Front Wing Testing (d)

### 4.3.2 Rear Wing Test



Figure 4.50: Go-kart's Rear Wing

#### 4.3.2.1

#### Rear Wing (DRS OFF) Test



Figure 4.51: Go-kart's Front Wing (DRS OFF) Testing (a)

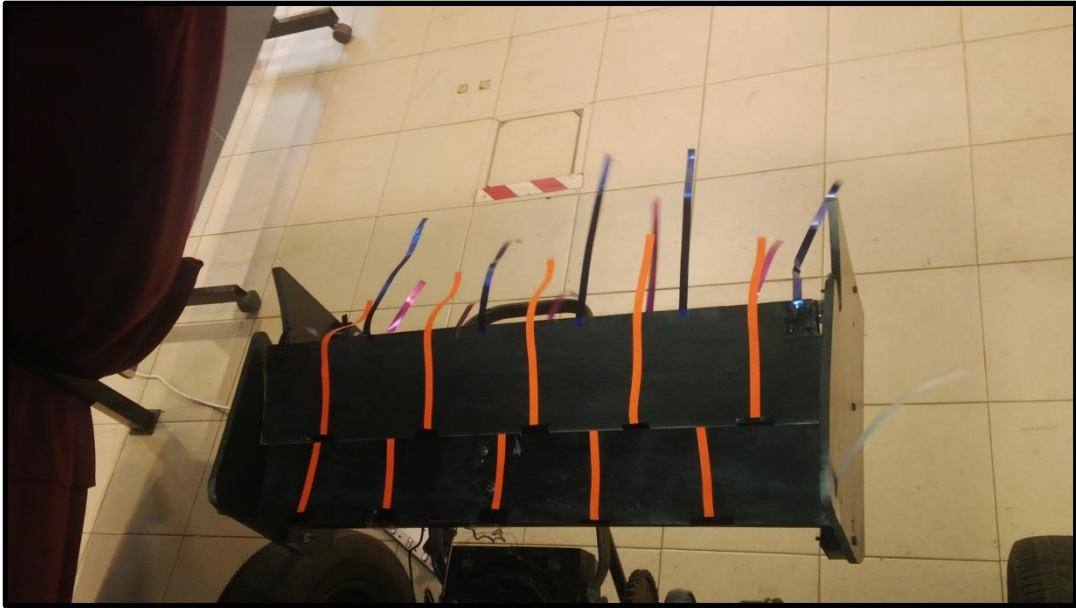


Figure 4.52: Go-kart's Front Wing (DRS OFF) Testing (b)



Figure 4.53: Go-kart's Front Wing (DRS OFF) Testing (c)



#### 4.3.2.1 Rear Wing (DRS ON) Test

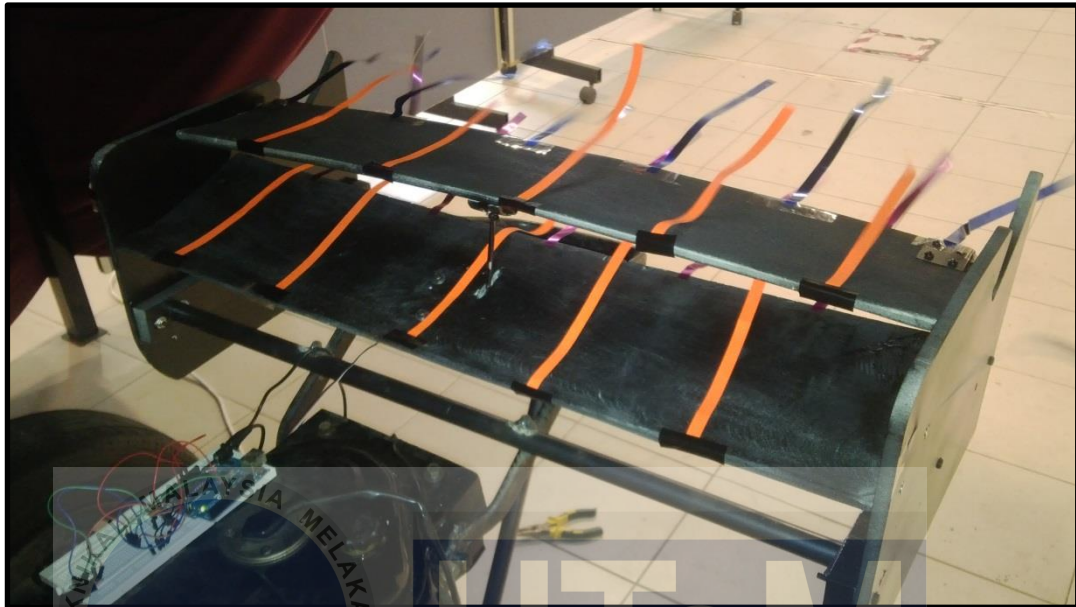


Figure 4.54: Go-kart's Front Wing (DRS ON) Testing (a)



Figure 4.55: Go-kart's Front Wing (DRS ON) Testing (b)

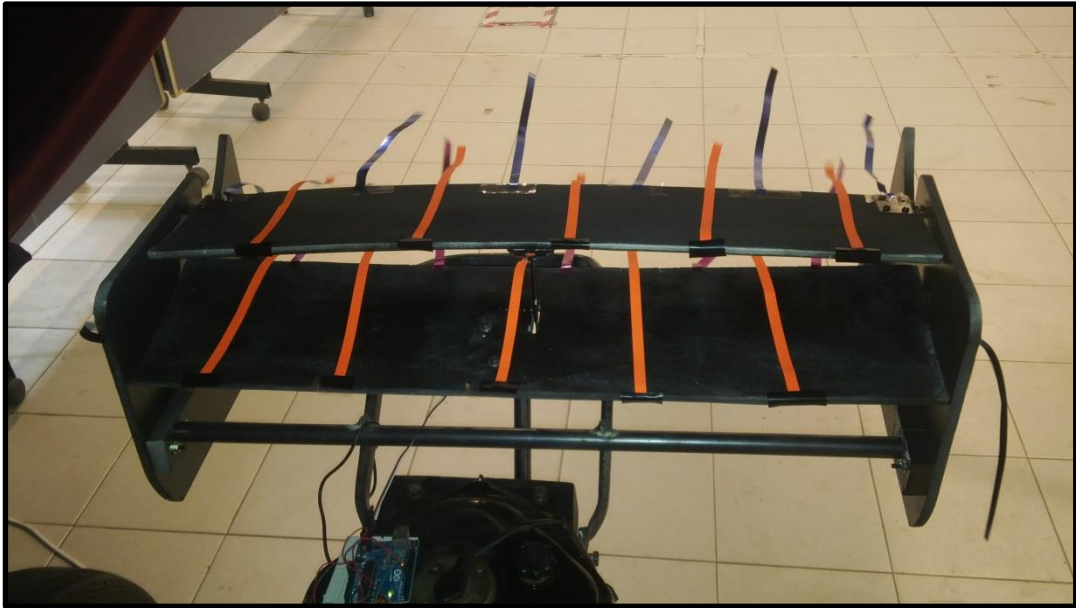


Figure 4.56: Go-kart's Front Wing (DRS ON) Testing (c)

## 4.4 Analysis

### 4.4.1 Front Wing Drag Force and Downforce

As seen in Table 4.1, front wing generates drag and lift force about 28.86750081 N and -33.67683727 N. The negative value of lift force indicates negative lift or in other word, downforce. The total drag coefficient obtained is approximately 0.193206041 with current front wing design. For the lift coefficient, the downforce is approximately -0.225394239, where the force acting toward gravity pushing the car to ground.

Table 4.6: Go-kart's Front Wing Pressure Simulation Result comparison

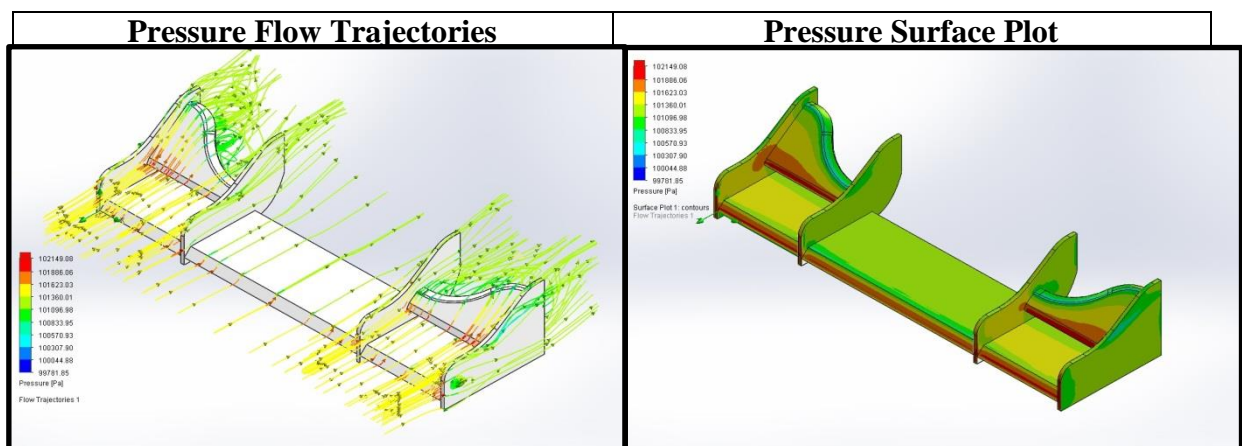


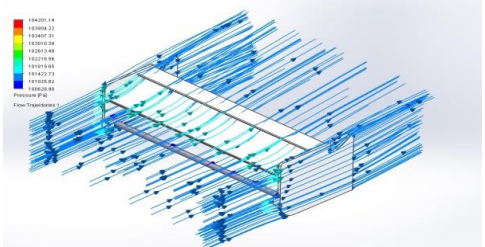
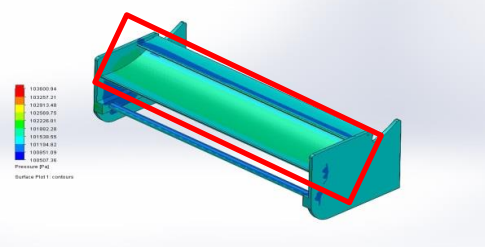
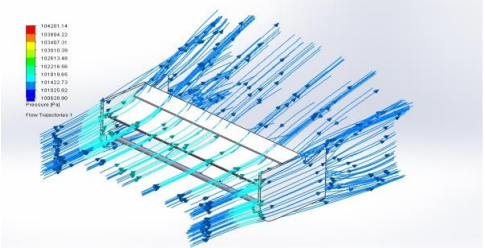
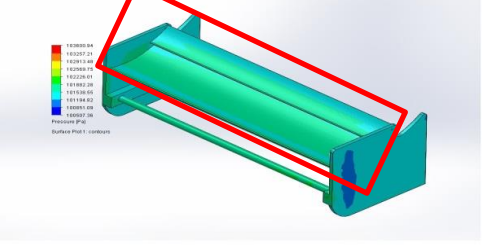
Table 4.6 shows the total pressure through the front wing. The pressure distribution reveals a high pressure region in front of the wing, at the first contact surface due to air slows down. Then the pressure decreases as the flow accelerates over the surface of the wing. This condition creates unwanted lift, in the same time decrease the normal force. As a result, this phenomenon creates a drag force. Downforce acting perpendicular to the drag force increasing and always larger than drag force. The red area of pressures distributions shows the stagnation pressure where the velocity is zero and the static pressure is at maximum value.

#### 4.4.2 Rear Wing DRS OFF and DRS ON

From the result of the simulation, rear wing generate more negative lift (downforce) force compare to drag force. At condition of the flap wing or aileron wing in 10mm position (DRS OFF), rear wing generate -72.04246262N and 43.09434726N in lift and drag force respectively. During the flap wing in 50mm position away from main plane (DRS ON), rear wing generate -68.03264103N and 29.27609195N in lift and drag force respectively. From the result obtained, during DRS was activated, drag force reduce almost half from initial force or in condition DRS OFF. This shows that by moving the flap wing away from main plane will reduce the force that opposes the forward direction. At the same time, during DRS activated, downforce simultaneously reduce along with drag force and large drop in both forces.



Table 4.7: DRS OFF and DRS ON of Rear Wing comparison

DRS	Pressure Flow Trajectories	Pressure Surface Plot
ON	 <p>Flow Trajectories</p> <p>Pressure (Pa)</p> <p>104201.14 103984.22 103867.31 103750.40 103633.49 103516.58 103400.00 103283.00 103166.00</p>	 <p>Surface Plot 1 - contours</p> <p>Pressure (Pa)</p> <p>103984.22 103867.31 103750.40 103633.49 103516.58 103400.00 103283.00 103166.00</p>
OFF	 <p>Flow Trajectories</p> <p>Pressure (Pa)</p> <p>104201.14 103984.22 103867.31 103750.40 103633.49 103516.58 103400.00 103283.00 103166.00</p>	 <p>Surface Plot 1 - contours</p> <p>Pressure (Pa)</p> <p>103984.22 103867.31 103750.40 103633.49 103516.58 103400.00 103283.00 103166.00</p>

Figures of pressure distribution of rear wing in four different conditions are presented on Table 4.7. As can be seen on Table 4.7, there are slightly different in pressure distributions in two different conditions. As can be seen in marked region, the pressure distributions during DRS OFF larger compare to DRS ON. This shows that the pressure distribution high during DRS OFF and reduce during DRS ON. During DRS activated, the wing produce low-drag and in the same time downforce decrease. This is a reflection of the basic contradiction between the downforce and drag, where, low downforce comes with low aerodynamic drag and vice versa. When, DRS deactivated, the high pressure presses down the rear wing increasing the downforce as well as drag force.

Figures 4.57-4.60 shows the comparison graphs of aerodynamics forces and coefficients in two different conditions. The comparison graph shows clearer representation the difference between DRS ON and DRS OFF.

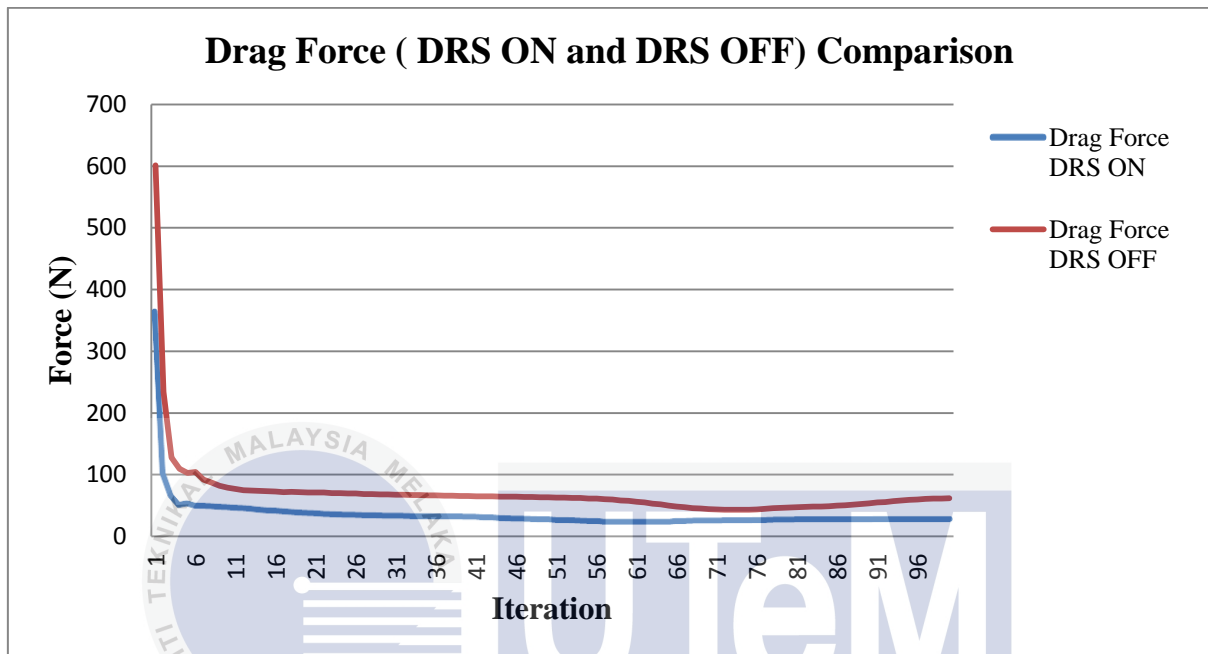


Figure 4.57: Graph of Drag Force of a Rear Wing during DRS ON and DRS OFF Comparison

Figure 4.57 shows the comparison graph of drag force versus number of iterations. As can be seen in Figure 4.57, drag force during DRS activated lower than the drag force during DRS in OFF condition. At iteration 1, the different of drag force during DRS ON and DRS OFF almost 50% in different. Then gradually drops almost more than half from initial value. During DRS OFF, the average force is about 55.23042715N, then the minimum and maximum force approximately 43.09434726N and 60.85225584N respectively. During DRS ON, the average force was about 29.28886545N, then the minimum and maximum force approximately 29.15813664N and 29.51081491N respectively. It can be observed that when DRS ON, the drag force decrease approximately 32.07% after the DRS activated.

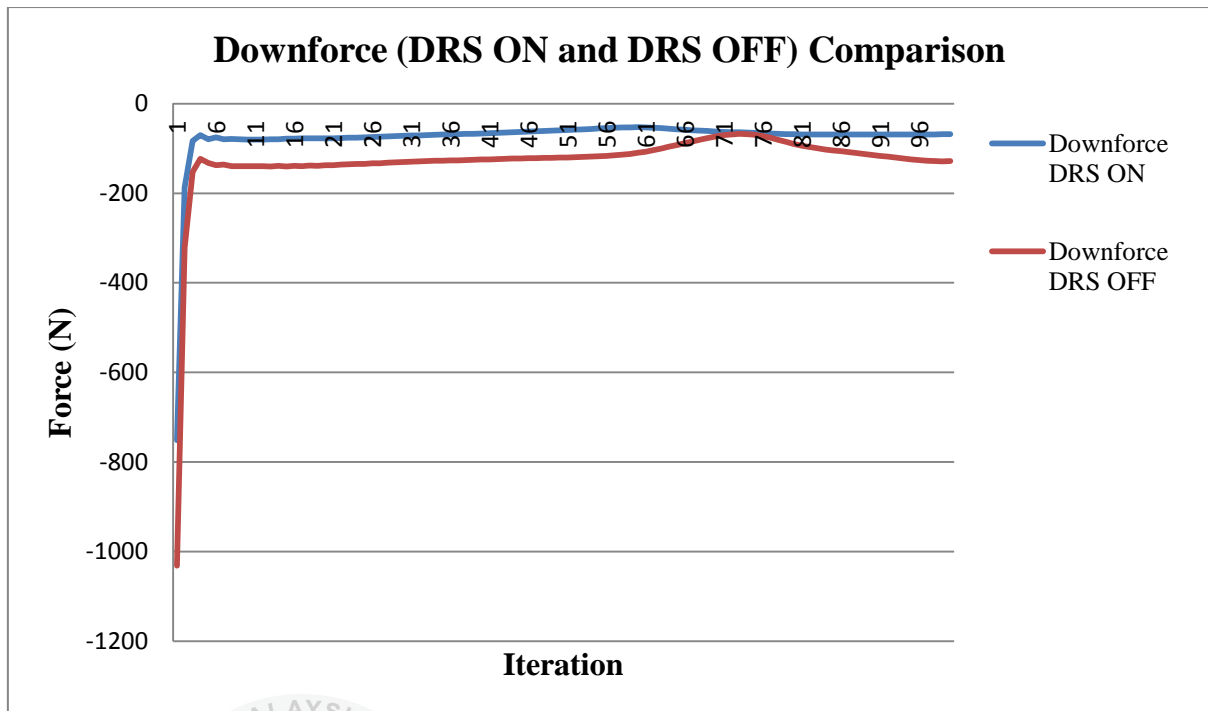


Figure 4.58: Graph of Downforce of a Rear Wing during DRS ON and DRS OFF Comparison

Figure 4.58 shows the negative lift force acting on the rear wing. Graph in Figure 4.58 shows the comparison of downforce (negative lift) of a rear wing in two set of conditions. To be noted that, the negative value is only a vector whereas represents the direction of the force. The negative lift shows the force acting towards the gravity, these phenomena known as downforce. At iteration 1, the difference of downforce during DRS ON and DRS OFF are approximately 20%. Then the both force gradually drop almost more than 80% from initial value. During DRS OFF, the average force is about -105.2466044N, then the minimum and maximum force approximately -72.04246262N and -117.190273N respectively. During DRS ON, the average force was about -67.99033602N, then the minimum and maximum force approximately -67.63386411N and -68.43785184N respectively. It can be observed that when DRS ON, the downforce decrease approximately 20% after the DRS activated.

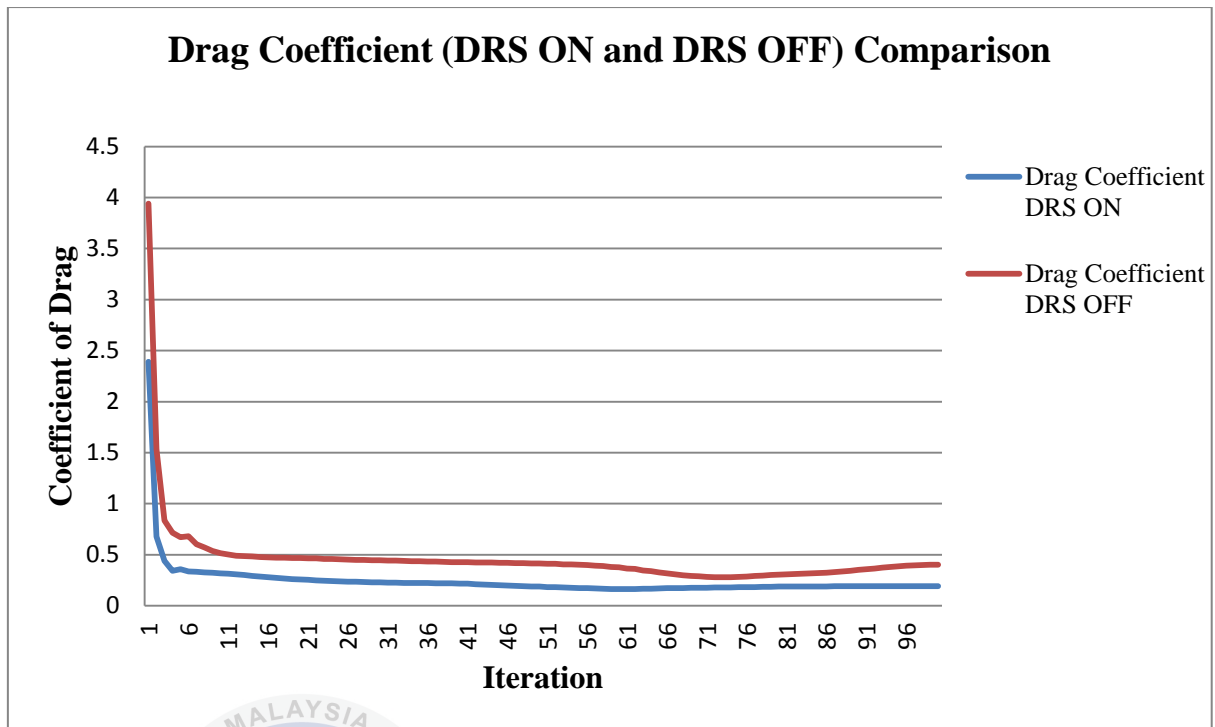


Figure 4.59: Graph of Drag Coefficient of a Rear Wing during DRS ON and DRS OFF Comparison

Figure 4.59 shows the comparison graph of coefficient of drag versus number of iterations. As can be seen in Figure 4.59, drag coefficient during DRS activated lower than the drag coefficient during DRS in OFF condition. At iteration 1, drag coefficient during DRS ON and DRS OFF almost 50% in different. Then both of the drag coefficients gradually drop almost more than half from initial its value. During DRS OFF, the average force is about 0.361838483, then the minimum and maximum forces approximately 0.28232976 and 0.398669521 respectively. Moreover, during DRS ON, the average drag coefficient was about 0.191884061, then the minimum and maximum force approximately 0.1910276 and 0.193338148 respectively. It can be observed that when DRS ON, the drag coefficient decrease almost 50% after the DRS activated.

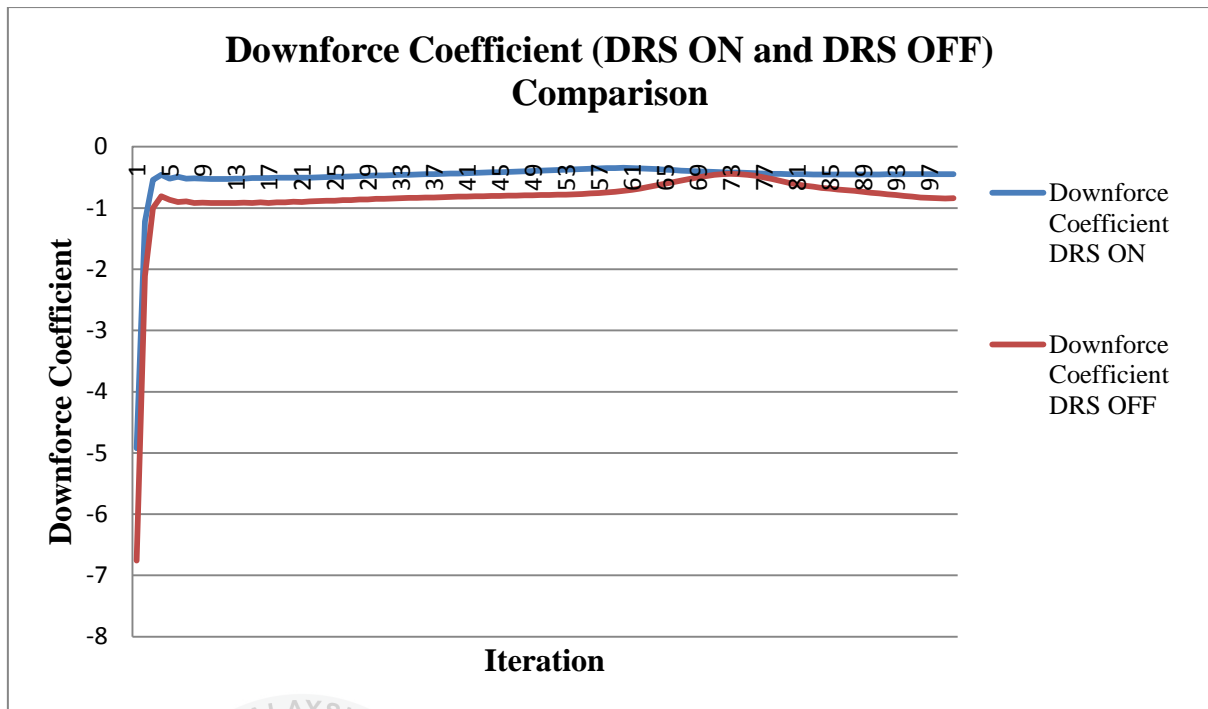


Figure 4.60: Graph of Downforce Coefficient of a Rear Wing during DRS ON and DRS OFF Comparison

Figure 4.60 shows the downforce (negative lift) coefficient acting on the rear wing. Graph in Figure 4.60 shows the comparison of downforce coefficient of a rear wing in two set of conditions. At iteration 1, downforce coefficient during DRS ON and DRS OFF approximately 20% in different. Then the downforce coefficients gradually drop almost more than 80% from initial value. During DRS OFF, the average force is about -0.689516154, then the minimum and maximum value approximately -0.767764308 and -0.47198142 respectively. During DRS ON, the average force was about -0.44543418, then the minimum and maximum value approximately -0.443098779 and -0.448366051 respectively. It can be observed that when DRS ON, the downforce decrease approximately 20% before the DRS activated.

#### 4.4.3 Full Scale Go-Kart Comparison

In this section, full scale of Go-kart analysis was performed in Solidworks Flow Simulation to investigate the pressure distribution and aerodynamics elements. The results analysed in two parts, comparison on pressure flow in three-dimensional simulation and comparison by using graph.

Table 4.8: DRS ON and DRS OFF of Full Scale Go-kart comparison

DRS	Pressure Flow Trajectories	Pressure Surface Plot
ON		
OFF		

Figures of pressure distribution of full scale in two different conditions are presented on Table 4.8. As can be seen on Table 4.8, pressure distribution through the Go-kart in both condition are almost the same. The pressure distribution reveals low pressure region in all parts of the Go-kart in both DRS conditions. There are no big changes in pressure distributions through the Go-kart. However, from the result of the simulation, at condition of the flap wing or aileron wing in 10mm position (DRS OFF), full scale go-kart generate 255.277854N and -55.0318996N in drag force and downforce respectively. Moreover, during the flap wing in 50mm position away from main plane (DRS ON), rear wing generate 254.4428811N and -55.70474255N in drag force and downforce respectively. From the result obtained, during DRS was activated drag force decrease to 0.83449729N or about 0.327% improvement.

Figures 4.61-4.64 shows the comparison graphs of aerodynamics forces and coefficients in two different conditions. The comparison graph shows clearer representation the difference between DRS ON and DRS OFF in Full Scale Go-kart.

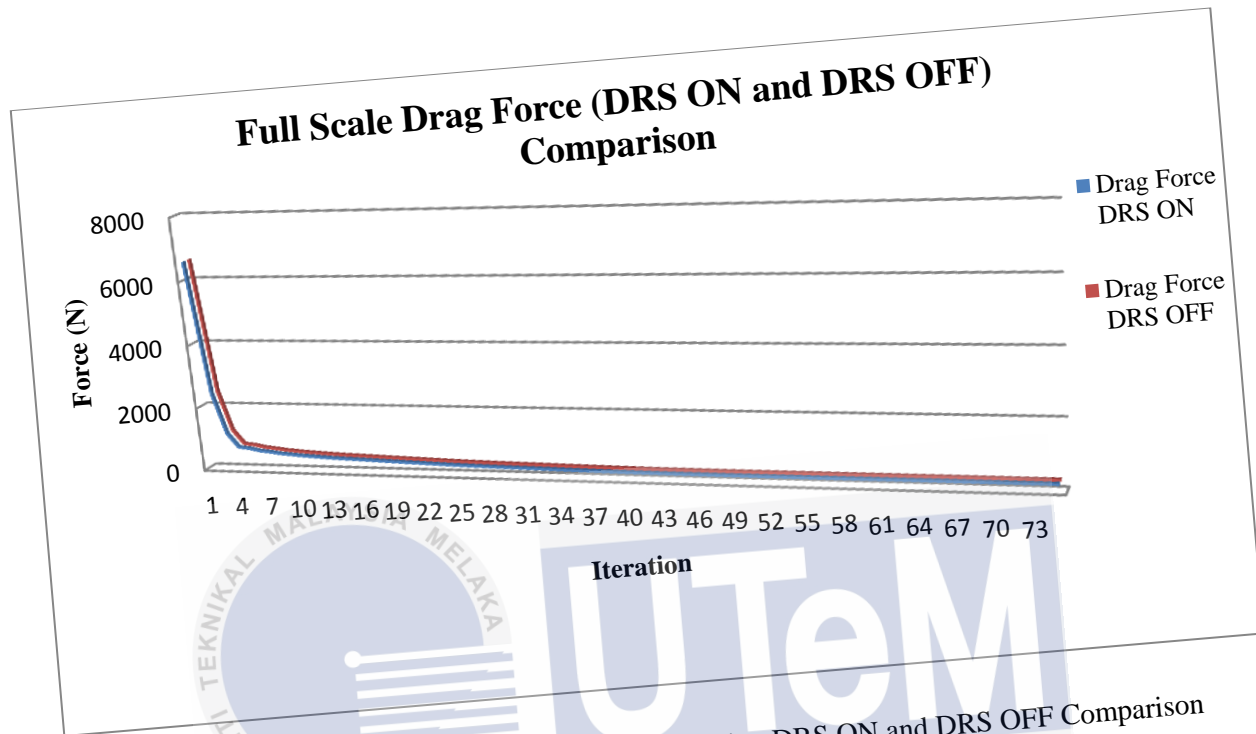


Figure 4.61: Graph of Drag Force of a Rear Wing during DRS ON and DRS OFF Comparison

Figure 4.61 shows the comparison graph of drag force versus number of iterations. As can be seen in Figure 4.61, there are no big difference of forces between DRS activated and DRS OFF. The average drag force during DRS OFF is about 253.2919693N, then the minimum and maximum force approximately 249.7055744N and 255.277854N respectively. During DRS activated, the average force was about 252.7436586N, then the minimum and maximum force approximately 249.5498352N and 254.7979508N respectively. It can be observed that when DRS ON, the drag force decrease only 0.5483053N or about 0.21% improvement in drag reduction.



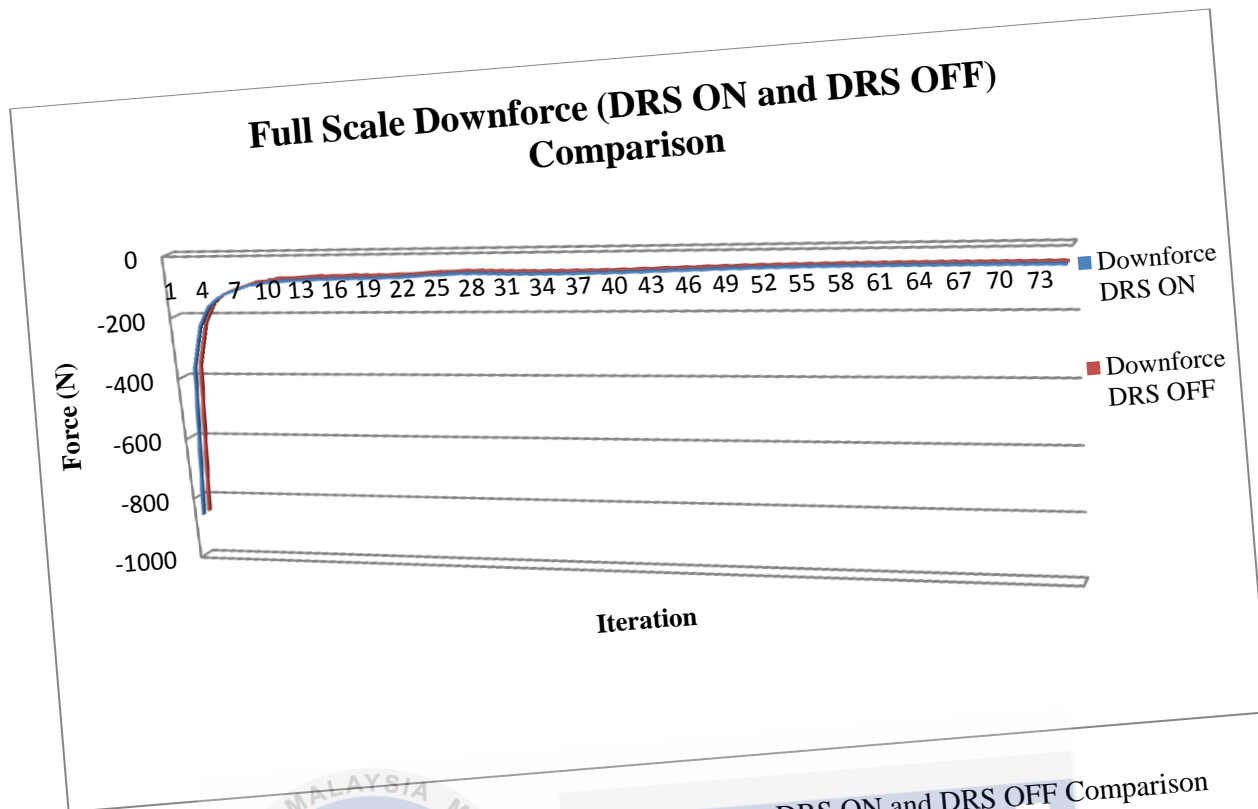


Figure 4.62: Graph of Downforce of a Rear Wing during DRS ON and DRS OFF Comparison

Figure 4.62 shows the comparison graph of downforce versus number of iterations. As can be seen in Figure 4.62, there are no big difference of forces between DRS activated and DRS OFF. The average downforce during DRS OFF is about  $-56.04434086\text{N}$ , then the minimum and maximum force approximately  $-54.84792629\text{N}$  and  $-59.41734485\text{N}$  respectively. During DRS activated, the average force was about  $-55.94515108$ , then the minimum and maximum force approximately  $-54.9912329\text{N}$  and  $-60.00904916\text{N}$  respectively. It can be observed that when DRS ON, the downforce increase about  $0.14330661\text{N}$  or about  $0.26\%$ . In this simulation, the downforce was increasing instead of decreasing.



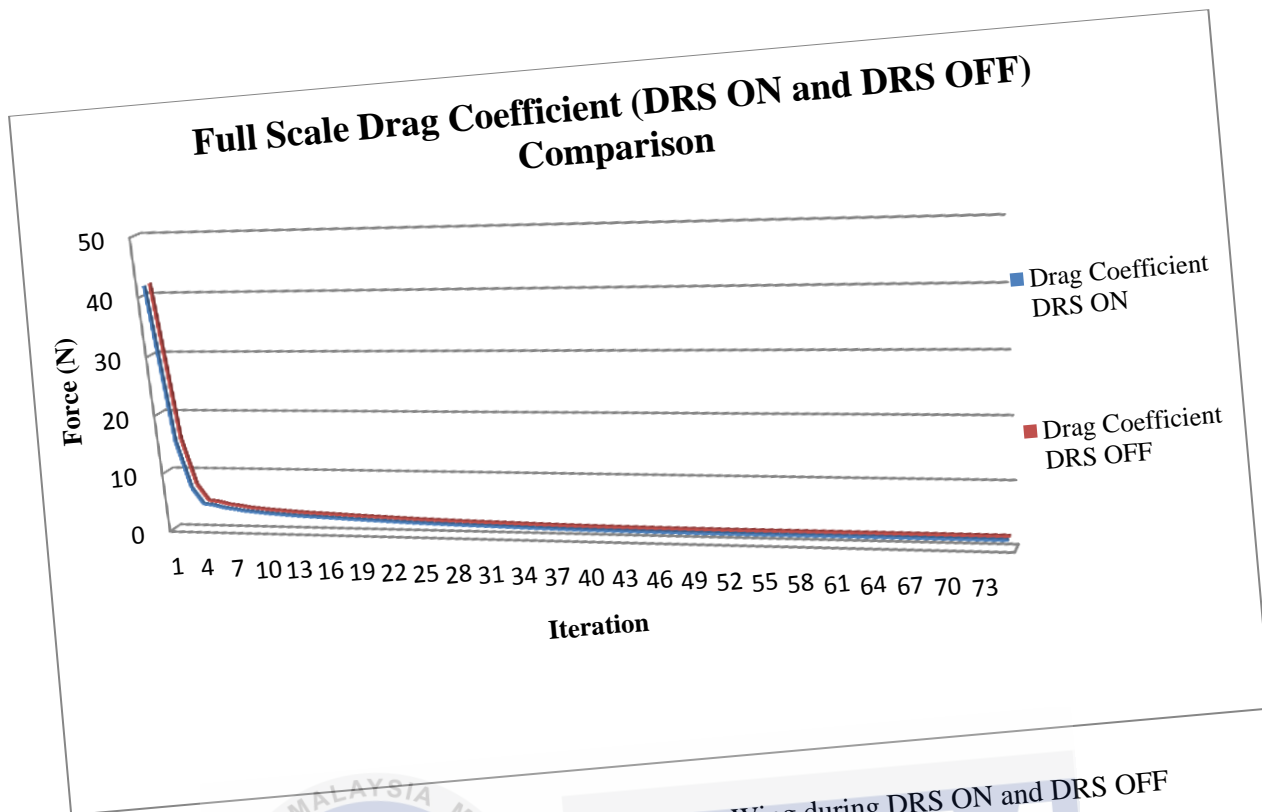


Figure 4.63: Graph of Drag Coefficient of a Rear Wing during DRS ON and DRS OFF Comparison

Figure 4.63 shows the comparison graph of drag coefficient versus number of iterations. As can be seen in Figure 4.63, there are no big difference of drag coefficient between DRS activated and DRS OFF. The average drag coefficient during DRS OFF is about 1.615345061, then the minimum and maximum coefficients approximately 1.580084838 and 1.615345061 respectively. During DRS activated, the average coefficient was about 1.599309201, then the minimum and maximum coefficients approximately 1.579099352 and 1.612308334 respectively. It can be observed that when DRS ON, the drag coefficient decrease only 0.016 or about 0.9927% improvement in drag coefficient reduction.

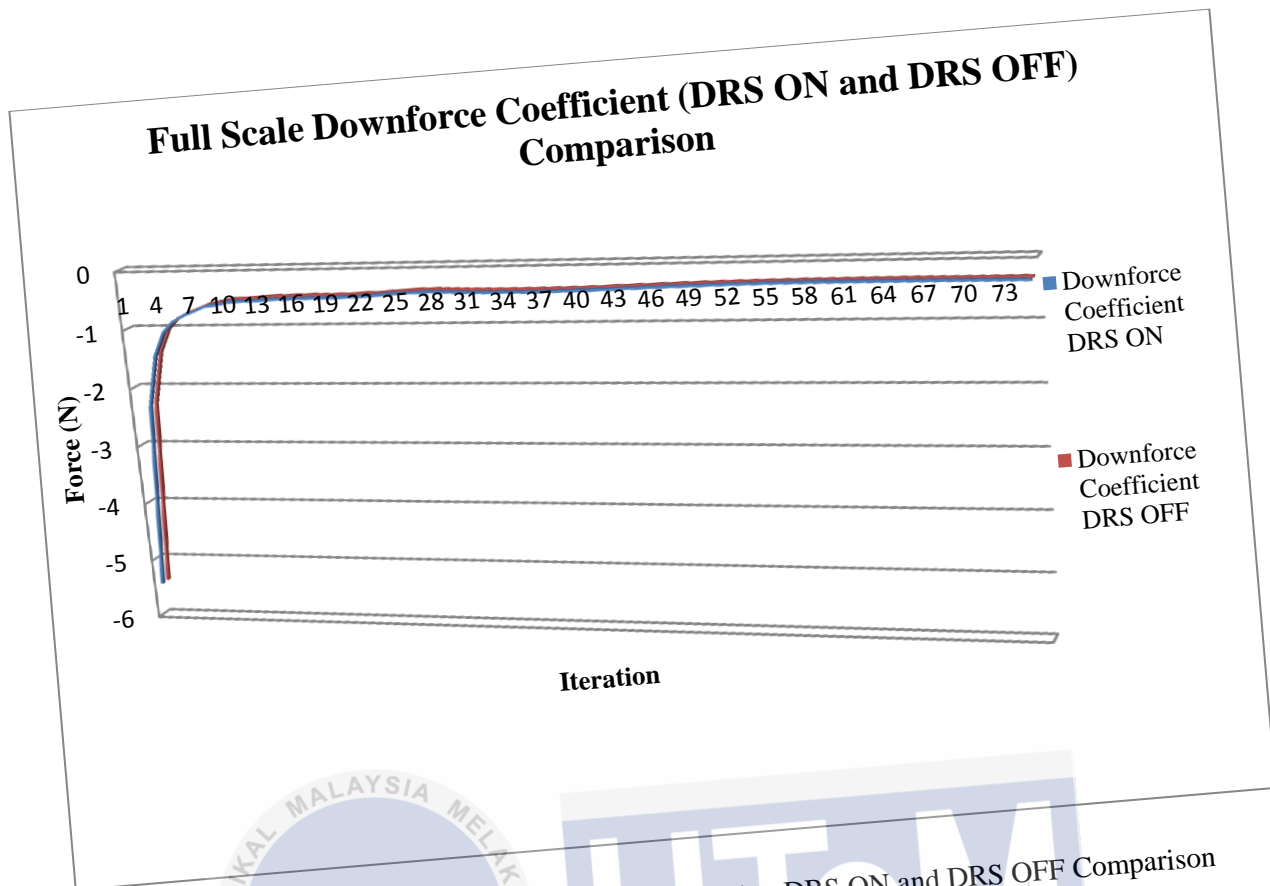


Figure 4.64: Graph of Drag Force of a Rear Wing during DRS ON and DRS OFF Comparison

Figure 4.64 shows the comparison graph of downforce (negative lift) coefficient versus number of iterations. As can be seen in Figure 4.64, there are no big difference of downforce coefficient between DRS activated and DRS OFF. The average downforce coefficient during DRS OFF is about -0.35463691, then the minimum and maximum coefficients approximately -0.347066248 and -0.375980576 respectively. During DRS activated, the average coefficient was about -0.352488002, then the minimum and maximum coefficients approximately -0.347973062 and -0.379724757 respectively. It can be observed that when DRS ON, the downforce coefficient increase about 0.0021 or about 0.606%. In this simulation, the downforce coefficient was increasing instead of decreasing.

4.4.4 Simulation and static test result comparison

Table 4.9: Flow trajectories of Rear Wing comparison (Isometric View)

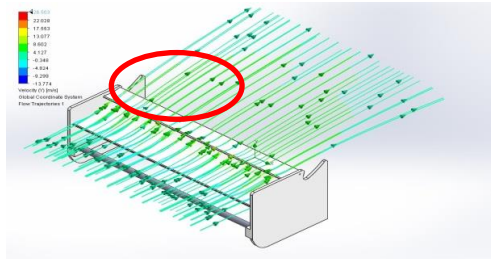

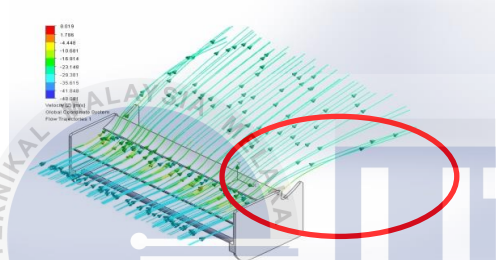

Test Type	Simulation	Static Test
DRS OFF		
DRS ON		

Table 4.10: Flow trajectories of Rear Wing comparison (Side View)

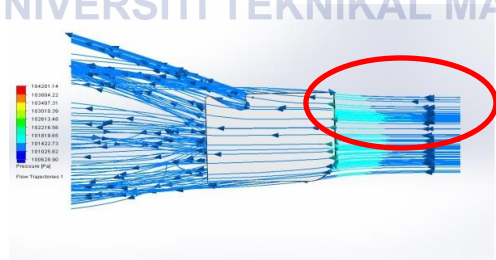

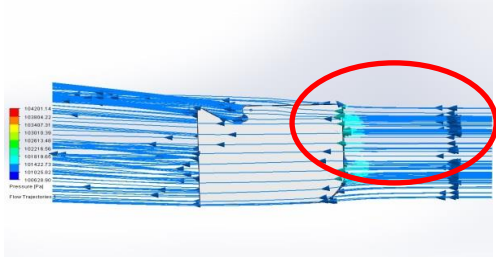

Test Type	Simulation	Static Test
DRS OFF		
DRS ON		

Table 4.11: Flow trajectories of Rear Wing comparison (Isometric View)

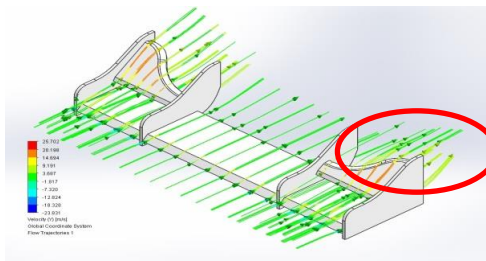

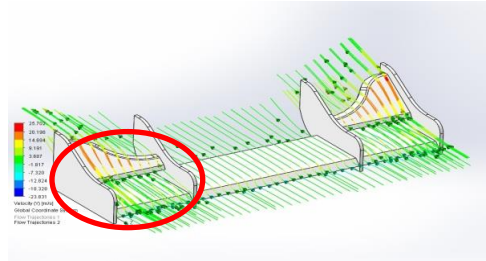

Test Type	Simulation	Static Test
<b>Downforce</b>		
<b>Drag Force</b>		

Table 4.9 - 4.11 show the comparison of flow trajectories simulation with static test in real world environment results. As can be seen in marked each area, there is slightly identical or similarity in flow trajectories between simulations and static tests.

## 4.5 Discussion

As mentioned earlier, during DRS ON race car experiences decreasing in drag force and downforce. From the simulation result, this theory has proven where both forces decrease during DRS was ON. The result confirms that actuated rear wing (DRS) increase the overall performance in aerodynamic, decreasing in both drag force and downforce. From the results, DRS reduce the drag force almost quarter or to more accurate about 32.07% from its initial value (during DRS OFF). Studies from [8], the drag improvement was about 32%, reduce in drag of rear wing only (not in full scale). However, this only valid for rear wing simulation results but not the full scale result. In full scale result, drag force reduce only in 0.9927%. In paper [11], author claims wings are considered ineffective at low operating speeds. However, the small improvement has shown significant benefit could be achieved in closed circuit lap times even considering the low operating speeds.

The purposes of downforce in race car are given car better traction [18] and the consequences decreasing in downforce may result lost car's stability. In order to avoid this problem, DRS will be turned on in straight-line track. The reasons are during cornering, the probability of the race car will oversteer is high compared to straight-line track. This also been stated at 2013 Formula One Technical Regulations, where adjustable bodywork (Drag Reduction System) only can be activated at a pre-determined point on the track during race [21].

Based on the simulation results, rear wing also contributes improving in downforce and reducing the drag force. Combinations of these aerodynamics elements may result improving in overall race car's performance.

There are several factors affecting the results in this study such as Go-kart's body structure, motion of Go-kart through the applied air flow and the air flow itself. Absence of aerodynamics car's body is the major factor affecting the result in this study. Due this factor, the air flows through the Go-kart are in proper streamlines of air. The airflow around the Go-kart separated causing existing of air turbulence.



However, the result from the simulation and static test in a real world environment does not really reliable. This is due to several constrain in static test such as the flow of air during testing, lack of equipment, the air flow from fan does not constant and other several factors. This is a major limitation in this study due to no proper equipment (such as wind tunnel) or other approach (such as different CFD analysis) to validate the results from simulations.



## CHAPTER 5

### CONCLUSION AND RECOMMENDATIONS

#### 5.1 Introduction

In the previous chapter, the outcome and result of the project has been presented. In this chapter contains a brief summary of this project and a recommendation as well.

#### 5.2 Conclusion

As a conclusion, the result confirms that actuated rear wing (DRS) increase the overall performance in aerodynamic, decreasing in both drag force and downforce. From the results, DRS reduce the drag force almost quarter or to more accurate about 32.07% from its initial value (during DRS OFF). In full scale result, drag force reduce only in 0.9927%. However, the small improvement has shown significant benefit could be achieved in closed circuit lap times even considering the low operating speeds.

A study is performed on aerodynamic front wing and rear for Go-kart in term of drag force and downforce. Both the forces on the wing and the flow trajectories are studied from an experimental and a simulation using Solidworks Flow Simulation approach. The main challenge of the present study is to compare aerodynamics element, deduced from experiments and simulation, with each other.



The Drag Reduction System (DRS) has been developed and the performance simulated using Solidworks Flow Simulation and tested in real world test. From the result of the simulations undertaken on this study, it can be conclude that DRS reduce the drag force as well as the downforce.

The front wing and rear wing has been developed and fabricated by using PVC form. Then, the completed wings attached to the Go-kart.

### 5.3 Recommendation

In order to make improvement to this project, there are some parameter needs to be considered. Firstly, go-kart is an open-wheeled car which means that effect the total area touch by the airstream. Therefore, the designs of the front wing have to be considering this matter in order to achieve optimum aerodynamic effects.

To validate the results from simulation, wind tunnel is required in order to obtain proper and accurate data. Instead of using wind tunnel, the results have to be compare with other simulation software such as ANSYS Fluent, Falcon Flow Simulation, and Catia Flow Simulation.

## REFERENCES

- [1] Yang,Z, Gu. W, Li. Q. Aerodynamic design optimazation of race car rear wing. *IEEE Journal.National Basic Research Program of China* , pp. 642-646.
- [2] Devaiah, B. N, Umesh. S. Enhancement of Aerodynamic Performance of a Formula-1 Race Car using Add-On Devices. *SASTECH Journal* . Bangalore , 2013, Vol. 12.
- [3] Adjustable rear wing - Drag Reduction System. Technical F1 - Dictionary. [Online] [Cited: november 1, 2013.] [http://www.formula1-dictionary.net/drs\\_wing\\_rear\\_movable.html](http://www.formula1-dictionary.net/drs_wing_rear_movable.html).
- [4] Jawad, B. and Longnecker, M., "Aerodynamic Evaluation on Formula SAE Vehicles," *SAE Technical Paper 2001-01-1270*, 2001, doi:10.4271/2001-01-1270.
- [5] Bruce .R. M, Donald .F. Y, Theodore .H .O,. *Fundamentals of Fluid Mechanics*. s.l. : John Wiley & Son Inc, 1998.
- [6] Yang,Z, Gu. W, Li. Q. Aerodynamic design optimazation of race car rear wing. *IEEE Journal.National Basic Research Program of China* , pp. 642-646.
- [7] Bao. H. Study the effect of rear spoiler on car aerodynamics characteristic. *The 6<sup>th</sup> International Conference on Computer Science & Education (ICCSE 2011)*. pp 460-463, 2011.
- [8] Wordley. S, Saunders. J. Aerodynamic for formula SAE : initial design and performance prediction. *SAE International*. 2006-01-0806. 2005
- [9] Devaiah, B. N, Umesh. S. Enhancement of Aerodynamic Performance of a Formula-1 Race Car using Add-On Devices. *SASTECH Journal*. Bangalore, 2013, Vol. 12.
- [10] Xin. Z. zerihan. J. Aerodynamic of a double-element wing in ground effect. *AIAA Journal*. Vol.41, No. 6, pp 1007-1016. 2003
- [11] Badih. A. J, Maria. M. L. Aerodynamic Evaluation on Formula SAE Vehicle. Society of Automotive Engineers Inc. 2001-01-1270, pp. 333-339.

- [12] McKay, N. and Gopalarathnam, A., "The Effects of Wing Aerodynamics on Race Vehicle Performance," *SAE Technical Paper 2002-01-3294*, 2002, doi:10.4271/2002-01-3294
- [13] Zhigang. Y, Gu. W, Qiliang. L. Aerodynamic design optimization of race car rear wing. *IEEE Conference Publications*. Vol. 3, pp. 642-646.2011
- [14] Jie. C, Gang. S, Xin. J. Intelligent Aerodynamic Design for Airfoil Based On Artificial Neural Network Method. *IEEE Journal*. Vol. 5, pp 289 – 293.2010
- [15] Chang.Y. J. Development of NURBS Based Wing Design Optimization. *School of Transportation System Engineering*. Korea.
- [16] Matsushima, K.; Iwamiya, T., "Aerodynamic shape design of wings using an inverse problem approach," High Performance Computing on the Information Superhighway, 1997. HPC Asia '97 , vol., no., pp.271,276, 28 Apr-2 May 1997doi: 10.1109/HPC.1997.592159 [17] Pehan. S, Kegl. B. Aerodynamics Aspects of Formula S Racing Car. *International Design Conference – Design 2002*. May 14-17 2002. Pp 1109-1116
- [18] Golossop. T, Jinks. S, Hopton R. A1\_1 Can an F1 Car Drive Upside Down?. *Journal of Physics Special Topics*. Department of Physics and Astronomy, University of Leicester, Leicester, LE1 7RH. Feb 1, 2011
- [19] Xin. Z, Willem. T, Jonathan. Z. Ground Effect Aerodynamics of Race Car. *Journal of ASME*. Jan 2006, vol. 59. Pp 33-49
- [20] P. V .Valkenburg. Race Car Engineering and Mechanics. 1<sup>st</sup> Edition. America: ISBN, 2000.
- [21] 2013 Formula One Technical Regulations, 2012 *Fédération Internationale de l'Automobile*, 2012

## APPENDICES





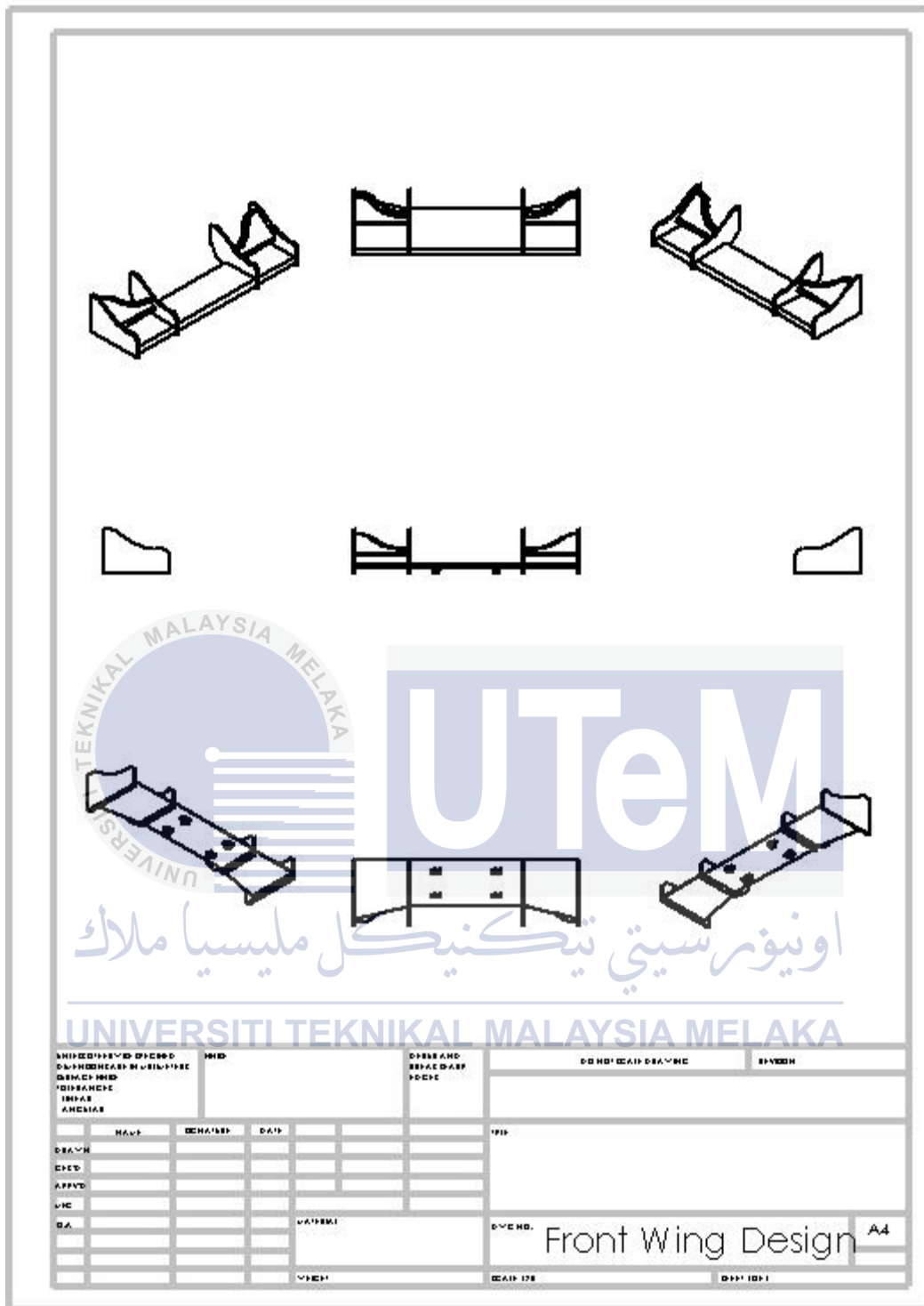


Figure A2: Front wing solidworks drawing dimension

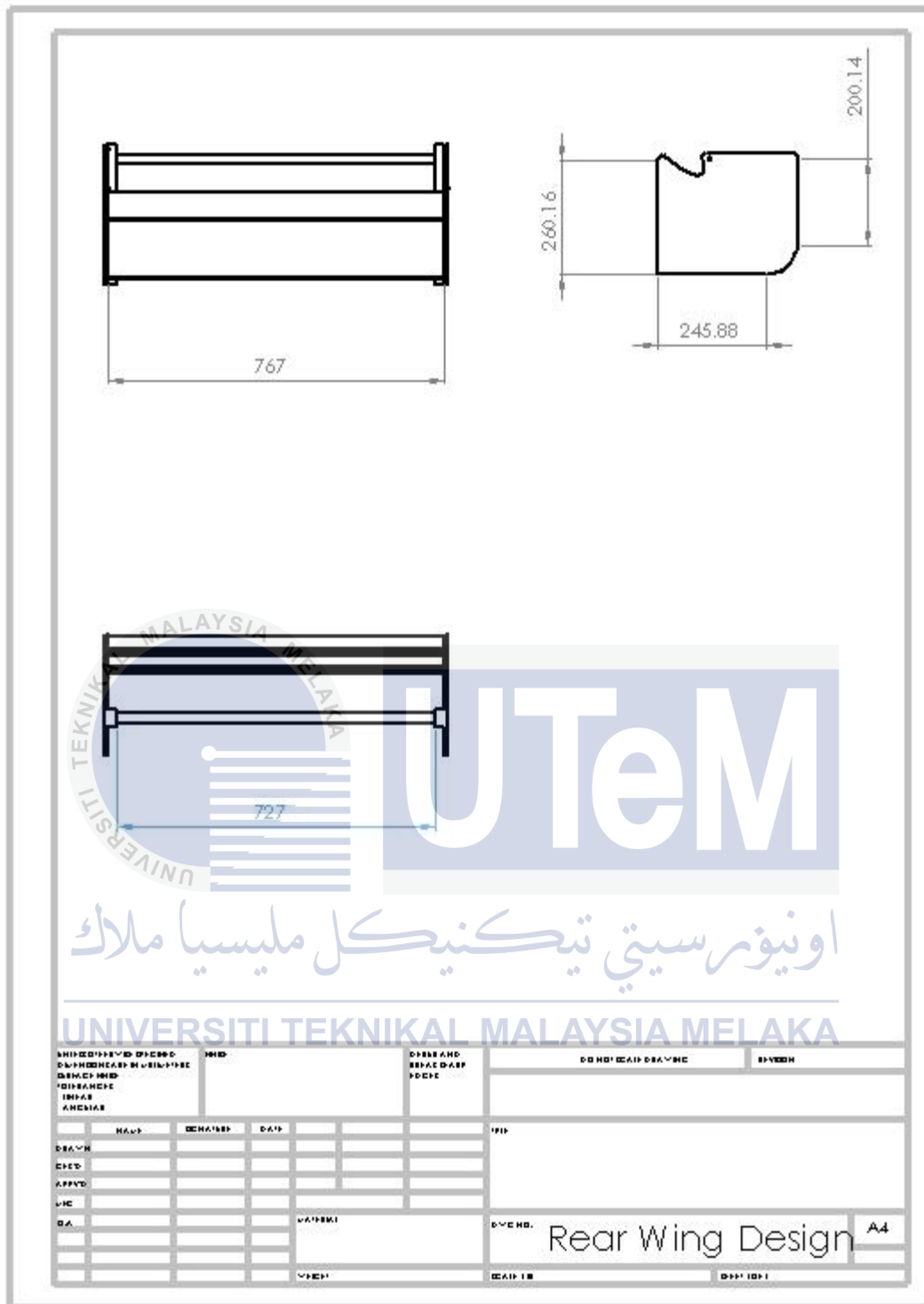


Figure A3: Rear wing solidworks drawing dimension



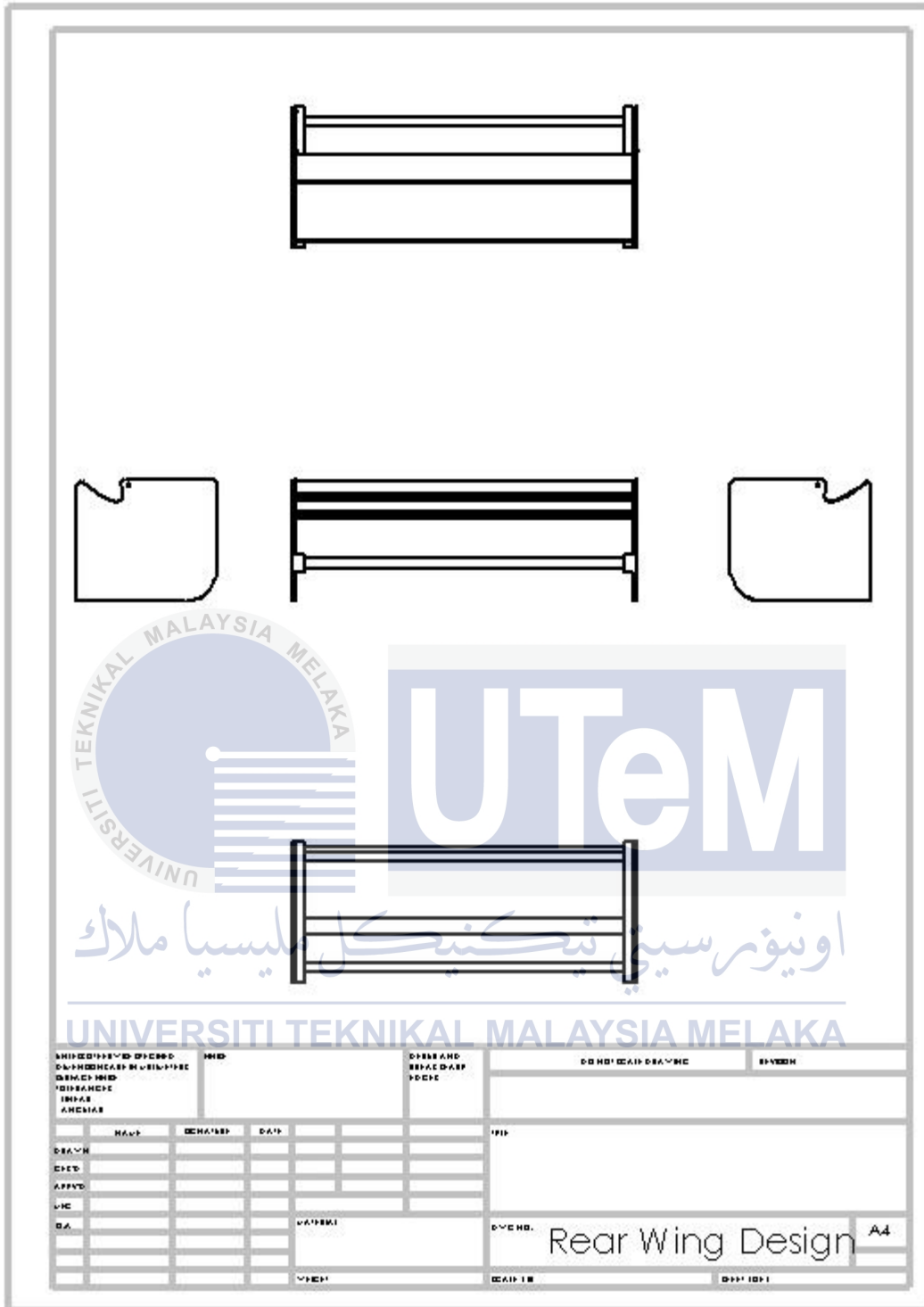


Figure A4: Rear wing solidworks drawing dimension







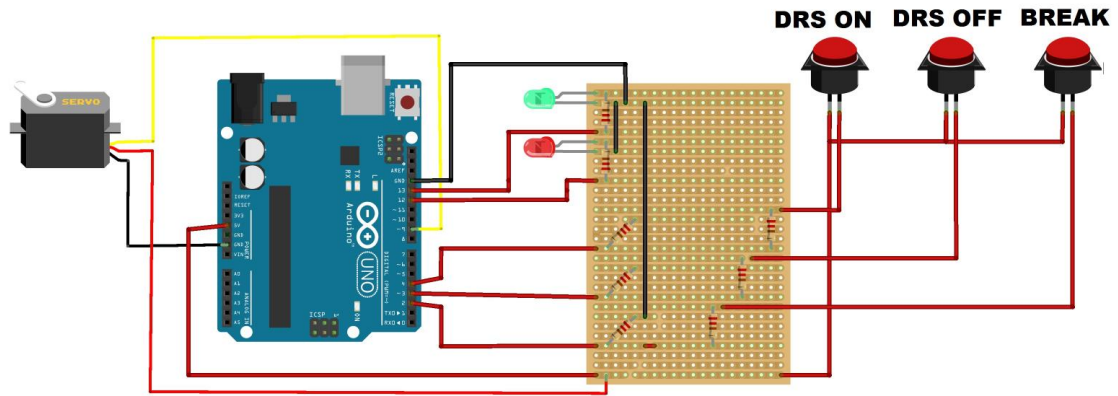


Figure C1: Circuit Diagram

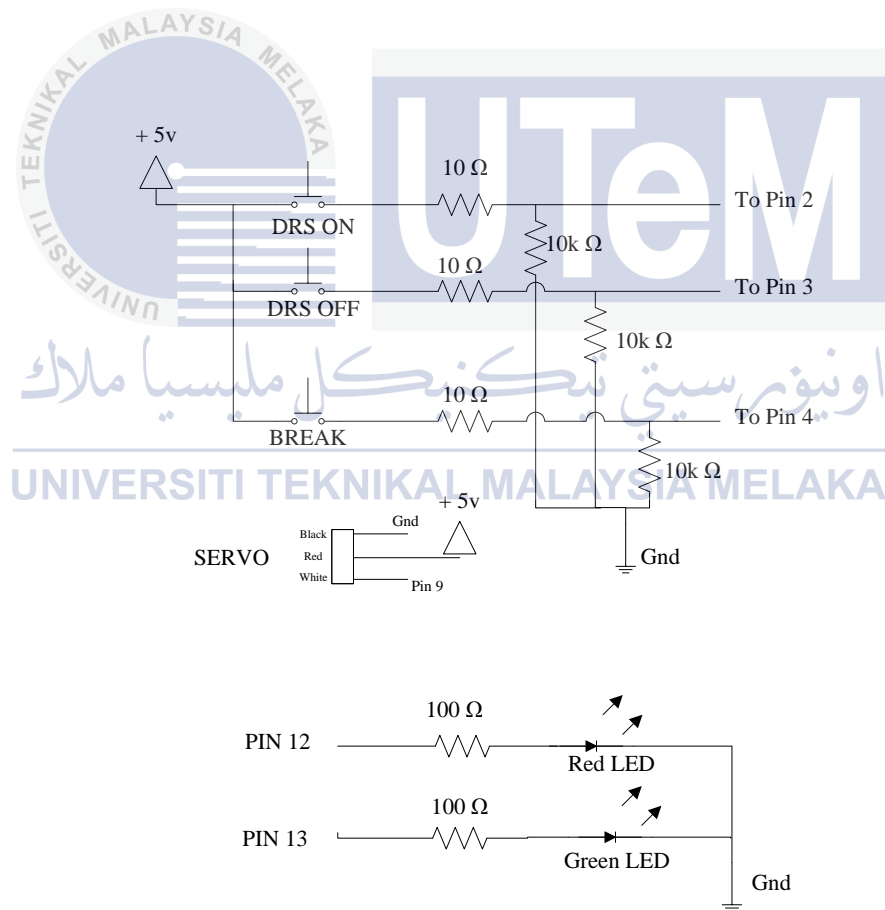


Figure C2: Circuit Schematic



```

#include <Servo.h>
Servo myservo; // create servo object to control a servo
int button2=0; // DRS ON Push Button
int button3=0; // DRS OFF Push Button
int button4=0; // Break Push Button
int pos=90; // initial position
int led1Pin = 12; // Red LED
int led2Pin = 13; // Green LED
void setup()
{
  pinMode(2, INPUT); //declare pin 2 as input (DRS ON)
  pinMode(3, INPUT); //declare pin 3 as input (DRS OFF)
  pinMode(4, INPUT); //declare pin 4 as input (BREAK)
  myservo.attach(9); //servo on pin 9
  pinMode(led1Pin, OUTPUT); // declare Red LED as output
  pinMode(led2Pin, OUTPUT); //declare Green LED as output
}
void loop()
{
  button2=digitalRead(2); //read push button DRS ON value
  button3=digitalRead(3); //read push button DRS OFF value
  button4=digitalRead(4); //read push button BREAK value
  myservo.write(pos); //servo turn to initial position
  delay(5); //delay 5ms
  pos=constrain(pos,0,180);
  if(button3==1 && button2==0)
  {
    pos++;
    digitalWrite(led1Pin, HIGH); // turn Red LED ON
    digitalWrite(led2Pin, LOW); // turn Green LED OFF
  }
  if(button4==1 && button2==0)
  {
    pos++;
    digitalWrite(led1Pin, HIGH); // turn Red LED ON
    digitalWrite(led2Pin, LOW); // turn Green LED OFF
  }
  if(button4==0 && button2==1)
  {
    pos--;
    digitalWrite(led1Pin, LOW); // turn Red LED OFF
    digitalWrite(led2Pin, HIGH); // turn Green LED ON
  }
}

```



